Electrochemical biosensing array for simultaneous detection of urinary metabolites for disease profiling

Fernando Perez

A thesis submitted in partial fulfilment of the requirements of the University of Brighton for the degree of Doctor of Philosophy

July 2023

Abstract

Overactive bladder (OAB) is a multifactorial disease that affects up to a third of the population. OAB is a syndrome where dysfunction in bladder storage presents with increased urinary urgency, frequency, and nocturia. Often OAB is diagnosed when other urinary pathophysiology is not present. The condition can be socially isolating for the sufferer. Given the majority of the symptoms associated with OAB are due to functional changes in the bladder, there is an assumption that changes in signalling molecules within the bladder may be root cause of OAB.

Signalling molecules are released from the bladder urothelium, which is the outer most layer of the bladder and is in direct contact with urine stored within the bladder. These signalling molecules play a pivotal role in regulating bladder function such as relaxation and contraction of the bladder smooth muscle. The three main urothelium signalling molecules are acetylcholine (ACh), adenosine triphosphate (ATP), and nitric oxide. However, these signalling molecules when released from the urothelium are easily metabolised making detection difficult. However, their respective metabolites choline, xanthine, and nitrite, are stable and thus provide the ability to serve as indirect measure of urothelium signalling molecules in urine.

To measure the metabolites of urothelium signalling molecules, we utilised electrochemical detection, where multiple electrochemical sensors could be utilised for simultaneous detection of all metabolites within a single urine sample.

For simultaneous measurements, four carbon platinum black composite working electrodes consisting of carbon nanotube and platinum black were produced and tailored to directly detect nitrite and peroxide. Two of these electrodes were used to detect peroxide generated by choline oxidase and xanthine oxidase. The third electrode served as a null electrode as well as for the detection of nitrite. The fourth electrode is used to subtract for the nitrite sensor.

By using these four sensors we detected choline, xanthine, and nitrite in rat urine from an OAB animal model. We observed no difference in choline levels, a significant decrease in

xanthine levels and significant increase in nitrite level in the urine of the OAB animal model. Both xanthine and nitrite showed clear correlations with bladder functional measures and inflammatory score.

Overall, our findings highlight that metabolites of urothelium signalling molecules can provide insight into changes with OAB that are directly related to functional changes. These findings can have significant potential in the development of a point-of-care diagnostic technology for early detection of OAB.

Contents

List of figures

List of tables

Abbreviations

ACh	Acetylcholine
AChE	Acetylcholinesterase
ADP	Adenosine 5’-diphosphate
ATP	Adenosine 5’-triphosphate
AU	Artificial urine
AWG	American wire gauge
BGMD	Blood glucose monitoring device
BSA	Bovine serum albumin
BuChE	Butyrylcholinesterase
CE	Capillary electrophoresis
CHT1	High-affinity choline transporter
CTL	Choline transporter-like protein
CV	Cyclic voltammetry
DPV	Differential pulse voltammetry
EDX	Energy-dispersive x-ray spectrometry
ELISA	Enzyme-linked immunosorbent assay
FSCV	Fast scan cyclic voltammetry
GAG	Glucose-aminoglycan
GA	Glutaraldehyde
GC	Gas chromatography
GPRC	G-protein
HPLC	High performance liquid chromatography
IHC	Immunohistochemistry
LOD	Limit of detection
LUTS	Lower urinary tract symptoms
MWCNT	Multi-walled carbon nanotubes
Nafion™	Sulfonated tetrafluoroethylene polymer
NANC	Non-adrenergic, non-cholinergic

NO	Nitric oxide
NOS	Nitric oxide synthase
OAB	Overactive bladder
OCT	Organic cation transporter
PAG	Periaqueductal grey
PdB	Palladium black
PMC	Pontine micturition center
PPD	Poly(phenylenediamine
PtB	Platinum black
qPCR	Quantitative polymerase chain reaction
TRPV1	Transient receptor potential cation channel subfamily V member 1
UF-AU	Urea free artificial urine
UTI	Urinary tract infection
VAChT	Vesicular acetylcholine transporter

Acknowledgements

I wish to thank everyone that contributed towards the completion of the thesis and the support provided to me along the way.

First and foremost, I extend my deep gratitude to my supervisor Professor Patel, for providing me the opportunity to embark on this journey, and for providing guidance and inspiration despite the unprecedented challenges.

An extra special thanks to Professor Michael Winder and the team at Sahlgrenska for introducing me to research and their excellent contributions that helped shaped the thesis.

Thanks to Dr Yeoman, Dr Marcus Allen, and Professor Cragg for their expertise and insight in approaching the project.

I am grateful to Dr John Young and Prof Anastasia Callaghan for their part in the project.

I thank past and present members of the Patel Group for the camaraderie and motivation during challenging times. Your friendship has made this journey enjoyable and memorable. I thank Dr Aya Abdalla for patiently teaching me the basics of electrochemistry, Mareike Herrmann and Dr Nadezhda Velichkova for burning those long hours in the lab. Ricoveer Shergill for his infinite energy and motivation; Ana, Emily, and Ryan for all the help with biology.

I send my love to everyone in the PhD office, past, present, and future. Particular thanks to Dr Gheed Al-Hity, Dr Haya Intabli, Dr Marta Falcinelli for their advice and support. Thanks to Dr Emma Ward for your unparalleled kindness and unfaltering work ethic. And thanks to Andra, Chloe, Natalia.

I want to express my gratitude to all the authors, researchers, and scholars whose works I have cited in this thesis. Their contributions to the field have been fundamental to the development of my research.

I would like to acknowledge the support of EPSRC whose financial assistance made this research possible.

To everyone who has played a part in shaping this thesis and myself, directly and indirectly, I extend my heartfelt thanks. Your contributions have been invaluable, and I am deeply grateful for your support.

Thank you all.

Declaration

I declare that the research contained in this thesis, unless otherwise formally indicated within the text, is the original work of the author. The thesis has not been previously submitted to this or any other university for a degree and does not incorporate any material already submitted for a degree.

Signed: Fernando Perez
Dated: 13/07/2023

Chapter 1: Introduction

1.1 Overactive Bladder

1.1.1 Incidence and prevalence

Overactive bladder (OAB) is a syndrome where dysfunction in bladder storage presents with increased urinary urgency, frequency, and nocturia (Haylen *et al.*, 2010). This exclusionary diagnosis can only be applied when the symptoms are not due to a urinary tract infection (UTI) or any other pathology (Haylen *et al.*, 2010). The American Urological Association considers increased urinary frequency as above eight episodes in 24 hours (Cox and Rovner, 2018) and used as a threshold in OAB trials, but this can be affected by numerous factors (fluid intake and fluid loss) as well as patient self-reporting (Stav, Dwyer and Rosamilia, 2009). Nocturia is generally defined as needing to wake up to void the bladder more than once during the night, with urgency being the key factor for identifying OAB (Bright *et al.*, 2014).

Over the past 20 years there have been wide ranges reported for the incidence of OAB due to differences in definitions, groups studied, and sampling strategies (Bedretdinova *et al.*, 2016). For the UK the yearly incidence is thought to be around 8.8% (Dallosso *et al.*, 2004). Initial estimates of 16.0% prevalence in men and 16.9% in women came from the NOBLE study performed in 2003 via a telephone survey in the US (Stewart *et al.*, 2003). In 2005 the EPIC study included western European countries and reported OAB to affect 18% of men, 31% of women (Irwin *et al.*, 2006). This disparity between the sexes has been confirmed with the more recent epidemiology of lower urinary tract symptoms (EpiLUTS) study revealing

rates of 27% and 43% in men and women respectively (**Figure 1.1**) (Coyne *et al.*, 2012), and in the OAB poll with 17% and 30% (Coyne *et al.*, 2013).

The consolidation of the terminology for lower urinary tract symptoms (LUTS) points towards recent estimates of OAB prevalence being more accurate. Despite this high prevalence, it is thought to be under reported due to patient embarrassment (Coyne *et al.*, 2013) and the misconception that urinary incontinence is just part of ageing. Though it is the case that OAB and symptom severity increases with age (Hannestad *et al.*, 2000; Wennberg *et al.*, 2009), it is clear that the syndrome has underlying causes that could benefit from tailored treatment (Peyronnet *et al.*, 2019).

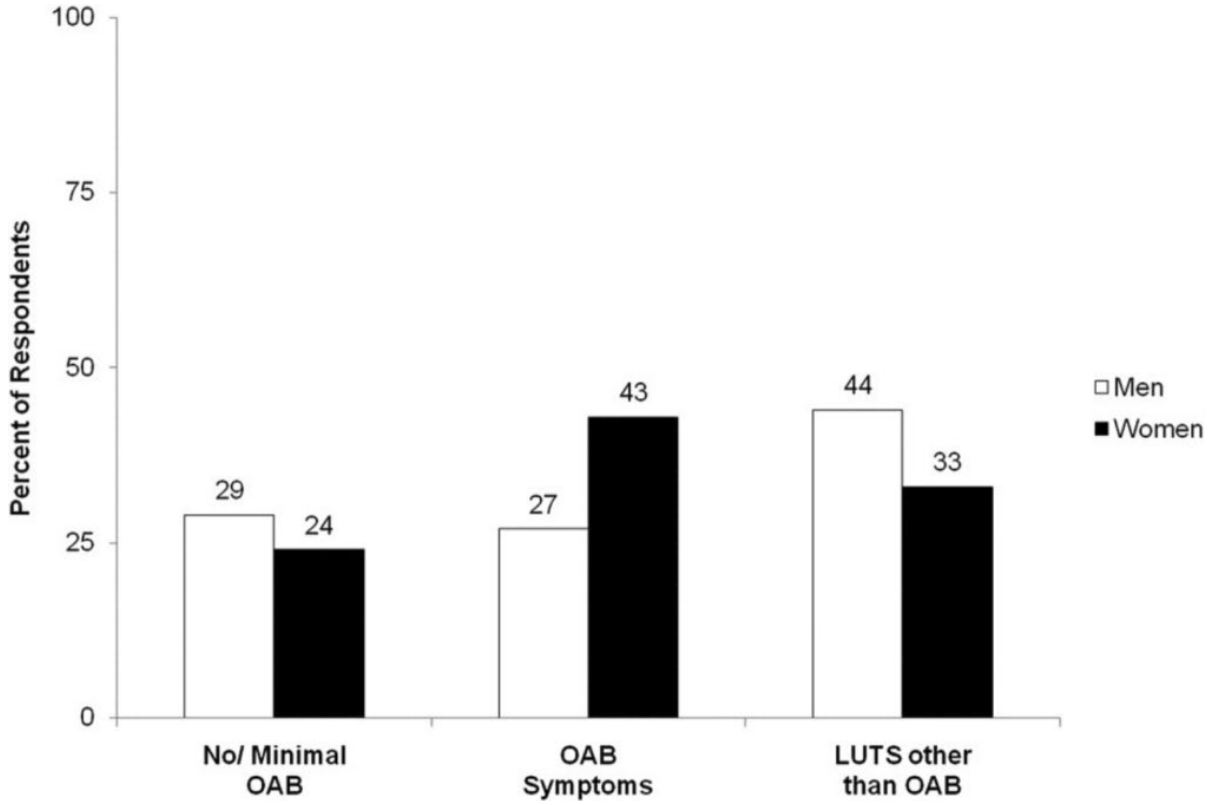

Figure 1.1.
Percentage of men and women reporting OAB symptoms 'sometimes' as part of the EpiLUTS survey. Milsom, I. *et al.*, 2012.

1.1.2 Impact

The key symptom of OAB is the acute urgency sensed by the patient, that doesn't necessarily result in incontinence. OAB can be further broken down in patients that don't suffer from urinary incontinence (OAB dry), and those that do (OAB wet). The proportion between the two groups is roughly 2:1 (dry to wet) (Tubaro, 2004) and shown to worsen with time (Wennberg *et al.*, 2009). This is a huge problem as OAB patients suffer a decreased quality of life from the discomfort of the urge and the increased urinary frequency (Agarwal *et al.*, 2014), as well as the financial burden of purchasing continence pads. This cost is then picked up by the NHS which spends £80 million for incontinence pads (NHS England, 2018), often supplemented by the individual if supply is insufficient (Turner *et al.*, 2004; Uchil *et al.*, 2006). Furthermore, OAB symptoms contribute to an increase risk in falls (Soliman, Meyer and Baum, 2016; Szabo *et al.*, 2018) which cost the NHS £2.3 billion (NICE guideline, 2013) in hospital and nursing home admissions (Milsom *et al.*, 2014). This is concerning as patients only refer to a healthcare professional once symptoms become severe, resulting in years of poor quality of life which could have been prevented with lifestyle and pharmacological treatment.

Impact	Number of participants (%)
Affects daily living	44.1
Causes depression	37.3
Avoids going out	27.0
Plans life around condition	32.3

Table 1.
Impact of bladder dysfunction on daily life (*n = 763*). Uchil *et al.*, 2006.

It is therefore important to review the anatomy of the bladder and how it functions normally, as to then explore the changes that occur with disease that could be responsible for the dysfunction in OAB.

1.1.3 Bladder anatomy

The bladder is a musculomembranous organ vital for the storage and voluntary elimination of urine (Miftahof and Nam, 2013). To serve this function the bladder base is shaped like an inverted triangle (known as the trigone), from which two inferolateral surfaces meet the bladder neck, and above is the superior surface (Drake *et al.*, 2020). The superior surface is domed inwards and balloons upwards as the bladder fills, taking space in the pelvic cavity and lower abdomen. The trigone is fed by two ureters which enter obliquely at the top and close during detrusor contraction as to reduce backflow as bladder pressure increases during filling (Corcos, Ginsberg and Karsenty, 2015). These drain towards the neck of the bladder where the urethra is located, which despite different nerve connections it is anatomically and functionally indistinguishable (Corcos, Ginsberg and Karsenty, 2015).

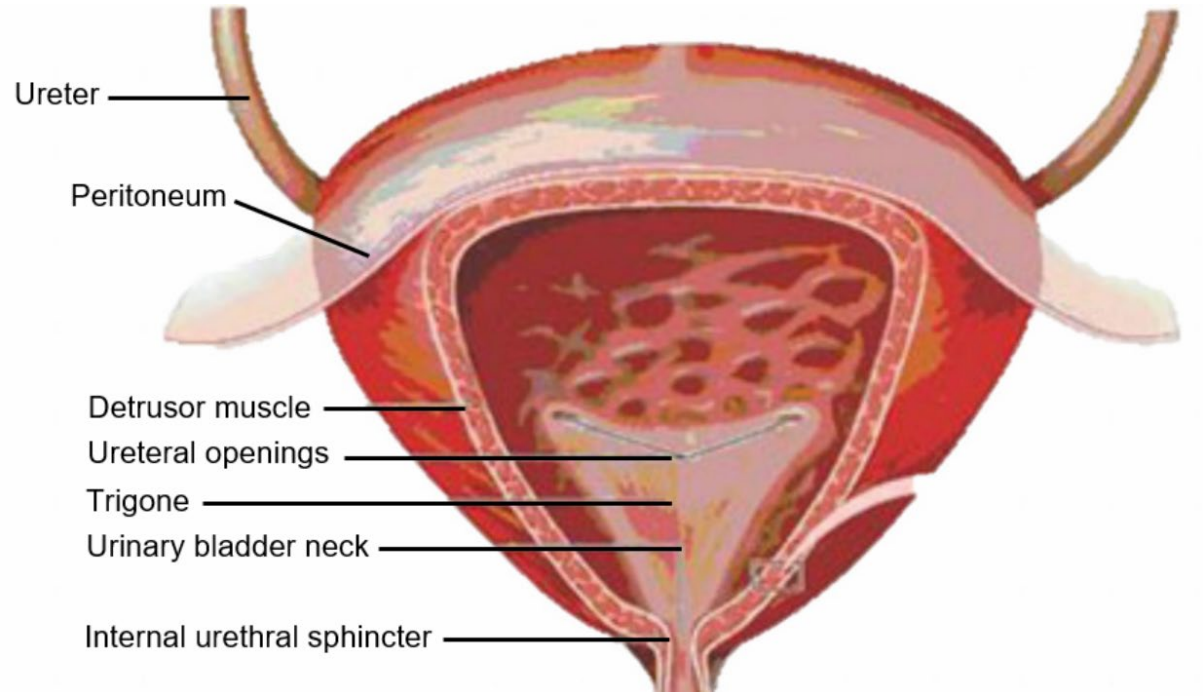

Figure 1.2.
Diagram of anatomy of lower urinary tract (LUT). Miftahof, R. N. *et al.*, 2013.

There are sex specific urethral anatomical differences that affect bladder storage and voiding. In females the pubovesical ligament wraps around the bladder neck, whilst in males the puboprostatic ligament blends with the fibrous capsule of the prostate that surrounds the bladder neck (**Figure 1.3**) (Drake *et al.*, 2020). The longer (18-20cm) male urethra contains the internal urethral sphincter consisting of smooth muscle fibres which continue from the detrusor into circularly arranged fibres fed by sympathetic nerves (Wallner *et al.*, 2009). This proximal sphincter promotes continence and prevents retrograde semen ejaculation, whilst the distal sphincter is composed of striated voluntary muscle in a horseshoe shape with an inner layer of smooth muscle (Chapple, Steers and Evans, 2020). This means that in males even if the proximal sphincter and bladder neck are completely non-functioning, continence can be maintained by the voluntary distal sphincter alone (Chapple, Steers and Evans, 2020). The female urethra is only about 4cm long with the proximal sphincter (urethral rhabdosphincter) taking up to two thirds of the length and is surrounded by circular striated muscle (Corcos, Ginsberg and Karsenty, 2015). This is

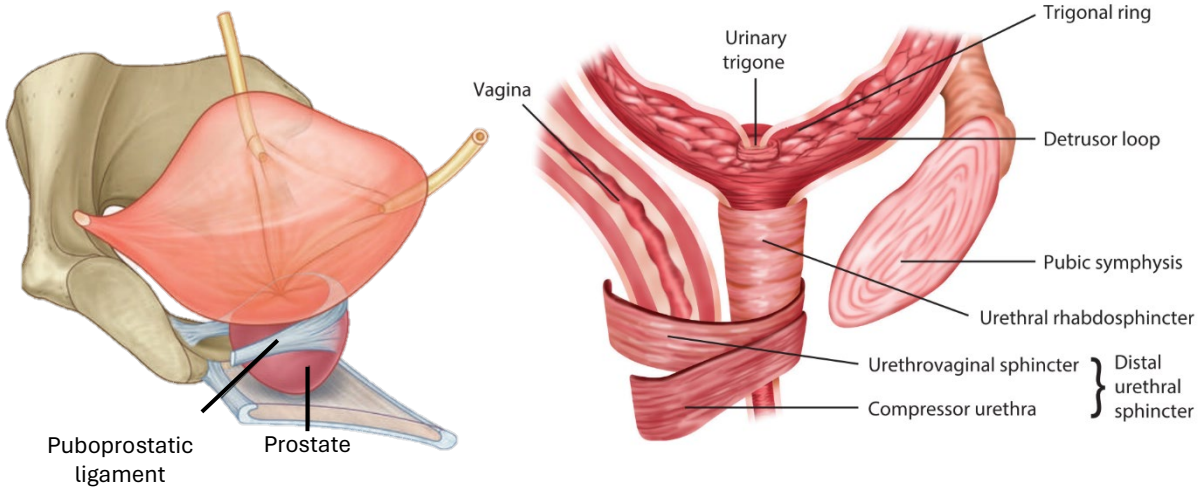

Figure 1.3.
Diagram of male ligaments and urinary bladder (left), Drake, R. L. *et al.*, 2020. Diagram of female urethral sphincters (right), Corcos, J. *et al.*, 2015.

followed by the distal sphincter which consists of two striated muscle bands which form the urethrovaginal sphincter and the compressor urethra (**Figure 1.3**) (Corcos, 2001).

The bladder wall is the same in both sexes, and is vital due to its ability to stretch and maintain tension during storage, and contract during micturition. The three main layers consist of the urothelium, the lamina propria, and the detrusor muscle (**Figure 1.4**) (Aoki *et al.*, 2017).

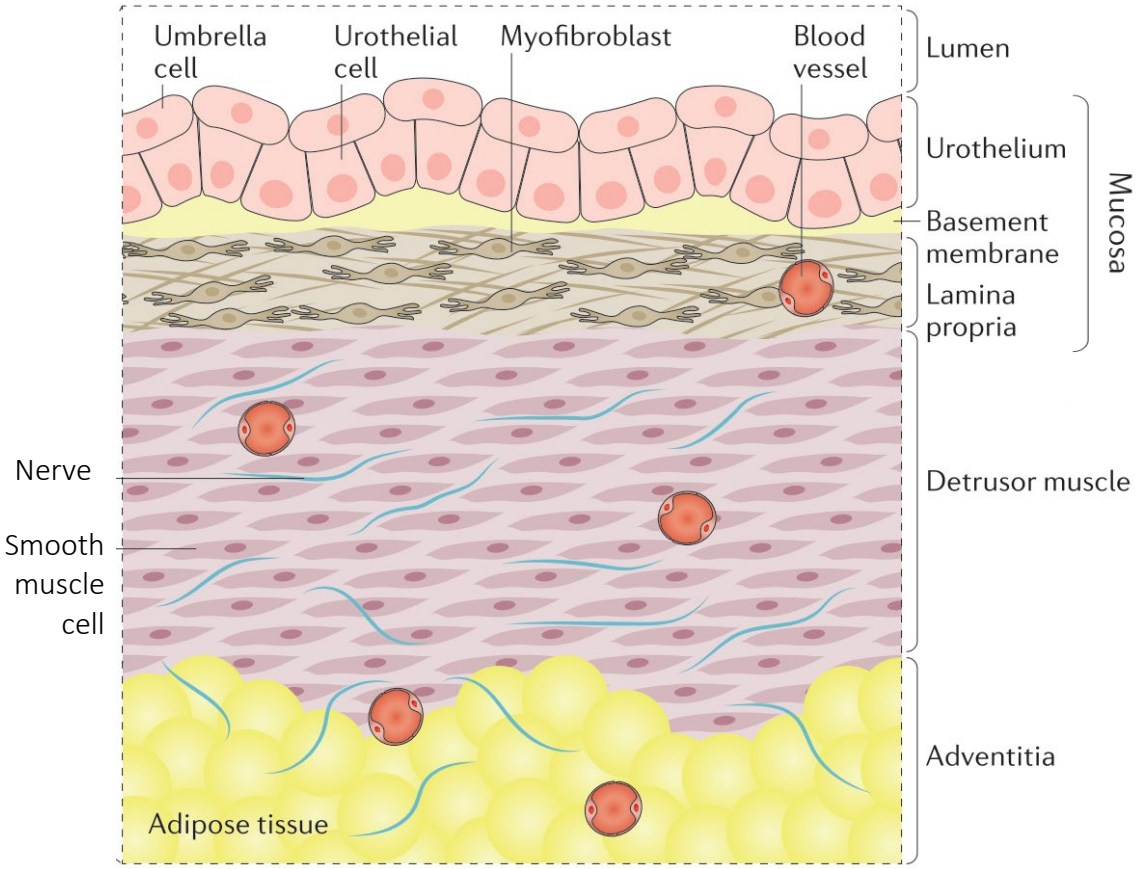

Figure 1.4.
Cross-section of the urinary bladder wall showing the distinct cell layers as determined by histology. Aoki, Y. *et al.*, 2017.

Beneath the umbrella cells the human urothelium contains up to five intermediate cell layers followed by smaller basal cells (Jost, Gosling and Dixon, 1989). This is followed by the lamina propria which contains afferent nerve terminals, blood vessels, fibroblasts and myofibroblasts (Hicks, 1975; Fry *et al.*, 2007) between loose fibrous connective tissue made

of collagen and elastin (Miftahof and Nam, 2013). The next layer is the detrusor smooth muscle cell layer, which has interlacing fibres traveling in all directions up until the bladder neck, where they are orientate into inner longitudinal, middle circumferential, and outer longitudinal muscle layers required for the bladder neck and urethral sphincter (Elbadawi, 1996). The outermost layer is fibrous connective tissue known as the adventitia or serosal layer (William C. de Groat and Yoshimura, 2015).

For the bladder to fill and void correctly the detrusor muscle, internal and external sphincters need to contract and relax appropriately. Therefore, it is important to know how these muscles are innervated to map out where dysfunction occurs in OAB.

1.1.4 Innervation

The micturition cycle can be split into two phases, bladder filling and bladder voiding. To achieve this the urinary bladder is controlled by parasympathetic, sympathetic, and somatic nerves (**Figure 1.5**) (Hanno *et al.*, 2014).

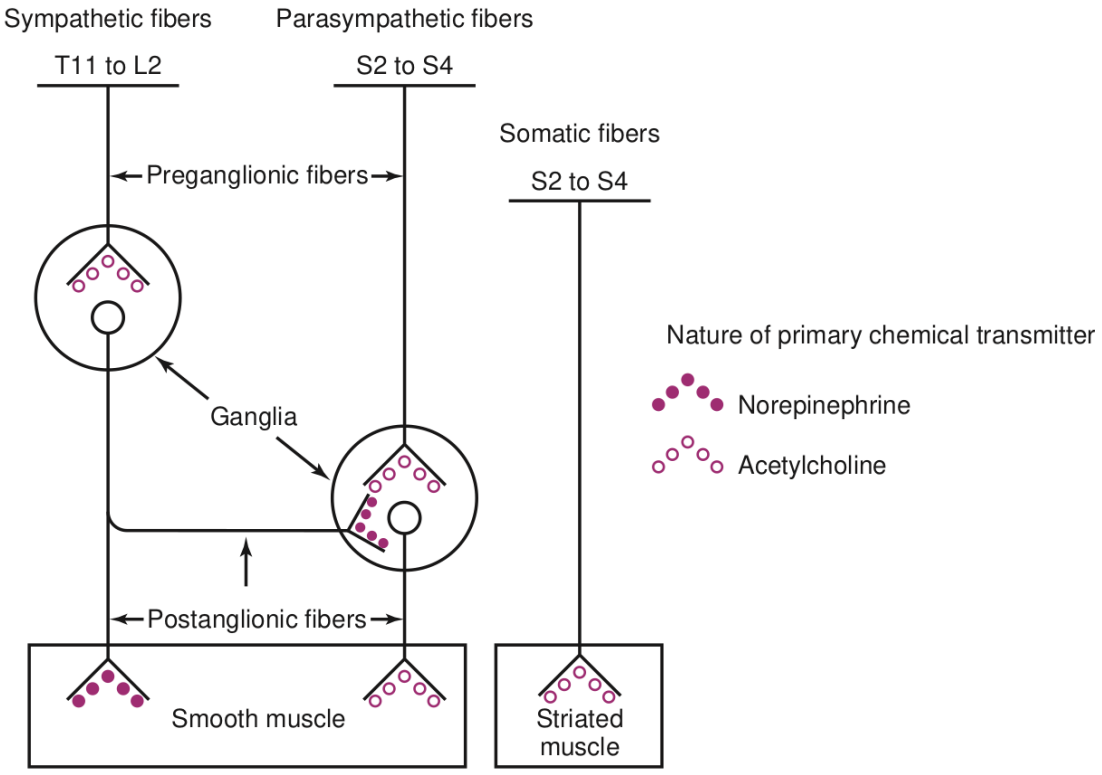

Figure 1.5.
Schematic of efferent nerves of the urinary bladder. Hanno, P. M. *et al.*, 2014.

During the storage phase the sympathetic nervous system signals to detrusor smooth muscle cells to relax. These nerves project from the spinal cord at T11-L2 via the hypogastric nerve, reaching the inferior mesenteric ganglion and then the bladder. Signals can also pass through the paravertebral sympathetic chain ganglia, to the pelvic plexus through the pelvic nerve to the base of the bladder and urethra (William C de Groat and Yoshimura, 2015). Postganglionic nerves release noradrenaline onto α-adrenergic receptors at the base, and onto β-adrenergic receptors in the main body. Sympathetic stimulation causes contraction

of the urethra through α_{1A} receptors, and relaxation of the detrusor muscle through β_3 receptors (Nomiya and Yamaguchi, 2003). Furthermore, sympathetic nerve fibres also innervate parasympathetic ganglia in the detrusor, such that their activation causes inhibition of the parasympathetic system.

During voiding the parasympathetic nervous system carries signals to the detrusor smooth muscle to cause contraction. The pelvic nerve originates from S2-S4 in the spinal cord running to the pelvic plexus, the vesical ganglia on the bladder surface, and the intramural ganglia (Lincoln and Burnstock, 1993). Preganglionic neurotransmission occurs through the release of acetylcholine (ACh) onto nicotinic receptors, and then postganglionic pelvic nerves transmit excitatory signals by releasing ACh onto muscarinic receptors. Despite M2 receptors being the most abundant in the detrusor, contraction is mediated through M3 receptors also located on smooth muscle cells (Tobin and Sjögren, 1995). The pelvic nerve also feeds the urethra and trigger relaxation through the release of nitric oxide (NO) (Andersson and Persson, 1994).

Somatic nerves innervate the striated muscle fibres that control the external urethral sphincter and pelvic floor, carrying signals from Onuf's nucleus at S1-S3 via the pudendal nerve (Fowler, Griffiths and De Groat, 2008). Release of ACh on nicotinic receptors to promote contraction, whilst relaxation of the sphincter occurs through adrenergic nerves (Yoshimura and De Groat, 1997).

OAB is a storage failure thought to be due to detrusor overactivity. As these contractions are involuntary, it is important to map the afferent nerve activity that relays bladder sensation to the brain as part of the micturition cycle.

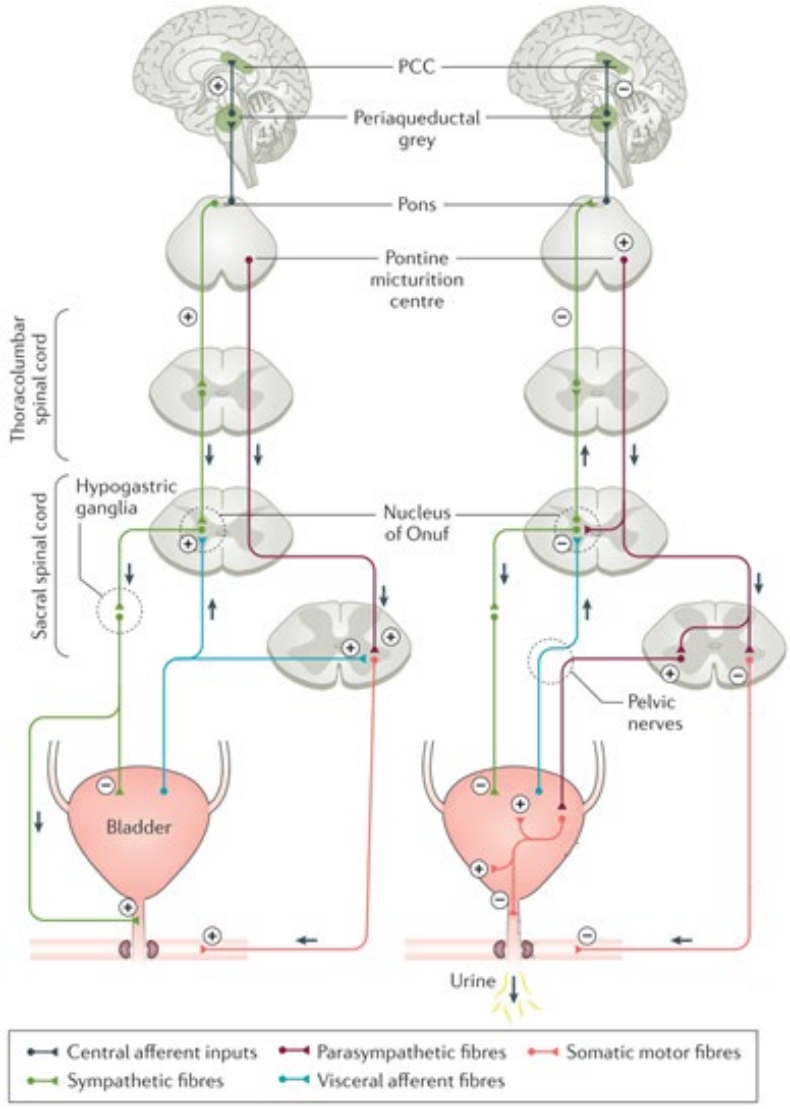

Figure 1.6.
Diagram of the central and peripheral pathways required for micturition. Aoki, Y. *et al.*, 2017.

The afferent nerves are myelinated Aδ and unmyelinated C-fibers which run from the bladder to the spinal cord via the hypogastric, pelvic and pudendal nerves (Kanai and Andersson, 2010; de Groat, Griffiths and Yoshimura, 2015) (**Figure 1.6**) (Aoki *et al.*, 2017). The Aδ nerves located in the detrusor muscle relay information regarding distension during bladder filling (Jänig and Morrison, 1986) whilst C-fibers respond to nociceptive stimulation and are thus located in the lamina propria, close to the urothelium (Häbler, Jänig and

Koltzenburg, 1990). These signals travel up the spinal cord to the periaqueductal grey (PAG) then to the pontine micturition center (PMC) (Griffiths and Fowler, 2013). This is thought to inhibit sympathetic activity in the bladder and promote parasympathetic activity for micturition to occur (Noto *et al.*, 1989).

It is therefore suggested that in OAB the dysfunction could be due to increased afferent firing due to hypersensitivity of the bladder. The mechanism by which afferent activity is initiated would be from a release of signalling molecules from the innermost lining of the bladder, the urothelium.

1.1.5 The urothelium

The innermost layer is the urothelium, and it consists of stratified epithelial cells known as umbrella cells (Khandelwal, Abraham and Apodaca, 2009). These are polyhedral (hexagonal) in shape when flat with diameters between 25-250μm (Khandelwal, Abraham and Apodaca, 2009). These cells interlock with tight junctions of claudin and occludin to form what is thought to be the most impermeable barrier in the body (Kreft *et al.*, 2010). This is further helped through the use of apical uroplakins (Wu *et al.*, 2009) and a glucose-aminoglycan (GAG) mucus layer (Klingler, 2016).

The urothelium was initially thought to just act as a passive barrier to protect the bladder from urine (Jost, Gosling and Dixon, 1989), but is now regarded as a dynamic sensing organ that releases signalling molecules to regulate neuronal activity, detrusor smooth muscle cells and bladder function (Apodaca, 2004; Winder *et al.*, 2014).

1.1.6 Signalling molecules

a) Acetylcholine

In both the afferent and efferent pathways, the release of signalling molecules determines contraction or relaxation of the smooth muscle in the detrusor. Acetylcholine (ACh) was first extracted and identified in 1914 by Sir Henry Dale (Dale, 1914), and then shown by Loewi to pharmacologically slow down a frog's heart when released from the vagus (Dale, 1934). This has led to many pivotal discoveries regarding its release at synapses in the brain and neuromuscular junctions(Van Der Kloot and Molgó, 1994), cholinergic autonomic and somatic nerves (Burnstock, 2013), and its effects in disease (Cruz *et al.*, 2015; Rizzi and Tan, 2017; Sun *et al.*, 2022).

Acetylcholine is an organic ester synthesised enzymatically from choline and acetyl-CoA through choline acetyltransferase (Yoon, Choi and Park, 2022), or via carnitine acetyltransferase in some cells (White and Wu, 1973; Hanna-Mitchell *et al.*, 2007). Neuronal ACh synthesis is thought to be limited by the intracellular availability of choline, which is brought inside through high-affinity choline transporter 1 (CHT-1) (Okuda *et al.*, 2000), choline transporter-like proteins (CTL1-5) (Traiffort, O'Regan and Ruat, 2013), and organic cation transporter (OCT) (Lips *et al.*, 2007). Once formed the ACh is transported into vesicles through the vesicular acetylcholine transporter (VAChT) and then released through calcium mediated exocytosis (Shen and Yakel, 2009). Parasympathetic nerves release ACh to post-synaptic muscarinic receptors which can either be excitatory (M1, M3, M5) or inhibitory (M2, M4) (Mansfield *et al.*, 2005; Winder *et al.*, 2014). These receptors are located on afferent nerve terminals, detrusor smooth muscle cells, or the urothelium.

This is important as it means that when the urothelium is stretched, non-neuronal ACh release can also stimulate these receptors (**Figure 1.7**). Activation of muscarinic receptors triggers local detrusor contraction and increased afferent nerve activity (Hanna-Mitchell *et al.*, 2007; Yoshida *et al.*, 2010; Moro, Uchiyama and Chess-Williams, 2011).

After unbinding from the receptor extracellular ACh is broken down through acetylcholinesterase (AChE)(wakabayashi *et al.*, 1995) and butyrylcholinesterase (BuChE) (Kawashima and Fujii, 2008) so that choline re-uptake can occur (Okuda *et al.*, 2000).

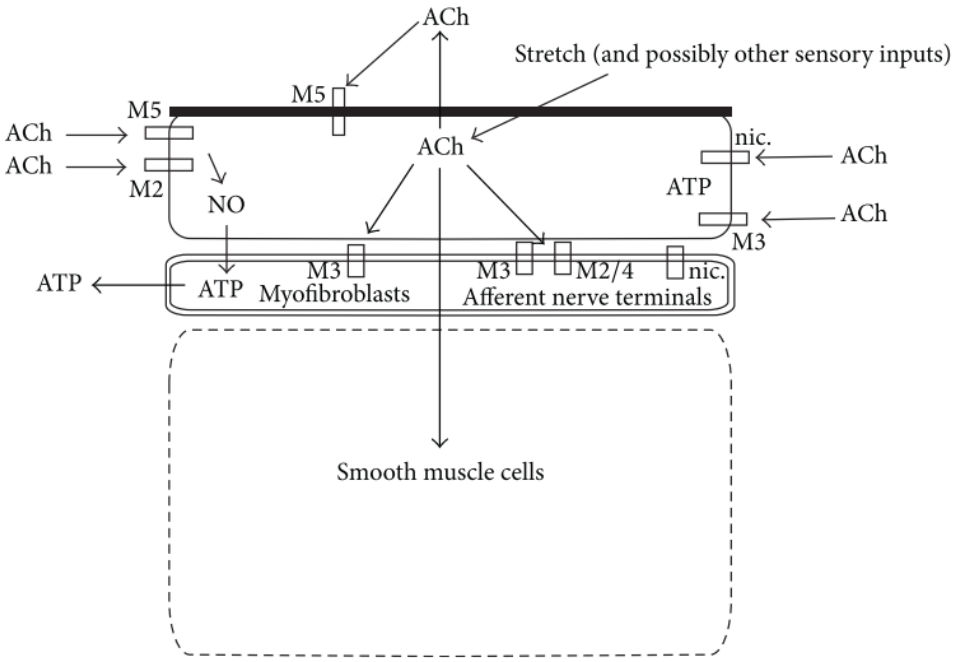

Figure 1.7.
Diagram showing the non-neuronal acetylcholine release and its targets in the bladder wall. Winder *et al.*, 2014.

b) Adenosine Triphosphate

Another important signalling molecule is adenosine 5'-triphosphate (ATP). It can be released from urothelial cells via a uridine triphosphate mediated calcium-dependent mechanism, or by carbachol-mediated calcium-independent mechanism (Sui *et al.*, 2014). Though neuronal release occurs through parasympathetic stimulation resulting in ATP release (Giglio *et al.*, 2007), it does not seem to be a component in healthy human bladder physiology (William C. de Groat and Yoshimura, 2015).

Mechanical deformation of the urothelium (namely stretching) causes ATP release, acting on afferent nerves to relay bladder filling. This is thought to be through $P2X_2$ and $P2X_3$ receptors which are ligand gated ion channels permeable to sodium or calcium (Cockayne *et al.*, 2005). ATP is thought to be part of the non-adrenergic non-cholinergic transmitters

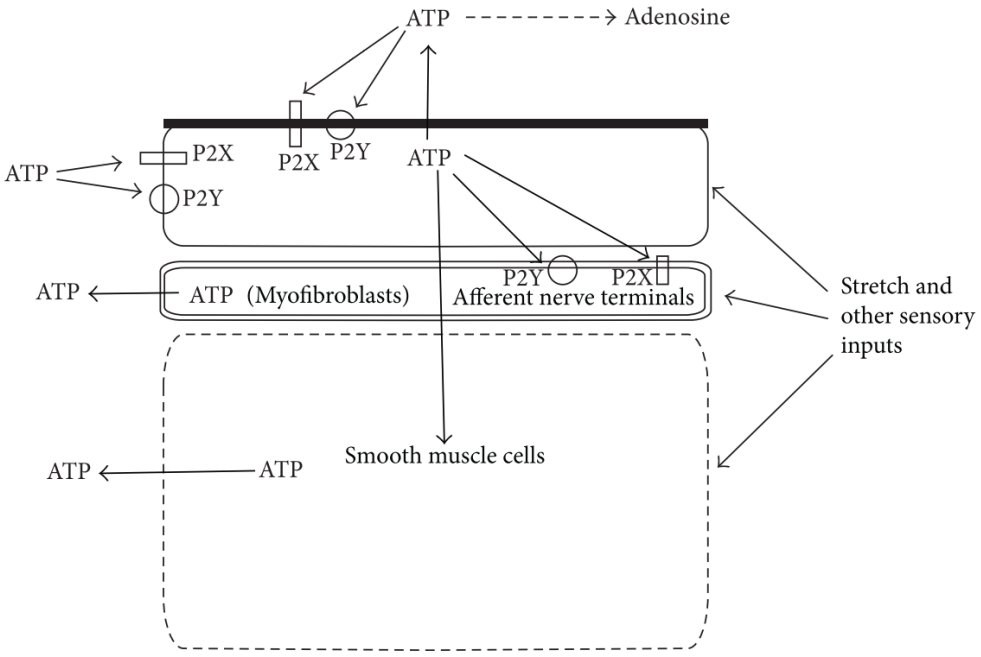

Figure 1.8.
Diagram of ATP release and its targets in the bladder wall (Winder *et al.*, 2014)

responsible for contraction during atropine resistance (Burnstock, Dumsday and Smythe, 1972), and therefore a component of contraction during voiding.

c) Nitric oxide

Nitric oxide (NO) is a gaseous molecule which was shown in 1980 to cause smooth muscle relaxation (Furchgott and Zawadski, 1980), initially identified as endothelium-derived relaxing factor(Nicholls, 2019). It is released from the parasympathetic nerves to regulate relaxation of the bladder (Veselá *et al.*, 2012). It is also released from the urothelium during stretching, muscarinic, β-adrenergic, and vanilloid receptor activation.

NO is formed from nitric oxide synthase (NOS), which can be endothelial, inducible, or neuronal. The isoforms eNOS and nNOS are calcium dependent, whilst iNOS is not. iNOS is upregulated in the urothelium during inflammation in cystitis and acute tissue damage, with detection of NO in urine. However, eNOS expression also increases when the inflammation peaks, whilst nNOS is involved in afferent signalling.

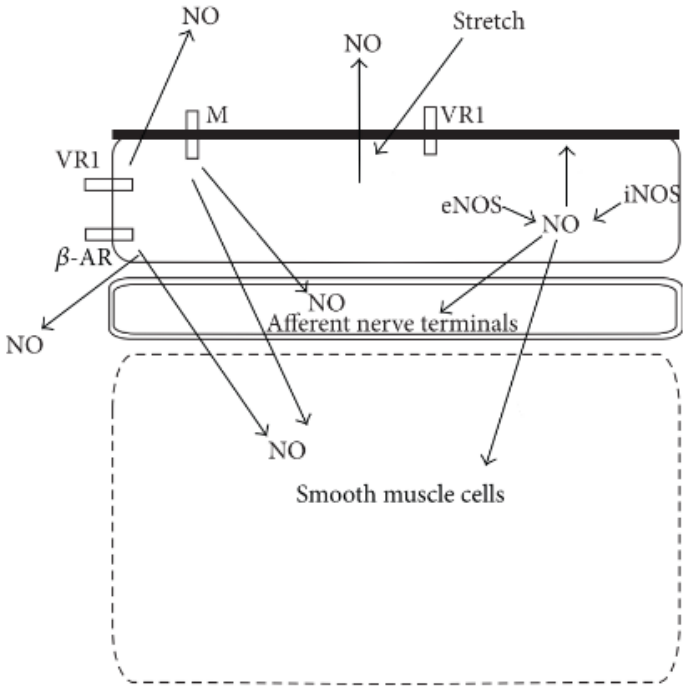

Figure 1.9.
Diagram of nitric oxide (NO) release and its targets in the urinary bladder wall (Winder *et al.*, 2014).

1.2 Methods of exploring bladder function

1.2.1 Pharmacological approach

The neuronal and non-neuronal control of the bladder has been explored through the use of techniques that relate pharmacology to function. The use of agonists, antagonists, and electric field stimulation on *ex-vivo* tissue in conjunction with a force transducer allows changes in muscle contraction to be quantified. Excised tissue can have external factors controlled such that metabolism and downstream pathways do not affect the experimental setup. This is then validated through the use of immunohistochemistry (IHC) (Winder *et al.*, 2016), qPCR (Mansfield *et al.*, 2005), and western blot (Stenqvist *et al.*, 2017) to match receptor quantity and location. This can be quite robust as agonists and antagonists can be specific to a receptor subtype, which then can build an accurate model of how contractions are regulated in the bladder.

A weakness in these methods is that it neglects the effects of the central nervous system as well as reflexes as nerves are severed upon tissue excision. Furthermore, responses to a signalling molecule can be confounding due to a complex interplay where other molecules are released and have opposing effects, resulting in a weak correlation that needs further exploration to elucidate their effects. This is particularly problematic for our models of OAB as both contractile and relaxatory molecules are released upon tissue stretching, and their effect on afferent nerves could be the source of the impulse for urinary urgency.

This could be resolved through the simultaneous detection of multiple signalling molecules.

1.3 Strategies for the detection of signalling molecules

The detection of signalling molecule concentration allows function to be explored precisely as changes in concentration match changes in response. Models can be made more robust through the detection of multiple signalling molecules so that their interplay and effect on function can be studied.

The strategies used for detection need to exhibit certain properties for them to be fit for purpose, but also have unique strengths and weaknesses.

All techniques need to have adequate sensitivity to monitor physiological concentrations of the desired analyte. The technique needs to be specific for the analyte without being affected by other molecules in the matrix, so that only the analyte affects the signal being measured. The detection time of the molecule needs to be fast enough such that its concentration can be related to a functional change.

Other features such as cost and accessibility are often part of the trade-off that a technique has. For example, a highly sensitive technique might require expensive specialised equipment that cannot be miniaturised, limiting the amount of data that can be collected for a disease.

1.3.1 ELISA

One of the most common approaches for the measurement of signalling molecules is the use of enzyme-linked immunosorbent assays (ELISA). This technique was developed in the 1970s for the detection of small biomolecules in science and clinical practice (Borges, Dermargos and Hatanaka, 2022). There are four main ELISA techniques (**Figure 1.10**); direct, indirect, competitive, and sandwich, which all use the specificity of antibodies to antigens to quantify biomolecules through a colour change (Aydin, 2015).

Direct ELISA were initially designed by coating the bottom of a plate with an antigen or antibody relevant to the antibody/antigen to be detected (Engvall, Jonsson and Perlmann, 1971). The detection occurs by using an enzyme conjugated antigen/antibody that binds with the coated antibody/antigen. Provided that there is no non-specific binding (prevented by PBS washing or blocking with BSA) addition of enzyme substrate will produce a quantifiable colour change proportional to the biomolecule concentration (Engvall and Perlmann, 1972).

Indirect ELISA uses two antibodies such that the primary antibody binds to the protein of interest, and the secondary enzyme linked antibody binds to the primary antibody (Lindström and Wager, 1978). Though this allows it to be cheaper and sensitive as only the secondary enzyme is labelled, there is an increased risk of cross reactivity.

A sandwich ELISA offers the highest sensitivity due to the capture antibody coated on the microplate which bind to the antigen, followed by an enzyme-conjugated secondary antibody known as a detection antibody. Again, unbound antibody is washed away, enzyme

substrate is added such that the amount of product generated by the detection antibody is proportional to the antigen in the sample (Alhajj, Zubair and Farhana, 2023).

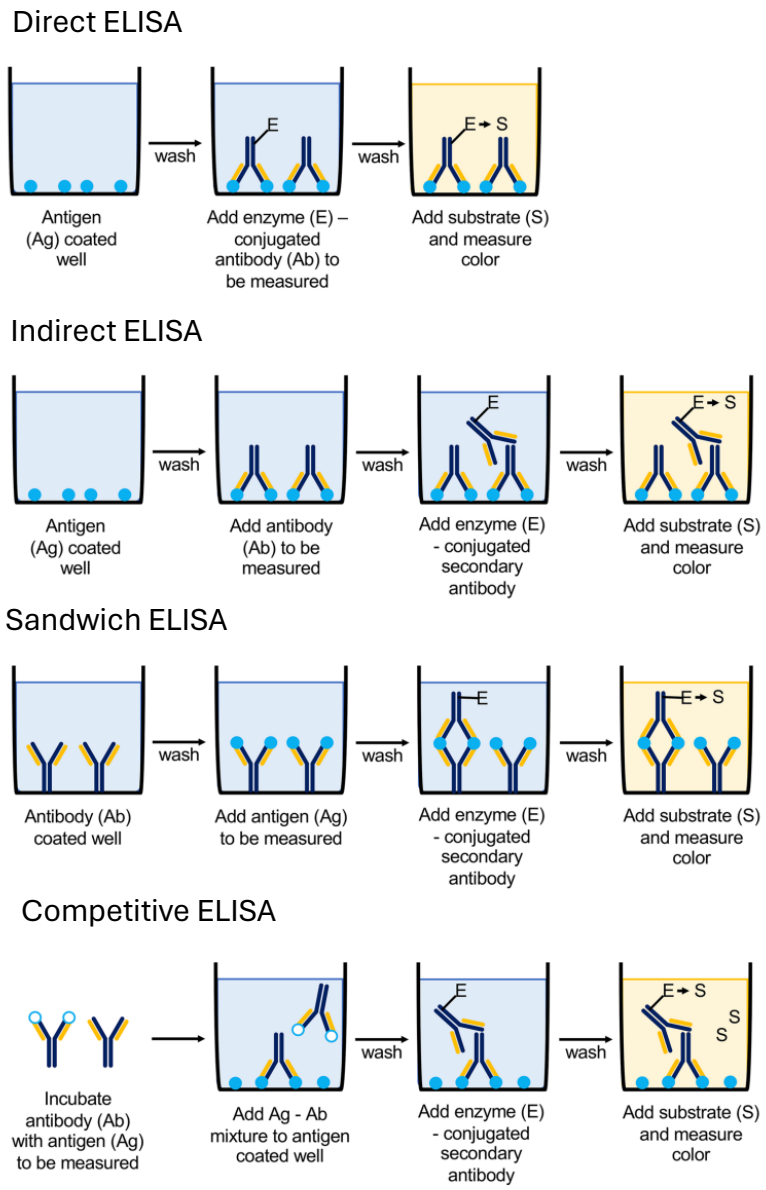

Figure 1.10.
Diagram showing the main types of ELISA and how they function; direct, indirect, sandwich, and competitive (Boguszewska *et al.*, 2019).

For small molecule biomarker detection competitive ELISA is the most widely used method as the size of the molecule is unsuitable for two binding points required for a sandwich assay (Yorde *et al.*, 1976). Like previous assays the base of a 96-well microtiter plate is coated with a specific quantity of antibody so that an appropriate amount of labelled analyte is used(Wild *et al.*, no date). The labelled analyte (tracer) competes with the analyte in the biological sample for the available antibodies, such that signal is inversely proportional to analyte concentration (Clark, Lister and Bar-Joseph, 1986).

The high specificity and selectivity have allowed ELISA to become the gold standard in research and diagnostics, particularly when compared to other assays such as radioimmunoassay (RIA) and polymerase chain reaction (PCR) (Engvall, 2010). However, it does have drawbacks that limit its use in the field such as the requirement of high-cost antibodies tagged with fluorescent labels, requirement of pipettes, a lab, a plate reader, and a trained operator to perform the technique (Chatziharalambous *et al.*, 2016). To overcome some of these drawbacks recent research has focused on developing immunoassays that can occur in 3D printed reactionware (Su, 2021) with detection being quantified by a smartphone's ambient light sensor (Singh *et al.*, 2015; Yang *et al.*, 2018). Even if cost of equipment is mitigated through smartphone use validation is required to exclude measurement bias through matrix effects, and it may be unavoidable to have to perform lengthy sample preparation. This highlights the currently unavoidable time-consuming nature of using the technique.

In the context of our work, the crucial disadvantage of ELISA is the inability to detect dynamic changes in biomolecule concentration (Boguszewska *et al.*, 2019). Detection in changes of

signalling molecule metabolite concentrations could reveal information regarding the relationship between these molecules, where time could be a factor. The detection of multiple metabolites over time would be prohibitively expensive using ELISA.

1.1.1 Separation methods

Separation is an essential aspect in analytical chemistry or chemical measurement science. With the capability to separate components within a sample into individual bands or zones distributed spatially or/and temporally, separation makes the analysis or measurement more accurate. By separating different components into individual fractions, you can reduce or even eliminate the interference from sample matrix species. Such a power also makes separation an important tool to purify components of interest from mixtures or natural products for further investigations. Meanwhile, separation can make a subsequent analytical method more sensitive through enriching or concentrating the components of interest in the samples to be tested (Janoš, 2003). Modern separation science and techniques have been well established and are quite mature, making them widely employed in routine scientific research and practices.

Some of the most widely used techniques for the measurement of signalling molecules are capillary electrophoresis (CE), gas chromatography (GC) (Beale *et al.*, 2018) and high performance liquid chromatography (HPLC) (Ocque, Stubbs and Nolin, 2015).

There have been many studies conducted in measurement of signalling molecules using chromatographic techniques. These are widely useful approaches as they provide the ability to measure a wide range of molecules within a single timepoint but require extensive sample preparation due to the complexity of biological samples.

These are all destructive to the sample, require expensive equipment, and a secondary method to detect the analyte (mass spectrometry). Often sample pre-treatment is necessary which adds to analysis time and consume solvents and columns (HPLC).

1.1.2 Electrochemical biosensors

The term “biosensor” refers strictly to chemical sensors where a biological macromolecule acts as a sensing element that is coupled to a physical-chemical transducer, for the purpose of detecting the concentration or activity of a specific analyte in a sample matrix. The various key elements of a biosensor are shown in **Figure 1.11**. Biosensors can be utilised in portable devices allowing for real-time measurements in remote environments (Watson, 2016).

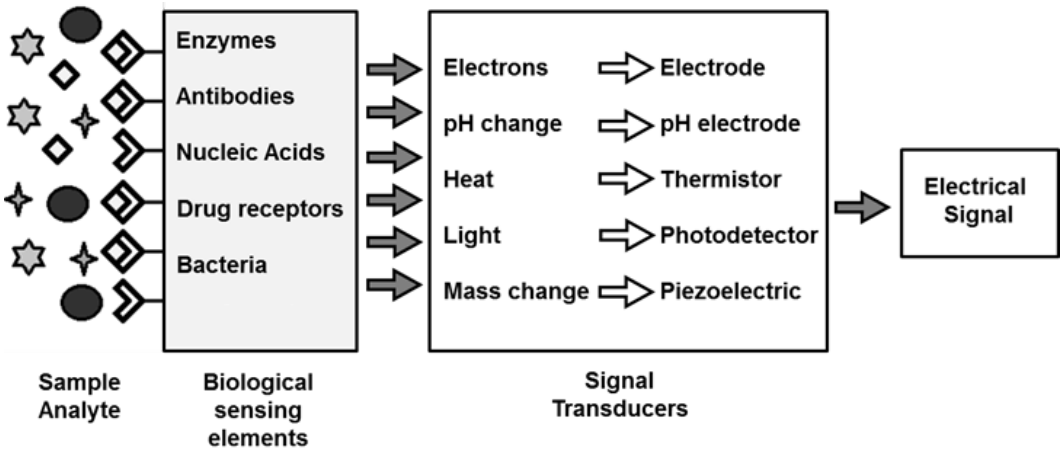

Figure 1.11.
Diagram of the various components in a biosensor.

A variety of biological macromolecules have been utilised within biosensors such as nucleic acids, antibodies and enzymes, of which the latter is the most commonly used biological sensing element. Due to the various biological sensing elements utilised, a host of compounds from sample organic structures to large biomolecular compounds can be easily monitored using such analytical devices. For the transducer element of the biosensor, a variety of analytical techniques have been utilised. These include electrochemical, optical

and piezoelectric. However, electrochemical biosensors have found the most widespread utility in measurement of biological signalling molecules.

Electrochemical biosensors can be constructed and validated such that no sample pre-treatment is necessary. High selectivity is achieved through the use of an enzyme specific to the analyte, as well as through the choice of electrode material and working potential (Watson, 2016; Patel, 2021). Although interferences in the matrix could still affect biosensor function, validation can be done to ensure their contribution to the signal is well below that of the analyte.

Biosensors can run miniaturised reactions cheaply. A small working electrode can use minimal amounts of noble metals, relying on screen printed carbon to carry current (Luong and Vashist, 2016). Cheap enzymes can be used instead of expensive antibodies, provided that an electrochemical reaction proportional to analyte concentration can occur.

Electrochemical biosensors are only limited by the speed of the reaction and mass transfer to the electrode. This can almost occur in real time and allow dynamic changes in analyte concentration. The production of multiple different biosensors in a small geometric area can allow the measurement of multiple analytes in a specific location.

1.4 Thesis aim and objectives

The aim in this project is to develop simple and robust approach to measure important urothelium signalling molecules within urine and understand how they alter with OAB. The following objective will be explored to achieve this aim:

1. Development of a simple strategy for the development of robust electrochemical sensors for the detection of hydrogen peroxide to serve as electrodes for oxidase based electrochemical biosensors.
2. To develop and characterise electrochemical sensors for the detection of choline (metabolite of acetylcholine), xanthine (metabolite of ATP) and nitrite (metabolite of NO) within urine.
3. To conduct physiological measurements from an animal model system of OAB to understand the functional changes that occur.
4. To simultaneously conduct measurement of choline, xanthine and nitrite from urine samples obtained from an animal model system of OAB
5. To evaluate if there are any correlative changes in the level of the different signalling molecules present within the urine and functional changes that occur due to OAB.

The current hypothesis is that in a diseased state the urothelium will release more signalling molecules which in turn would result in an increase in downstream metabolites detected in urine.

Chapter 2: Optimisation the fabrication of electrochemical sensors for the detection of peroxide to serve as first generation oxidase biosensors

2.1 Introduction

2.1.1 Introduction to electrochemistry

Electrochemistry is the study of electron movement in an oxidation or reduction reaction at an electrode surface. As an analyte requires a specific potential for the addition or removal of electrons, a reaction could be specific enough to use as an analytical technique (Bard and Faulkner, 2001).

Electroanalytical sensors can explore real time changes of an analyte in a solution by using fundamental principles of electrodes and their electrical properties (Bard and Faulkner, 2001). The underlying principle for detection to occur is the oxidation or reduction of an analyte preferentially to other molecules in the chemical system. The quantity of molecules oxidised or reduced per unit time is related to the number of electrons that are picked up at the electrode surface and therefore the bulk concentration of the analyte in the sample is determined. There are numerous parameters that influence the dynamics of an electrode reaction: analyte reactivity, electron transfer, mass transfer, and the electrode surface (Fisher, 1998).

To study electrochemical reactions a three-electrode system is generally used. This consists of a working electrode where the reaction occurs, a reference electrode to apply the correct voltage at the working electrode, and a counter (or auxiliary) to return electrons to the system (Figure 2.1).

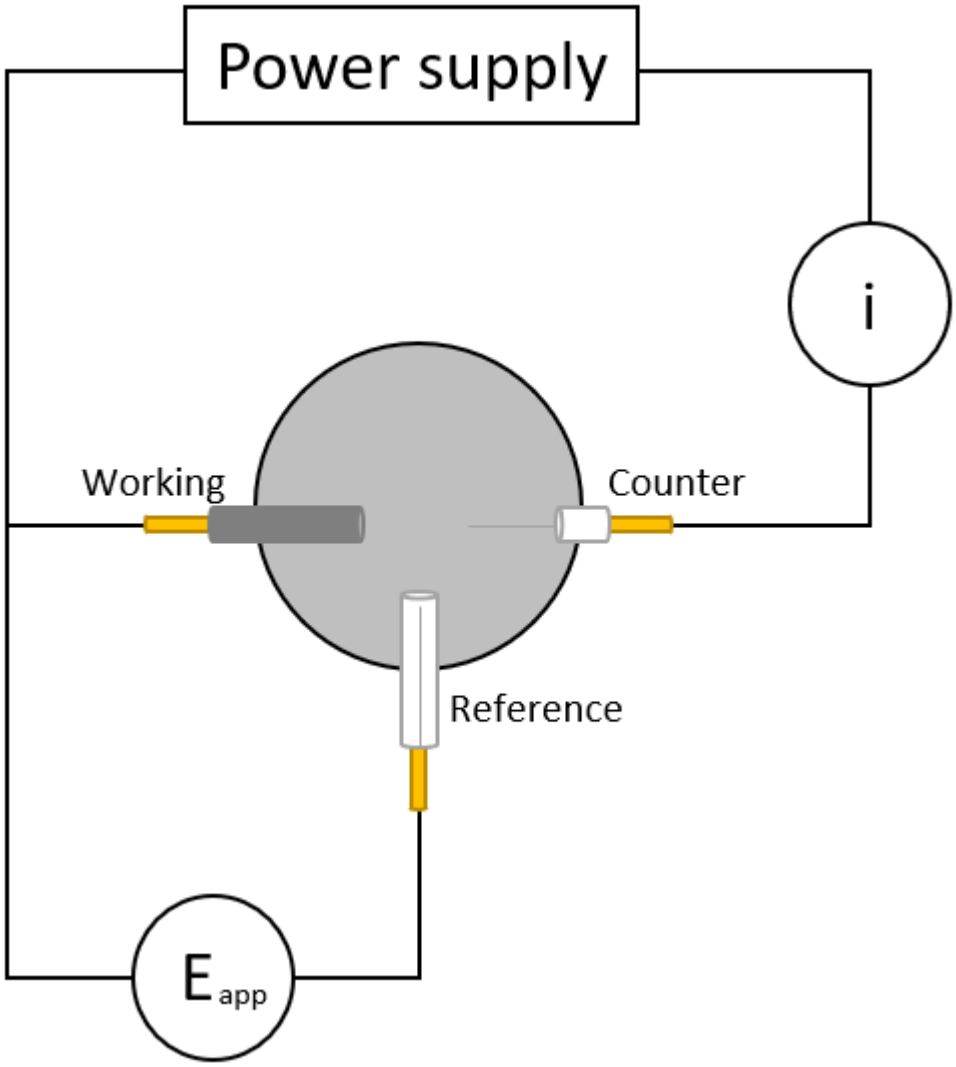

Figure 2.1.
Equipment required to perform electrochemical measurements. Adapted from Watson, D. *et al.*, (2016) with permission.

At the working electrode not only must the voltage be sufficient to drive the electrochemical reaction but the surface is tailored to detect the analyte of interest. The reference electrode (for example Ag|AgCl, consisting of a silver wire in a 3M KCl solution separated from the solution by a porous frit) is the electrode used by the system to accurately apply the voltage to the working electrode. The counter electrode can be of any conductive non-reactive material, usually platinum, and its function is to take or return electrons back to the system, as to ensure no current passes through the silver reference electrode affecting its voltage. A potentiostat is connected to the three electrodes and controls the voltage applied between the working and reference electrode and monitors the current at an ammeter which is positioned between the working and counter electrode.

2.1.1 Electron transfer and mass transfer

In an electrochemical reaction the overall rate of reaction is governed by four main factors. These are electron transfer, surface reactions, chemical reactions prior to electron transfer, and mass transfer (Bard and Faulkner, 2001).

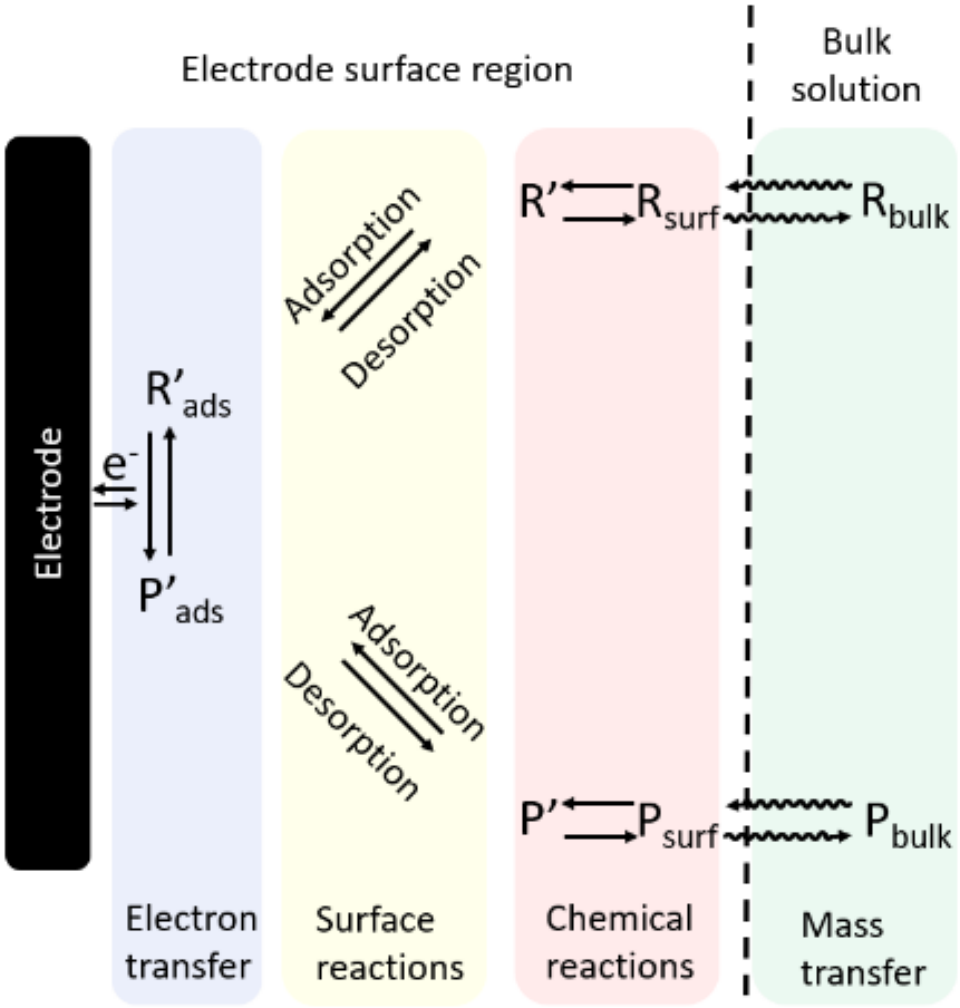

Figure 2.2.
Processes governing a general electrode reaction (Bard, A. et al., 2001).

The complexity of the reaction will affect how each of these rates will affect the final rate of reaction. This is important to understand for each reaction as the final rate of reaction will affect the current which is then related to concentration. For example, in the simplest of reactions a chemically reversible redox reaction is driven by a suitable voltage so that

heterogeneous electron transfer occurs (without requiring adsorption) and there is mass transfer of the product away from the electrode. In more complex reactions, the final rate will be limited by the slowest step/rate determining steps.

Electron transfer must occur for a current to be measured, and the more facile the kinetics the higher the ease of transfer (measured in cms^{-1}). Electrochemical reversibility is a ratio of electron transfer over mass transfer. Therefore, an electrochemically reversible reaction will require lower potentials than an irreversible reaction (Nicholson and Shain, 1964).

Mass transfer refers to the way which the reactant reaches (and product leaves) the electrode surface from the bulk solution. This is rate is governed by three main processes: diffusion, migration, and convection. After polarising the electrode, reactant is oxidised to the product and a concentration gradient between the bulk concentration of the solution and the electrode surface is established (Fisher, 1998). The chemical potential gradient drives reactant to the electrode surface, as well as product away from the electrode surface. Migration occurs due to the electric field that is generated at the electrode/solution interface, which exerts an electrostatic force on the surrounding ions thus inducing movement towards or away from the electrode (Fisher, 1998). Convection affects mass transfer through natural convection such as thermal gradients or forced convection through the use of external mechanical means such as stirrer bars.

Though convection brings the analyte closer to the electrode surface through turbulent flow, the layers of fluid closer to the electrode slow down to laminar flow due to friction causing a reduction in energy. The layer closest to the electrode surface is termed the Nernst diffusion layer, and as it cannot be disrupted by convection the analyte has to diffuse across the final

layer. This layer changes thickness based on the analyte depletion which depends on how long voltage is applied to the electrode.

2.1.2 Cyclic voltammetry

Voltammetry is the application of a time-dependent variation of the potential at an electrode and the current is measured as a function of applied voltage (Maloy, 1983). The plot of current against applied potential is known as a voltammogram and it provides quantitative and qualitative information about the analyte being oxidised or reduced (Maloy, 1983).

In cyclic voltammetry (CV) the voltage is swept linearly in one direction (anodic or cathodic) and then back again, giving the applied waveform a triangular shape (Kissinger and Heineman, 1983). When a slow triangular waveform is applied at a macroelectrode in solution containing a reversible redox couple, a duck shaped voltammogram is generated (Elgrishi *et al.*, 2018).

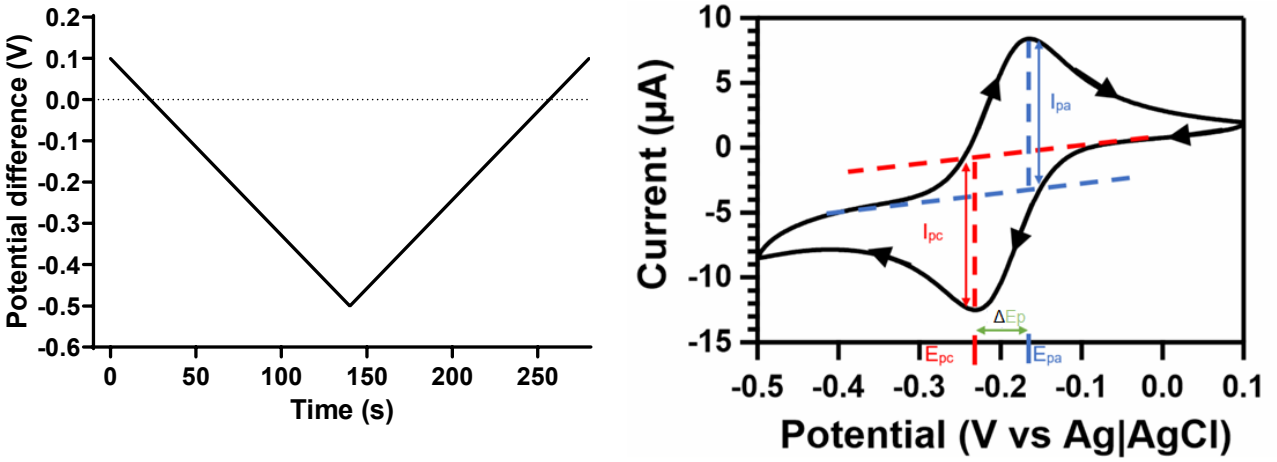

Figure 2.3.
Example cyclic voltammogram of 1 mM ruthenium hexaamine in 1 M KCl using a 3mm glassy carbon working electrode. Features labelled are peak reductive and oxidative current (I_{pc} and I_{pa} respectively), and their voltages (E_{pc} and E_{pa}), as well as change in peak potential (ΔEp). Scan rate 0.05 Vs^{-1}.

The voltammogram is analysed by measuring its features. The example shown in Figure 2.3 is for the redox probe ruthenium hexaamine which is initially reduced. As the voltage sweeps negative, the current increases until a peak response is formed at a specific voltage (known

as the cathodic peak potential, E_{pc}). The current amplitude of the E_{pc} peak is the cathodic peak current (I_{pc}). As the scan continues, past the E_{pc}, the current decreases due to the hinderance of ruthenium hexamine molecules aiming to reach the electrode surface from those that are diffusing away after being reduced at the electrode surface. As this reaction is electrochemically reversible, the rate is limited by electron transfer prior to the peak current, then by mass transfer after the peak.

2.1.3 Amperometry

Amperometry is a pulsed technique where the electrode is held at a constant potential and the resultant current is measured. Figure 2.4 shows an example of the waveform applied at the working electrode and the output current of the fixed potential.

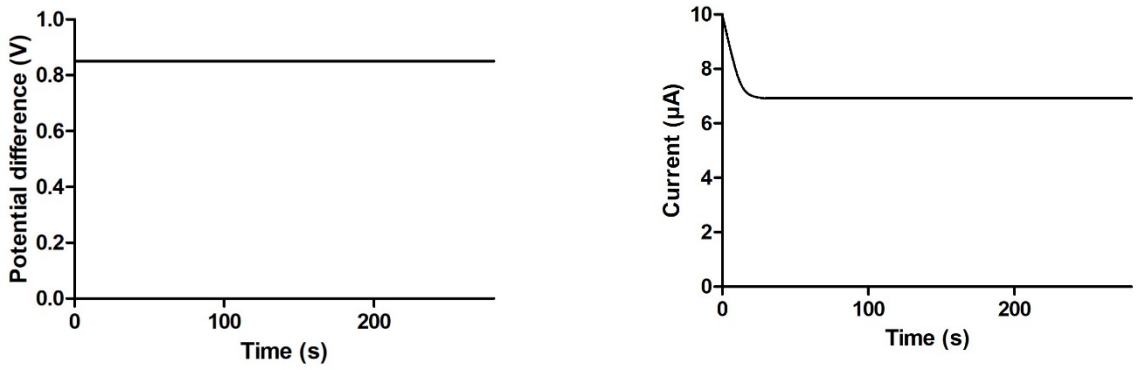

Figure 2.4.
Example of an amperometric waveform applied to the working electrode (left) with resultant current output (right). Adapted with permission from Patel, B. A. *et al.*, 2021.

For the technique to work the applied potential must be sufficient to oxidise or reduce the analyte of interest (Watson, 2016). As the potential is held constant changes in current that happen in real time can be directly related to real time changes in analyte concentration making it an invaluable technique for dynamic detection in biological samples. This is advantageous as in biology many fluctuations occur on a rapid timescale (in the nano to millisecond range), which may not be picked up by fast scan cyclic voltammetry (FSCV), or pulse polarography. In FSCV the electrode is held at a fixed potential for a few milliseconds in-between applications of the triangular waveform to preconcentrate analyte at the electrode surface and minimise biofouling. This reduced sample rate means that FSCV detects changes in concentration with a larger delay than amperometry.

The applied potential chosen will depend on the analyte and the material of the electrode. An optimal potential is usually determined by running a CV with the analyte and identifying the peak potential. The applied potential must then be slightly larger (50-100mV either positive for oxidation or negative for reduction) to account for any drift of the reference electrode (Patel, 2021).

A unique disadvantage of amperometry is that the voltage may oxidise other molecules in the sample and not just the chosen analyte. The way this is avoided is by tailoring the electrode to detect the analyte over other electroactive interferences, at the lowest possible voltage. This is because different electrode materials can be more suitable for a molecule to dock at the surface and donate or receive an electron. Other approaches involve the use of permselective films, that can use size or charge to selectively allow the analyte through. Though films have had moderate success for specific analytes, they reduce the temporal resolution of the electrode whilst also reducing the ruggedness of the electrode. The final constraint for the applied potential is the background solvent and electrolyte. These can affect the potential window in which the analyte can be detected without current generated from electrolysis of the solution.

2.2 Biosensors

Biosensors incorporate a biological macromolecule which when in contact with an analyte generate a measurable signal proportional to analyte concentration (Bhalla *et al.*, 2016; Watson, 2016). This covers a wide range of sensors where the bioreceptor can be aptamers, cells, DNA, enzymes, nanoparticles, and the signal generated can be in any form of energy (heat, light, pH, mass) for data acquisition (Bhalla *et al.*, 2016). The use of the bioreceptor allows high specificity to the analyte within a complex matrix, resulting in high selectivity to the desired analyte (Zhang, Ju and Wang, 2008).

Electrochemical biosensors dominate the market for blood glucose sensing due to their small size and ability to show dynamic fluctuations in concentration. These features of biosensors also make them useful tools in research, as probing real time changes in concentration of analytes in *ex-vivo* tissue allows them to be related to behaviour, drugs, and other endogenous molecules.

Despite the variety of different types of biosensors, the majority use oxidoreductase enzymes due to their established and reliable biochemistry. Oxidase enzymes work by catalysing the analyte into a product with peroxide produced as a by-product. At a suitable electrode poised at a sufficiently high voltage the peroxide can be reduced and related to the initial analyte concentration. For glucose oxidase (GOx) glucose is catalysed into non-electroactive gluconic acid and peroxide as shown in equation 1 below. Equation 2 describes the oxidation of peroxide that can then occur at a suitable electrode.

$$Glucose + O_2 \xrightarrow{GOx} gluconic\ acid + H_2O_2 \quad (1)$$

$$H_2O_2 \rightarrow O_2 + 2H^+ + 2e^- (2)$$

A GOx membrane on a platinum electrode for peroxide detection is commonly defined as a first-generation biosensor. Despite reliability and simplicity of this generation of biosensors there are certain limitations which when overcome allow gains in biosensor selectivity and sensitivity.

The main disadvantage is the use of a platinum electrode for the detection of peroxide. This is because the voltage for reducing peroxide is sufficient to reduce other biomolecules in a sample matrix. This can compromise selectivity depending on the content of electroactive compounds (such as ascorbic acid, dopamine, serotonin, uric acid) in the matrix being studied. This in conjunction with the high cost of a solid metal electrode makes it unsuitable for a disposable point of care device. Therefore, development has gone towards methods of boosting selectivity or enhancing peroxide sensitivity.

Selectivity has often been addressed using permselective electrode coatings that use size, charge, or polarity of interferences to reduce their effect. These are can be constructed via self-assembly (through self-assembled monolayers) or by electropolymerisation. Common films include phenols (Patel *et al.*, 2011; Monti *et al.*, 2017), polypyrrole, poly(phenylenediamine) (PPD) (McMahon *et al.*, 2007; Killoran and O'Neill, 2008), polyaniline (PA) (Kausaite-Minkstimiene *et al.*, 2011), and Nafion (Wahono *et al.*, 2012).

However, the introduction of the coating will reduce the mass transfer of peroxide and consequently negatively impact the sensitivity and response time of the sensor (Hamdi, Wang and Monbouquette, 2005; Clay and Monbouquette, 2018). Therefore, the more

suitable option is to enhance peroxide sensitivity of the transducer. This can be done by enhancing the catalytic ability of the sensor, or by lowering the voltage required to oxidise peroxide so that the sensor operates at a voltage where the interferents are not oxidised (Wang, 2008).

The choice of transducer and its implementation is key for maximising the reliability and ruggedness of the sensor. Older first-generation biosensors used noble metals which were unsuitable due to their high cost and issues with sensitivity to peroxide relative to endogenous compounds. Furthermore, the high voltage required, and high rate of biofouling makes them a poor choice as a transducer. To overcome these disadvantages, sensors have explored the use of novel materials and compounds for peroxide sensing. The method used to incorporate the material on the electrode surface can increase the fragility of the electrode despite improvements in peroxide sensitivity. Common methods include coating, direct deposition, direct growth, and printing (Ahmad *et al.*, 2018), all of these suffer from the creation of multiple layers which add complexity and increase points of failure to the final sensor. This limitation can be avoided by incorporating the novel material throughout the electrode and consequently firmly embedded on the electrode surface. Hence to make a suitably rugged composite electrode it should consist of the least number of materials that together form an inert, easy to shape, biocompatible electrode for peroxide sensing. This ideal transducer can then be transformed into a biosensor through reliable methods used in commercial blood glucose monitoring devices (BGMD). The chosen transducer and fabrication method for BGMD is screen printing carbon electrodes and lithography due to their high throughput nature, but this is unsuitable for research due to the fragility of the

biosensor for use in *ex*-vivo detection as well as the high equipment cost and difficulty for electrode modifications to be made (Feldman *et al.*, 2000; Heller and Feldman, 2010). Therefore composite electrodes are more suitable to produce a point of care diagnostic device.

2.3 Composite electrodes

Carbon composite electrodes are were first introduced in the late 50s in the form of 'carbon paste' electrodes(McCreery, 2008). These initially consisted of graphite powder and a water-immiscible insulating liquid, but now represent carbon-based conductive material dispersed within a non-conductive binding agent. This electrode type comes with advantages and disadvantages that overall have made them ideal for commercial glucose biosensing. This is because composites can cheaply be produced with good geometric control whilst allowing them to be tailored for a specific analyte. Though the random array of conductive pathways throughout the composite cause higher variation than a uniformly conductive material, the electroactive areas allow radial diffusion and less opportunity for the diffusion layer to become depleted of analyte. This coupled with parallel pathways each generating signal with minimal electroactive surface area that would otherwise generate capacitive background allows a large faradaic response with increased signal to noise ratio (Simm *et al.*, 2005).

Advantages	Disadvantages
Cheap	Inter-batch variability
Easy to make	Surface variability
Electrodes can incorporate any conductive particulate material	Increased resistance (compared to solid materials
Fabricated into any geometry	
Mechanically robust	
Small Nernst layer relative to convective boundary layer resulting in reduced dependence on current to flow rate	

Table 2.
Advantages and disadvantages of carbon composite electrodes. Adapted with permission Patel, B. A. *et al.*, 2021.

2.4 Aims and objectives

The aim of this chapter is to:

1. Fabricate a robust electrochemical sensor for the amperometric detection of peroxide.
2. Improve and enhance sensitivity to peroxide.
3. Convert peroxide sensor into glucose biosensor.
4. Characterise glucose biosensor to establish sensitivity, kinetics, and stability.

2.5 Experimental

2.5.1 Materials

0.1 M PBS pH 7.4 composed of 1.37 mM NaCl, 14.7 mM KH_2PO_4, 81.0 mM Na_2HPO_4, 26.9 mM KCl, obtained from Merck (Gillingham, UK). Buffers had their pH adjusted using 1 M NaOH or 1 M HCl using a Hanna precision pH meter model 209. 1 mM hexaammineruthenium(lll) chloride in 1 M KCl as supporting electrolyte made fresh using 18.2 MΩ purified water.

30-50 nm diameter Multi-walled carbon nanotubes (MWCNTs) obtained from CheapTubes, VT, USA. Metal powders were obtained from Merck (Gillingham, UK) consisting of platinum black (PtB), palladium black (PdB), nickel powder (Ni), ferrocenecarboxylic acid, Potassium hexachloroosmate(IV). 50m 30 AWG; silver plated copper wire; black kynar insulated, 0.05 mm^2 obtained from R S Components Ltd. Epoxy resin RX771C/NC and Aradur hardener HY1300 obtained from Robnor Resins Ltd, UK.

2.5.2 Electrode fabrication

Recessed electrode casings with a 2 mm internal diameter and 1 mm depth were designed on Solidworks, sliced on Simplify3D then printed using Raise3D printer. Insulated copper wire was fed through the casing into the recess into which the composite paste would be packed.

Blank composite electrodes consisted of packing the recess with a mixture of 15% w/w MWCNT (Cheap tubes, VM) and 85% of epoxy resin and left to cure for 48 hours. Electrodes were then subjected to 400 grit silicon carbide sandpaper then polished with alumina slurry to reveal a macroelectrode disc.

Metal powders were integrated into the composite electrode by mixing them with the 15% w/w MWCNT. These were added to the composite as received from the supplier to create a mixture containing 10% w/w of the metal powder, resulting in a lower fraction of epoxy resin.

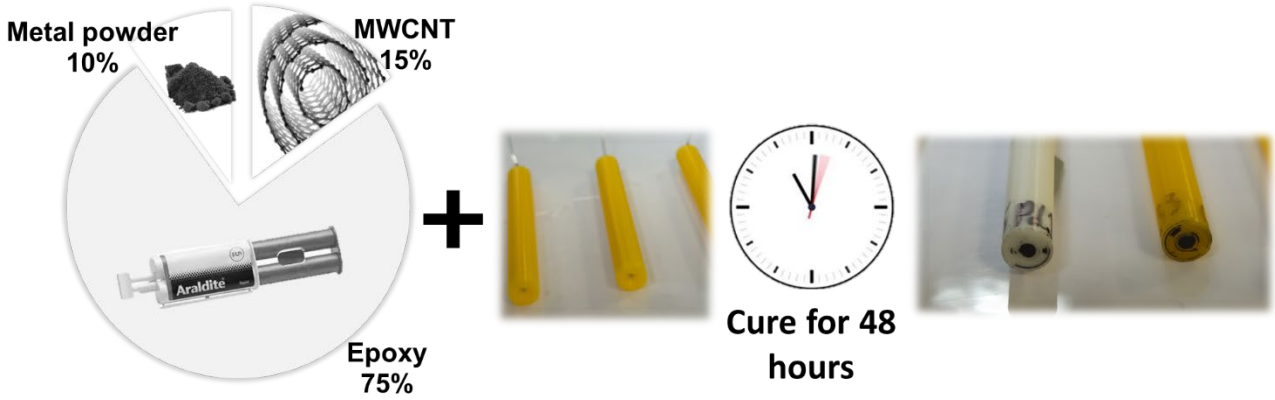

Figure 2.5.
Diagram of electrode fabrication process.

2.5.3 Fabrication of glucose biosensors

A solution of GOx 100U/mg (Merck) with 10% BSA 2μL glutaraldehyde in 0.01 M PBS of which 10 μL was drop cast on the electrode surface. This was left to crosslink for 2 hours then left to stabilise in PBS at 2-8°C.

2.5.4 Electrochemical characterisation of electrodes

Electrochemical measurements were obtained using a CHI 1009 potentiostat (CH instruments, Texas) a Ag|AgCl (3 M KCl) reference electrode, a platinum wire auxiliary electrode, and the composite electrode as the working electrode.

Electrodes were characterised in freshly prepared 1 mM hexaammineruthenium(lll) chloride (Ruhex) in 1 M KCl using cyclic voltammetry (CV). CV parameters for ruhex were scans at 0.05 Vs^{-1} between 0.1 V to -0.5 V.

Amperometric detection of peroxide was performed in stirred 0.1 M PBS pH 7.4 held at 0.85 V. This voltage was chosen as to ensure maximum detection of peroxide regardless of any variations in peak potential caused by the material.

2.5.5 Microscopy and spectroscopy analysis

Imaging was done using a Zeiss SIGMA field emission gun with a secondary detector operating in electron detection mode. The carbon surface was sufficiently conductive to allow native imaging without the use of any sputtering or coating. The Energy Dispersive X-

ray (EDX) spectroscopy was then used to identify the elements on the electrode surface, their dispersion and relative abundance.

2.5.6 Statistical analysis

Raw electrochemical data was exported from CHI and processed using WaveMetrics Igor Pro 4. Peak oxidation and reduction currents were determined through drawing manual tangents in CHI software and analysed using GraphPad Prism 9.

Peroxide calibration data was processed on Igor to remove capacitive background prior to plotting data in GraphPad Prism 8. Data is shown as mean ± standard deviation and plotted with a linear regression. Analysis was performed using 2way ANOVA with ad-hoc Tukey multiple comparisons test.

Biosensor calibration data was processed on Igor for smoothing and background subtraction prior to plotting with GraphPad Prism 9. Data was fitted with Michaelis-Menten enzyme kinetics to determine Vmax and Km. Limit of detection was defined as 3Sy/r where Sy is standard deviation of blank, r is sensitivity. Range of noise was determined using standard deviation of blank signal, and Michaelis-Menten was used to interpolate concentrations on GraphPad. Limit of Quantification (LOQ) was determined as ten times the range of the noise.

2.6 Results and discussion

2.6.1 Optimisation of electrode for peroxide detection

a) Composite electrode fabrication characterisation with ruthenium hexaamine

To test the fabricated electrodes, cyclic voltammetry (CV) was performed in 1 mM ruthenium hexaamine (ruhex) in 1 M KCl. Figure 2.6A shows the responses for an electrode after being subjected to increasing sanding cycles using 400 grit silicon carbide sandpaper. The voltammograms for the batch of electrodes (n = 7) were processed to compare their responses. Prior to sanding no distinct ruthenium peaks are shown (black), with a large separation between the anodic and cathodic peak potentials after one cycle (red), followed by a reduction in the difference between the anodic and cathodic peak potentials with increasing sanding cycles.

Figure 2.6B shows peak current (I_{pc}) decreasing as sanding cycles increase. Unsanded electrodes don't generate responses that can be quantified. Statistical analysis using one-way ANOVA with Tukey's multiple comparisons post test showed a significant decrease in I_{pc} after one sanding cycle ($p < 0.0001$) and after two cycles ($p < 0.001$) followed by no further decreases as sanding cycles increase.

As I_{pc} is related to electrode surface area as per the Randles-Ševčík equation the reduction and subsequent stabilisation of the current is due to removal of excess material until electrode surface area is uniform. After sanding a mean I_{pc} of 5 µA is obtained and using the Randles- Ševčík formula this calculates an electrode surface area of 0.0356 cm^2 which is 13% larger than the actual geometric area of 0.03146 cm^2. However, geometric area may not be a good proxy of electroactive area, as the composite only contains 15% conductive

material. Therefore, if only the conductive fraction of the surface is electroactive an area of 0.004719 cm^2 is expected, the current calculated area is 753% of the electroactive area.

Figure 2.6C shows a decrease and stabilisation of the different between the anodic and cathodic peak potentials (Δ*E*p) as sanding cycles increase, following the same trend seen with I_{pc}. Peak separation is a feature that reveals electron transfer kinetics of the redox couple, where low peak separation indicates facile electron transfer (Nicholson and Shain, 1964). As ruthenium hexaamine is expected to be surface insensitive and have facile electron transfer, the lower Δ*E*p which is seen post sanding follows the data generated at solid metal disk electrodes. Conversely, the pre-sanding currents are not limited by mass transfer due to the electrode's rough irregular shape.

In conclusion the composite fabrication method followed by a minimum of 3 sanding cycles produces electrodes of reproducible electrode with good kinetics.

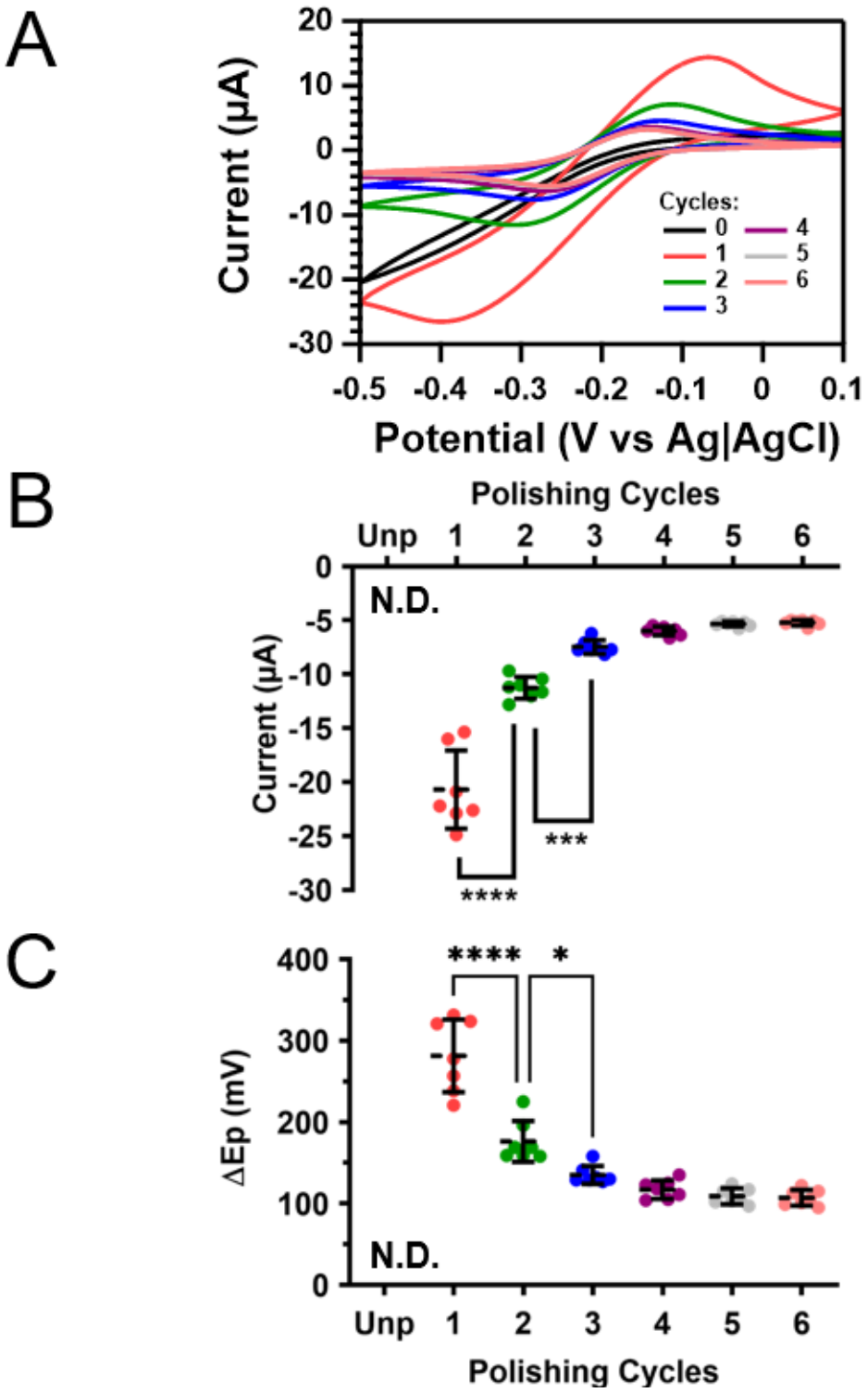

Figure 2.6.
Cyclic Voltammograms for 15% MWCNT composite electrodes in 1 mM $Ru(NH_3)_6^{2+/3+}$ in 1 M KCl generated at 0.05 Vs^{-1} scan rate. (A) Representative voltammograms as composite electrode is sanded. (B) Cathodic peak current (I_{pc}) for batch of composite electrodes. (C) Peak to peak separation (ΔE_p) for electrode batch. One-way ANOVA performed with Tukey's multiple comparisons post test, ****p < 0.0001, *** p < 0.001. Data shown as mean ± S.D. *n = 7*.

b) Effect of transition metals on composite electrode behaviour

Having optimised the preparation of the fabricated electrode for single component composite electrodes the next step was to enhance the sensitivity of the electrode for detection of hydrogen peroxide by the addition of a chemical component.

Materials chosen for testing were transition metals currently used in commercial blood glucose monitoring (BGM) devices. The most commonly used chemicals are ferricyanide (Xiang *et al.*, 2008), ferrocene derivatives (Vashist *et al.*, 2011), and osmium complexes(Jayakumar, Bennett and Leech, 2021) due to their ability to efficiently transfer electrons from the enzymatic reaction (Ballarin *et al.*, 2007). Electrodes used in research to detect reactive oxygen species involve electrocatalysts such as platinum black (PtB) coated platinum electrodes (Ikariyama *et al.*, 1989; Li *et al.*, 2013), as well as palladium nanoparticles (Lim *et al.*, 2005). Nickel has also been used in composite electrodes to detect glucose and acetylcholine (Shibli, Beenakumari and Suma, 2006; Gao *et al.*, 2021) with varying success.

Composite electrodes were constructed with 10% of metal powder mixed with 15% MWCNT. Powders were ferrocene carboxylic acid (FCA), nickel (Ni), potassium hexachloroosmate (Os), palladium black (PdB), and platinum black (PtB). Electrodes were tested in 1 mM ruthenium hexamine in 1 M KCl.

Figure 2.7A shows representative CV for each bicomponent electrode. All bicomponent electrodes generated voltammograms similar to those of blank composite electrodes.

Figure 2.7**Error! Reference source not found.**B shows the mean peak cathodic current (I_{pc}) with standard deviations for batches of 6 electrodes (Os $n = 5$). One-way ANOVA with Tukey's post-test showed a statistical decrease in I_{pc} when the blank was compared to FCA, Ni, and Os electrodes ($p < 0.001$). The PdB and PtB electrodes did not show a decrease in I_{pc} showing that these components did not hinder the response of the electrode for the measurement of ruthenium hexamine. However, in the case of electrodes made containing FCA, Ni and Os, the decrease in the current response could be attributed to the metal hindering the formation of conductive MWCNT pathways or a decrease in electroactive surface area.

Figure 2.7C shows the peak to peak separation (ΔE_p). Statistical analysis shows an increase in ΔE_p for FCA electrodes compared to blank electrodes, and a decrease in ΔE_p for reduced metal black electrodes ($p < 0.05$ and $p < 0.01$ using one-way ANOVA with Tukey's). This indicates fast electron transfer for PdB and PtB, and slow electron transfer with FCA (Kim *et al.*, 2013; Li *et al.*, 2013).

Overall the data shows that addition of different transition metals affects either conductivity or electrode surface area resulting in differing electron transfer of ruthenium hexaamine. This can be further explored through imaging of the electrode surface.

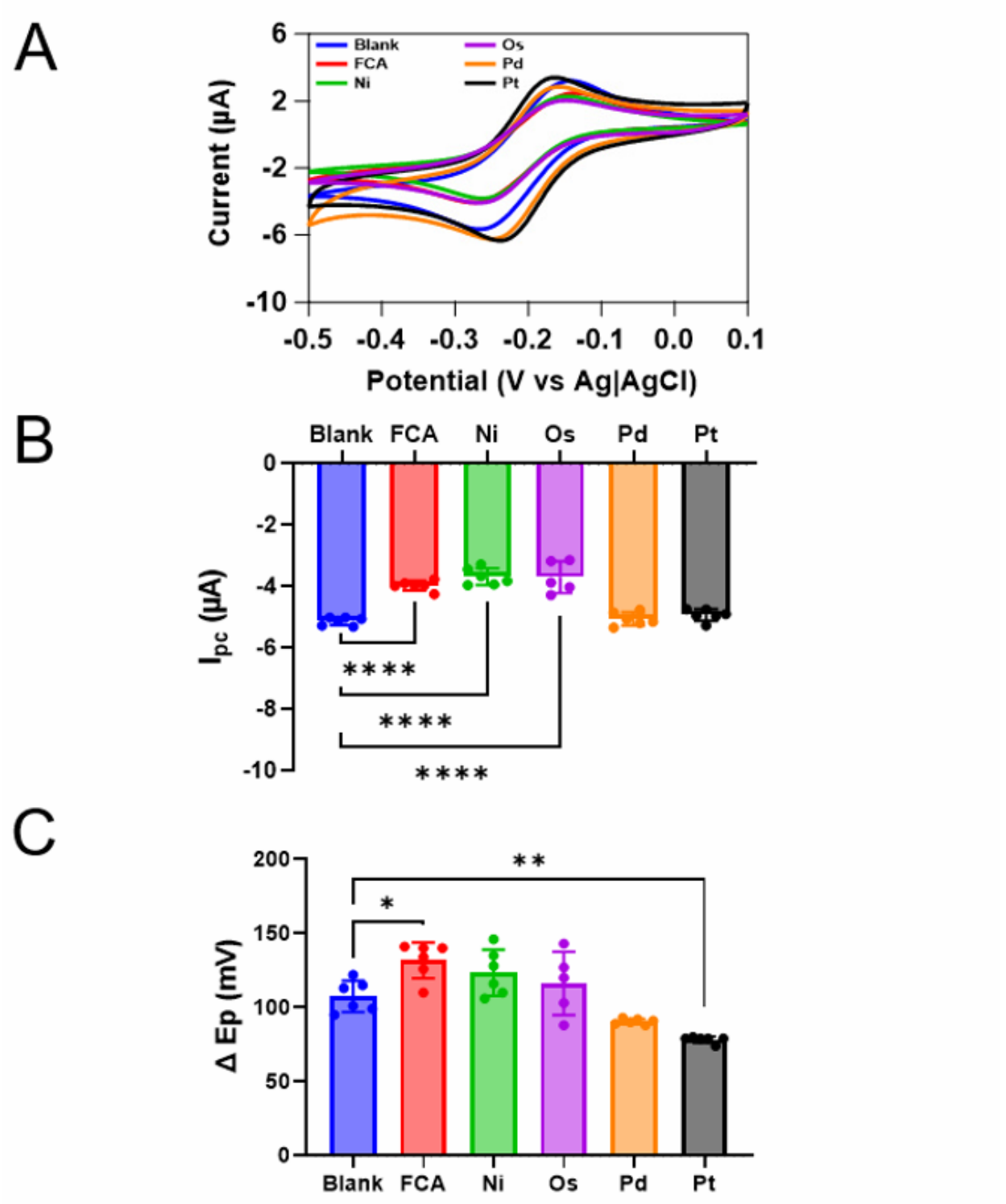

Figure 2.7.
Voltammetric responses of MWCNT and metal composite electrodes to 1 mM $Ru(NH_3)_6^{2+/3+}$ in 1 M KCl at 0.05 Vs^{-1}. (A) Representative CV for each electrode. (B) I_{pc} for composite electrodes, ****p < 0.001. (C) ΔE_p for composite electrodes, *p < 0.05, **p < 0.01. Data shown as mean ± SD. *n = 5* for Osmium, *n = 6* for all other batches.

c) SEM and EDX spectroscopy of composite surface

The differences in electrochemical activity of bicomponent electrodes can be due to the distribution of the metals on the electrode surface. Scanning electron microscopy (SEM) and Energy Dispersive X-ray (EDX) spectroscopy was used to identify the distribution of the metal additives on the electrode surface, as well as their relative abundance.

Figure 2.8A shows EDX spectra which maps the iron (Fe) content of the ferrocene carboxylic acid (FCA) which appears homogenously distributed throughout the electrode surface. Similarly, Figure 2.8B and C show fine and homogenous distribution of Nickel (Ni) and Osmium (Os) on the respective electrode surfaces. This contrasts the distribution of palladium in Figure 2.8D and platinum in Figure 2.8E which show some that the metal particles are clumped together. These findings are interesting as it would be assumed that more homogenous distribution of the metal particles around the MWCNT may provide enhanced current response, but this is not the case as shown in Figure 2.8. Current is instead enhanced when the particles are clumped together as key hot spot regions on the electrode surface. However, these findings do not highlight if there is variations in the quantity of the metals present of if their presence alters the distribution of MWCNT, which potentially could also hinder the current response observed.

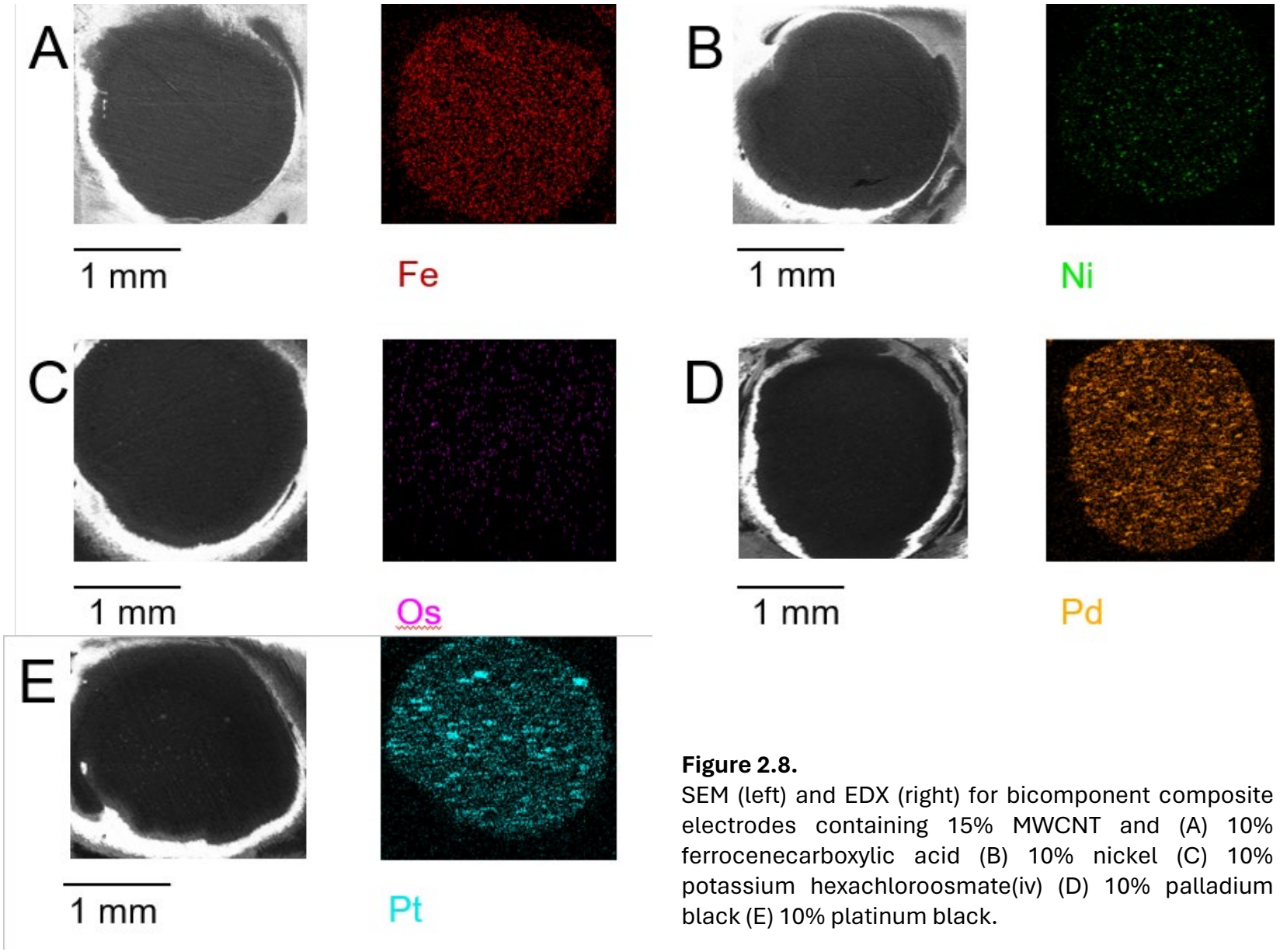

Figure 2.8.
SEM (left) and EDX (right) for bicomponent composite electrodes containing 15% MWCNT and (A) 10% ferrocenecarboxylic acid (B) 10% nickel (C) 10% potassium hexachloroosmate(iv) (D) 10% palladium black (E) 10% platinum black.

d) Sensitivity for detection of hydrogen peroxide

To evaluate which composition would be suitable for oxidase biosensing electrode responses to peroxide were investigated. Data was generated using amperometry in stirred 0.1 M PBS pH 7.2 at +0.85 V vs Ag|AgCl.

Representative traces for electrode response to peroxide are shown in Figure 2.9A. Mean responses with standard deviations for each batch ($n = 6$) are shown in Figure 2.9B.

Figure 2.9B shows that the PdB had the highest sensitivity to peroxide (6.92 μAmM^{-1}) followed by PtB (5.32 μAmM^{-1}). Analysis shows this to be statistically different above 350 µM through a two-way ANOVA ($p < 0.05$). The sensitivity of the blank electrodes is 3.48 ± 0.26 $nAmM^{-1}$, indicating that both PdB and PtB improve sensitivity by orders of magnitude. Figure 2.9B demonstrates that the remaining metal additives hinder the peroxide sensing ability of the MWCNT electrodes.

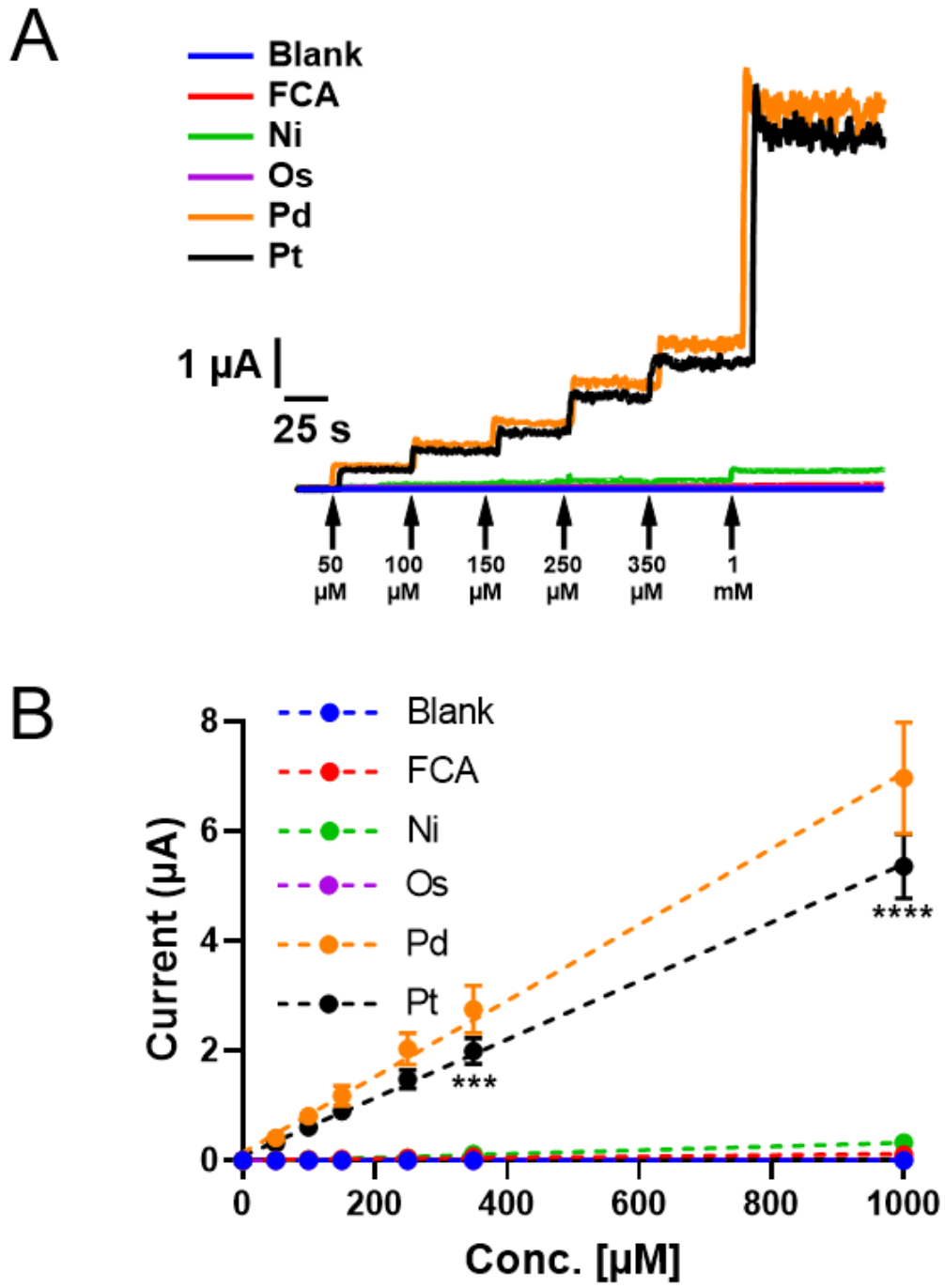

Figure 2.9.
Amperometric responses for 15% MWCNT and metal composite electrodes to cumulative additions of H_2O_2 in stirred 0.1 M PBS pH 7.2. All measurements carried out at +0.85 V vs Ag|AgCl (*n* = *6* for all batches, *n* = *5* for Os). (A) Representative traces for composite electrode with increasing concentrations of H_2O_2 every 50 seconds. (B) Electrode batch responses shown as mean ± S.D.

Comparison of these bicomponent electrodes to peroxide electrodes from the literature are usually done by considering electrode surface area. As the electrode surface is a disc with a diameter of 2 mm this produces an area of 0.03146 cm^2. For the blank 15% MWCNT electrode this results in sensitivity of approximately 0.111 $mAM^{-1}cm^{-2}$. This sensitivity is enhanced to 0.22 $AM^{-1}cm^{-2}$ and 0.17 $AM^{-1}cm^{-2}$ with PdB or PtB respectively.

In comparison, an amperometric platinated platinum microband electrode has a sensitivity of 6.02 $AM^{-1}cm^{-2}$ (Li *et al.*, 2013). Though this electrode has higher sensitivity, it is much more expensive due to both material and fabrication costs, as well as being much smaller and thus saturating at a lower peroxide concentration (1 mM) (Li *et al.*, 2013) making it unsuitable for our use case.

Composition	Sensitivity (μAM^{-1})	Sensitivity ($AM^{-1}cm^{-2}$)
15% MWCNT	3.48×10^{-3}	0.111×10^{-3}
10% PdB + 15% MWCNT	6.92	0.22
10% PtB + 15% MWCNT	5.32	0.17

Table 3. Peroxide sensitivity normalised by geometric surface area.

In relation to other cheap sensors, 3D printed Graphene/PLA sensors have a sensitivity to peroxide of 0.191 $mAM^{-1}cm^{-2}$, making them worse than all composite bicomponent sensors, despite their quick time for fabrication.

Figure 2.9 concludes that bicomponent composite sensors with electrocatalytic nanoparticles enhance sensitivity by orders of magnitude, whilst FCA, nickel, and osmium lower the sensitivity of native MWCNT composite sensors.

Another parameter that can be extracted from this dataset is the limit of detection (LOD). Like sensitivity this is a useful parameter to evaluate and compare sensors. The LOD is often defined as 3Sy/r where Sy is standard deviation of the blank signal, and r is the sensitivity(Loock and Wentzell, 2012). Thus the theoretical lowest concentration that can be detected is 1.15 μM for the PdB electrode and 2.7 μM for PtB.

e) Conductive volume fraction

Comparing sensitivity of the total area is crude as it does not consider the electroactive fraction of the surface area, or the roughness of the electrode surface. These factors are important to consider as an increase in electrochemical activity in a bicomponent sensor could be solely due to the increased addition of the conductive component. Calculating the conductive volume fraction of the electrode can be done using the mass of each of the components and their respective density (O'Hare, Macpherson and Willows, 2002; Abdalla *et al.*, 2021).

$$\boldsymbol{Volume\ fraction} = \frac{\left(\frac{mMWCNT}{mEpoxy}\right)\left(\frac{1}{\rho MWCNT}\right)}{\left(\frac{mMWCNT}{mEpoxy}\right)\left(\frac{1}{\rho MWCNT}\right)+\left(\frac{1}{\rho Epoxy}\right)} + \frac{\left(\frac{mPtB}{mEpoxy}\right)\left(\frac{1}{\rho Epoxy}\right)}{\left(\frac{mPtB}{mEpoxy}\right)\left(\frac{1}{\rho PtB}\right)+\left(\frac{1}{\rho Epoxy}\right)} \quad (3)$$

This gives a conductive volume of 9% for the 15% by mass MWCNT composite electrode. The addition of 10% PtB by mass results in a volume fraction increase by 20% to a total of 29%. This gives a conductive surface of 0.002831 cm^2 for MWCNT and 0.009123 cm^2 for PdB and PtB. Normalisation of the peroxide sensitivity by conductive area gives 1.23 $mAM^{-1}cm^{-2}$ for MWCNT, 0.759 $AM^{-1}cm^{-2}$ for PdB and 0.583 $AM^{-1}cm^{-2}$ for PtB.

The different method often used to determine electroactive surface area is by conductive atomic force microscopy (CAFM)(Colley *et al.*, 2006). Due to the large area it would be necessary to sample key areas of the electrode to give an idea where the majority of the electrode activity occurs. However, as conductivity may not always match the catalytic and electrochemical activity of an electrode, dividing the response of an analyte by the conductive volume fraction is more appropriate.

f) Batch variability for PdB and PtB composite electrodes

To confirm suitability of the bicomponent electrodes for peroxide detection, batch reproducibility required testing. This was determined by producing multiple batches on different days which were then subject to amperometric peroxide calibrations as in (d).

Figure 2.10A shows the mean peroxide sensitivity with standard deviation for batches of PdB electrodes ($n = 5$), with Figure 2.10B showing mean batch sensitivity for PtB electrodes. Analysis showed no statistical difference (ANOVA with Tukey's) in sensitivity between batches for both the PdB and PtB electrodes, indicating good reproducibility for composite electrodes.

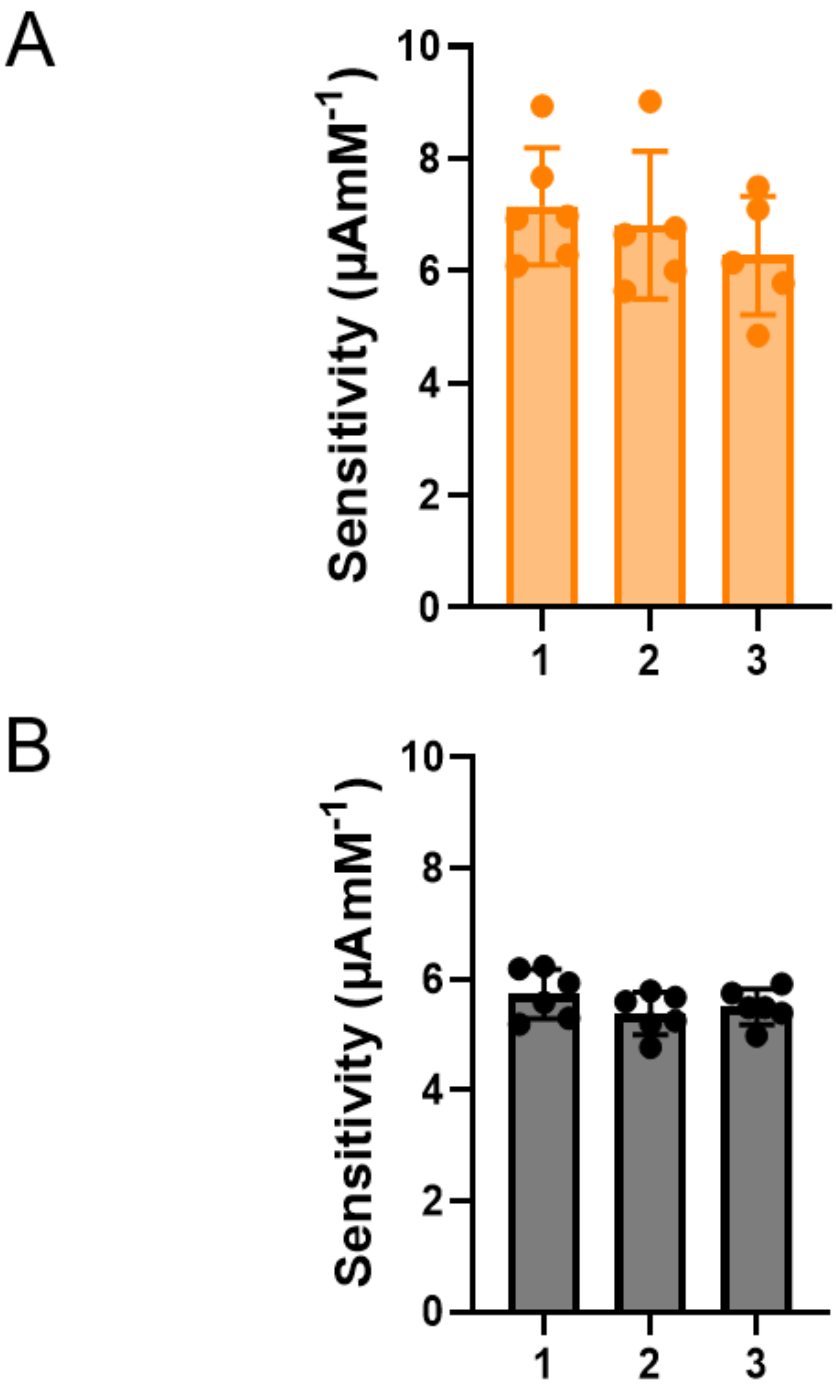

Figure 2.10.
Batch variability for PdB and PtB composite electrodes determined by sensitivity to peroxide from amperometric calibrations in stirred 0.1 M PBS at + 0.85 V vs Ag|AgCl. (A) Consecutive batches of PdB electrodes. (B) Consecutive batches of PtB electrodes. Data shown as mean ± SD *n* = *5* and *n* = *6* respectively. No significant difference between batches found using one-way ANOVA with Tukey multiple comparisons test.

Despite the same fabrication the data shows higher variation for the PdB composite electrodes compared to the PtB composite electrodes. Considering that the addition of a biosensing layer will add further variation to the sensor this supports the PtB electrodes being more suitable for analytical measurement. Despite the PdB electrodes having marginally higher sensitivity they may be unsuitable for detecting slight differences in concentrations and less useful for clinical measurements.

2.6.2 Comparison between of the performance of in glucose biosensors

Glucose oxidase is cheap and reliable oxidase enzyme perfectly suited for testing the incorporation of the enzyme. Composite sensors of PdB and PtB were adapted into glucose biosensors as described in section 2.5.3. Electrochemical performance with glucose was determined through amperometric calibrations at +0.85 V in 0.1 M PBS under stirred conditions.

a) Linear range and sensitivity

shows representative traces for the two biosensors, highlighting excellent range and sensitivity for both electrodes. Figure 2.11B shows the responses of a batch of glucose biosensors fitted with a Michaelis-Menten kinetic equation using graphpad prism 9. Statistical analysis was also use on the two batches showing a statistical increase in response with the palladium biosensor, compared to the platinum black biosensor. Enzymatic biosensors are often compared with parameters such as Km and Vmax, where Km is the concentration at which half of Vmax is achieved, and where Vmax is the saturation reaction rate. The PdB sensor had a Vmax of 1.64 µA and a Km of 7.23 mM, whilst PtB was calculated to have a Vmax of 1.38 µA and a Km of 10.1 mM. This indicates that the PdB sensor had a higher maximum rate compared to PtB, and its lower Km indicates a steeper curve where more activity is had with less substrate.

The calibrations show that a linear range can be forced on the data points with an r^2 above 0.9 for concentrations up to 10 mM (C). This gives a rough sensitivity of 0.103 µA mM^{-1} for the PdB sensor and 0.073 µA mM^{-1} for the PtB sensor.

A balance between sensitivity and linear range is important, as shown by other sensors fabricated for blood glucose measurements. Based off these examples our biosensor covers a similar linear range with a useable sensitivity for biological measurements.

Electrode	Sensitivity (μA mM^{-1})	Limit of detection (μM)	Linear range (mM)	Work
Graphene/AuNPs/GOD/chit	99.5*	180	0.2–4.2	Niu et al 2010
BPEI-Fc/PEDOT:PSS/GOx/SPCE	66*	NA	0.5–4.5	Ho et al 2013
GCE/Chi-Py/Au/GOx	0.58	68	1.0–20	Senel 2015
GOX-PoPD/PtNPs/PVF+Cl_{O4}-/Pt	17.4*	18	0.06–9.64	Yildiz et al 2014
GOD/TCT/AP/OMC/GCE	0.38	38	0.1–1.0	Farzin et al 2015
Nafion/GOD–OMCs/GE	0.053	156	0.5–15	Dong et al 2008
GR/PANI/GOx	0.92		1-25	Ramanaviciene et al 2021
Cu/Pd/PPD-GOx	4.46		0-6	
This work	**0.073**	**92.9**	**0.15-10**	**This work**

The fabrication method for the biosensor highlights low variability, considering other enzymatic biosensors have much more variable response due enzyme orientation, crosslinking, leaching, denaturing. The variation is well within the limits for commercial enzymatic biosensors.

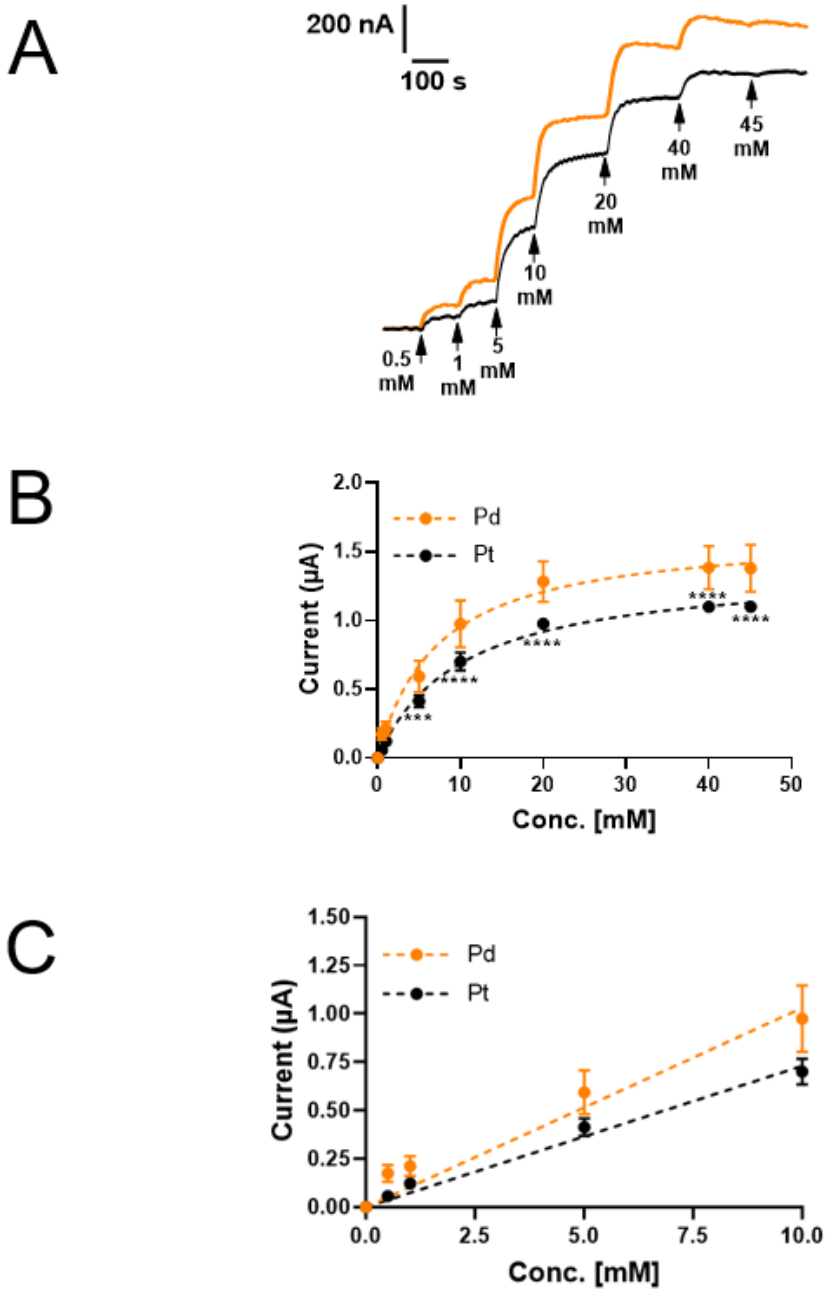

Figure 2.11.
Amperometric responses to cumulative concentrations of glucose on PdB and PtB MWCNT in stirred 0.1 M PBS pH 7.2. All measurements carried out at +0.85 V vs Ag|AgCl, *n* = 6. (A) Representative traces for PdB and PtB composites with crosslinked glucose oxidase. (B) Calibration of the responses shown as mean ± SD. (C) Linear range applied to glucose responses shown as mean ± SD.

b) Biosensor response time

An important parameter that can be extracted from the calibrations is the biosensor response time. This is useful information as the speed at which a concentration is determined can limit the use case of the sensor. As electrochemical biosensors acquire data continuously, they pull ahead of lab based biochemical techniques that take time and processing to provide a single snapshot of the concentration. However, if the dynamic concentration change occurs faster than the biosensor response time it cannot be used for that purpose.

To compare the response times of the glucose biosensors, the rise time for both was calculated at 10 mM using the time interval for the response to go from 25% to 75% of the total response. This would give an indication of the rate of reaction of glucose oxidase on the two different sensors, with minimal impact from the noise at baseline and max response.

Figure 2.12A shows a response for the PdB biosensor whilst Figure 2.12B shows that of a PtB biosensor. When analysed the PdB mean rise time was significantly faster ($p < 0.01$) than the PtB biosensors, as shown in Figure 2.12C.

Both biosensors have a rise time sufficiently fast for our use.

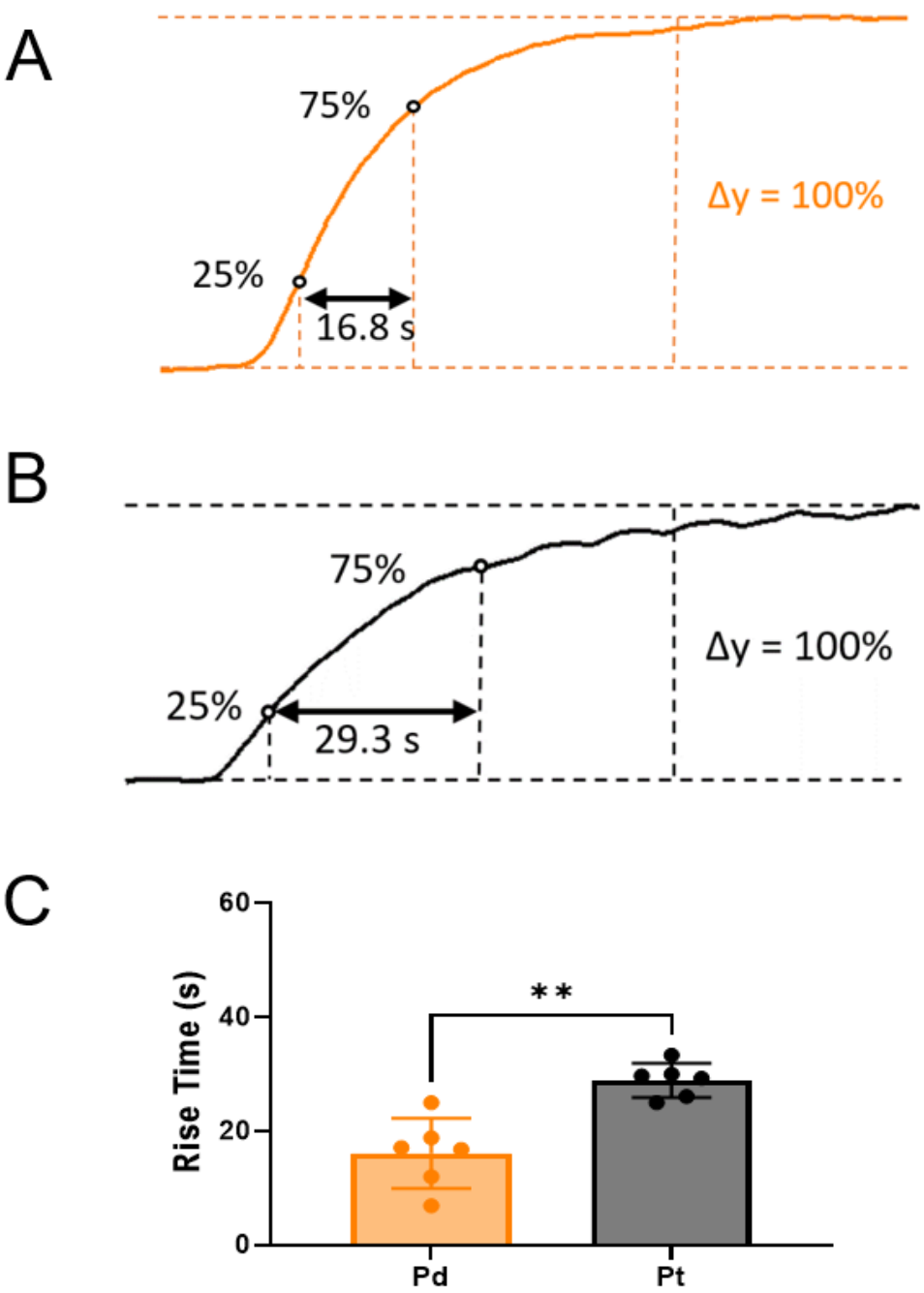

Figure 2.12.
Amperometric responses to cumulative concentrations of glucose on PdB and PtB MWCNT in stirred 0.1 M PBS pH 7.2. All measurements carried out at +0.85 V vs Ag|AgCl. (A) Representative trace for PdB biosensor. (B) Representative trace for PtB biosensor. Rise time shown as mean ± SD, *n* = 6.

As both batches used the same glucose oxidase layer fabrication method it is unlikely that the difference in rise time is due to this. To rule out that the difference is due to the electrocatalyst, analysis of the rise time with the peroxide calibrations could be performed. The fact that the peroxide responses are fast and visibly appear the same for both sensors indicate that the enzymatic layer is slowing down the responses to where one appears faster. This suggests that response time can be reduced by optimising the enzymatic layer. The enzymes within the layer are randomly oriented and rely on diffusion of the analyte across the layer to produce peroxide, therefore a thinner layer could reduce response time. Components within the layer would also affect diffusion, so an optimum amount of protein and enzyme within the layer could be established, as high amounts of protein would hinder diffusion, and low amounts of enzyme would reduce signal. Diminishing the amount of crosslinking would allow more enzyme to interact with the analyte, but at the cost of a less robust sensor.

Optimisation of the components in the enzyme layer is difficult due to the large variability within a batch of biosensors. This in conjunction with multiple components having a positive or negative impact depending on how they interplay makes optimisation a costly endeavour. For our use, optimisation would need to be undertaken with the enzymes required for our measurement, thus the current fabrication method is sufficiently reliable.

c) Biosensor stability

Biosensor stability is an important property for a sensor to be viable for commercial and research purposes. It is essential that all biosensors remain stable over the course of a measurement so that any changes in signal can be attributed to changes in analyte concentration and not sensor deterioration. Long term stability during storage is key for commercial sensors as to guarantee end user confidence in the data they collect. Stability during storage is also useful in research as it allows batches of sensors to be produced then used in timeframes that suite the researcher and sample collection.

To test stability a batch of each glucose biosensors were subjected to a glucose calibration on the day of their fabrication and every ten days thereafter. Whilst not in use the sensors were stored at 4°C in 0.1 M PBS, and subsequently brought to temperature prior to use. Figure 2.13A shows the calibrations of a representative PdB biosensor over time, with Figure 2.13B showing traces for a representative PtB biosensor. Despite fluctuations in individual biosensor response both PdB and PtB biosensors show no significant decrease in response over time. This is highlighted in Figure 2.13C where the Vmax was plotted as a percentage of day one response.

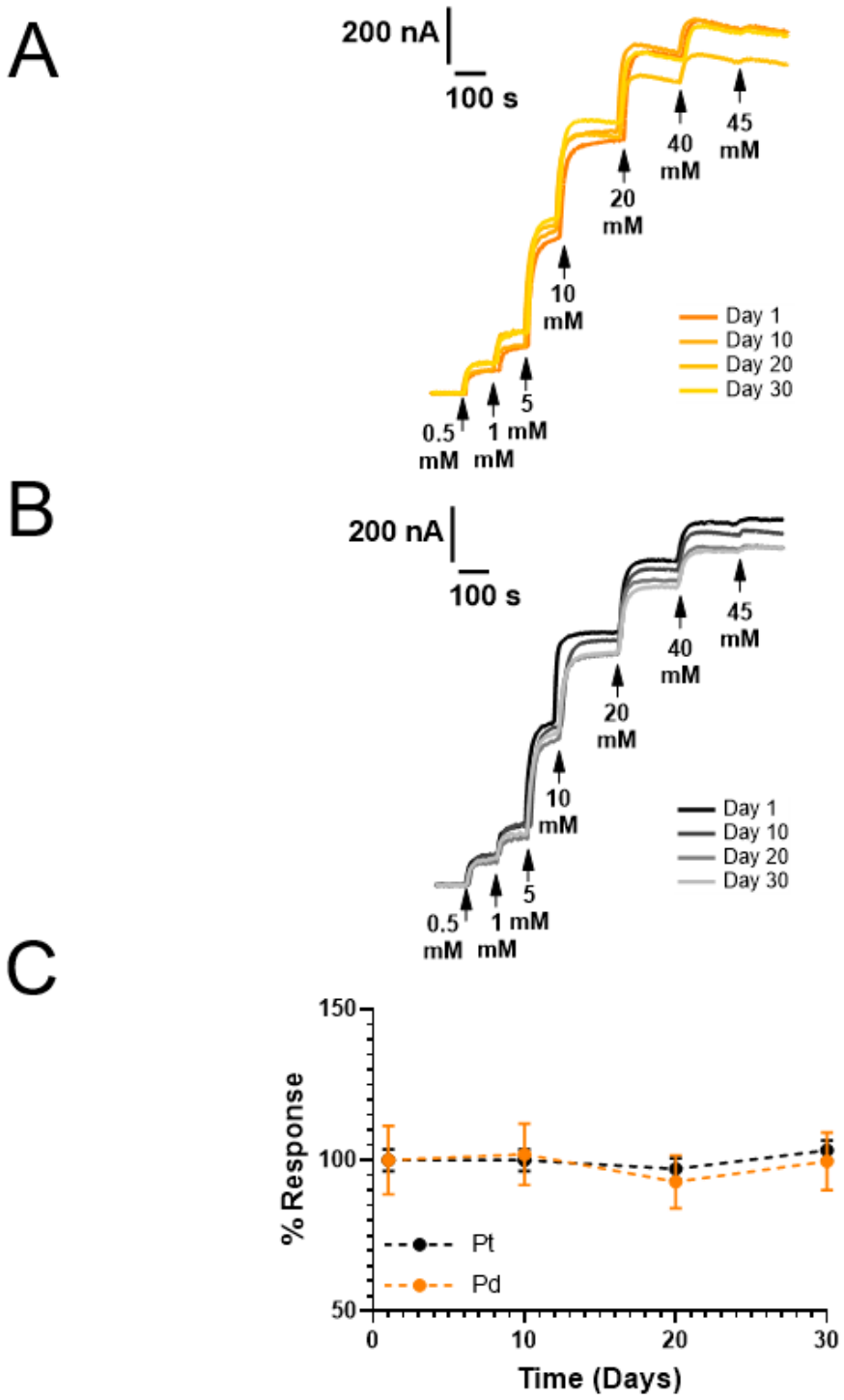

Figure 2.13.
Stability of PdB and PtB glucose biosensors evaluated by responses to glucose in stirred 0.1 M PBS pH 7.2. All measurements carried out at +0.85 V vs Ag|AgCl, *n* = 6. (A) Representative traces for a PdB glucose biosensor over time. (B) Representative traces for a PtB glucose biosensor over time. (C) Stability data for both batches of biosensors as a percentage of day 1 response.

The exceptional stability of both types of composite biosensors confirms the integrity of both the composite electrode and the enzymatic layer. The simplicity of the biosensor design reduces the points of failure that would usually compromise a biosensor over time. Methods of incorporating materials on an electrode surface often result in a sensitive yet fragile sensor often unfit for *in-vitro* and *in-vivo* measurement. Therefore our method of incorporating the electrocatalyst throughout the composite is proven to be a stable way of embedding it onto the electrode surface.

The enzymatic layer adhered well to the electrode surface, without any visible deterioration over time. The lack of any decrease in signal indicates that the entrapped enzyme does not leach out from the adhered layer. Although the data highlights that both biosensors can be used repeatedly, this would need further validation in biological samples due to the issues caused by biological and chemical fouling.

2.7 Conclusion

The data supports our method for producing a stable composite electrode with enhanced sensitivity to peroxide through the use of an electrocatalyst. The data suggests that for low intra-batch variation sensors with PtB are preferred to PdB despite the latter being marginally more sensitive. Furthermore, sensitivity is less of an issue as the PtB sensors show a tighter linear range which will need optimisation with our enzymes of interest. Both biosensors exhibited temporal resolution adequate for clinical measurements as well as excellent stability for storage.

This method of biosensor fabrication is perfect to optimise with enzymes related to ATP and ACh as to measure metabolites in urine.

Chapter 3: Biosensing of urinary metabolites related to overactive bladder

3.1 Introduction

Within the bladder urothelium, ATP, ACh and NO are key signalling molecules (as highlighted in Chapter 1). These signalling molecules play a key role in function of the bladder and thus changes in these molecules can have a significant impact with disease. However, when these molecules are released, they are metabolised and released in urine. Therefore, for conducting urinary analysis of these key signalling molecules, the breakdown products of ATP, ACh and NO are most suitable for measurement. ATP is broken down via many steps eventually to xanthine, ACh is broken down to choline and NO is broken down to nitrite. Therefore, development of electrochemical biosensors for the detection of xanthine, choline and nitrite provides a means of indirectly measuring key urothelium signalling molecules in a non-invasive fashion.

3.1.1 Electrochemical detection of choline

d) Direct detection approaches

Third generation biosensors offer high selectivity and low operating voltage due to the electron transfer occurring directly between the enzyme's redox centre and the electrode surface. Despite the production of third generation glucose sensors (Rahman *et al.*, 2010; Lee *et al.*, 2019; Jeon *et al.*, 2022) there are no direct choline biosensors in the literature. Choline itself is not electroactive as it cannot readily be oxidised or reduced at moderate potentials at physiological pH with known electrode materials. There are some non-enzymatic acetylcholine sensors that use metals such as copper (Balasubramanian *et al.*, 2019) or nickel (Sattarahmady, Heli and Vais, 2013) that may be able to detect choline due to the similar molecular structure, but this has not yet been explored. However, even if these electrodes were able to detect choline, they do have issues with stability, wearing out quickly with limited service life (Gu and Wang, 2021).

e) Choline biosensors

Unlike third-generation choline biosensors, there are many first- and second- generation biosensors that have been developed (Rahimi and Joseph, 2019). This is often in service of producing an acetylcholine sensor for *in-vivo* detection (Baker, Bolger and Lowry, 2015, 2017; Teles-Grilo Ruivo *et al.*, 2017). Acetylcholine biosensors require two enzymatic steps to produce the electroactive product peroxide, and therefore require an enzymatic choline sensor to take background choline measurements which are subtracted from the sensor containing both enzymes to obtain an accurate acetylcholine concentration.

The simplest biosensor for the detection of choline can be constructed using only one enzyme to generate electroactive peroxide (Ahlawat, Sharma and Shekhar Pundir, 2023).

$$\boldsymbol{Choline + 2O_2 + H_2O \xrightarrow{ChO} Betaine + 2H_2O_2} \quad (4)$$

As shown above choline oxidase (ChOx) catalyses choline to produce betaine and peroxide. Provided that the reaction is not limited by either enzyme or substrate, the concentration of peroxide detected will be proportional to the concentration of choline. Peroxide can be detected amperometrically at carbon (Amatore *et al.*, 2008; Fagan-Murphy *et al.*, 2016) or metal electrodes (Patel *et al.*, 2011; Li *et al.*, 2013; Qi *et al.*, 2022) from +0.248 V and 0.75 V (vs Ag|AgCl). As ChOx has a high activity, substrate catalysis quickly reaches steady state producing a stable signal. Selectivity therefore is an issue at the electrode surface where high potentials can oxidise other molecules from the matrix as well as peroxide. This can be minimised by tailoring the surface to peroxide detection, or by facilitating electron transfer to the electrode surface (Watson, 2016). Addition of layers to the electrode decreases response time consequently increasing wait time and impacting the relationships that can be established between analyte and physiology. Instead of increasing the complexity and adding points of failure to the biosensor, a simpler method is to run another electrode in parallel at the same voltage to oxidise all faradaic components in the matrix and subtracting it from the biosensor.

Of the choline biosensors developed, few have made it into *in-vivo* detection. The most notable is that made by Baker *et al.*, developed for the measurement of real-time changes in striatal extracellular choline (Baker, Bolger and Lowry, 2017). The electrode consisted of a platinum/iridium disc with poly(o-phenylenediamine) (PPD)

electrochemically grown on the electrode surface prior to dip absorption of various polymer layers. PPD is a permselective layer commonly used to screen out analytes such as ascorbic acid and dopamine for *in-vivo* monitoring yet still permeable to H_2O_2 making it suitable for first generation biosensors (Hamdi, Wang and Monbouquette, 2005). Other layers included glutaraldehyde (GA), bovine serum albumin (BSA) and polyethyleneimine (PEI) at varying concentrations as to enhance sensitivity and stability without compromising response time. The data collected *in-vivo* (Teles-Grilo Ruivo *et al.*, 2017) confirms the biosensor is fit for this purpose, but their fabrication time of three days as well as the use of a platinum electrode is expensive and unfit for a cheap point of care device (Baker, Bolger and Lowry, 2017).

In summary, due to the breakdown of acetylcholine to choline in urine, the detection of choline is likely to generate a larger signal that can be related to cholinergic bladder dysfunction. Therefore, the biosensor will be tailored for the detection of choline using Choline Oxidase (ChOx) immobilised on a composite electrode tailored to detect peroxide (Chapter 2). The biosensor will be characterised and optimised for the detection of choline in a urinary matrix.

3.1.2 Electrochemical detection of xanthine

The method selected to detect increased levels of ATP is through its breakdown metabolite xanthine. Purine levels are maintained by balancing *de novo* synthesis of inosine monophosphate (IMP) which is an energy intensive process, and the salvage pathway, which uses hypoxanthine and hypoxanthine-guanine phosphoribosyl transferase (HPRT) (Pedley and Benkovic, 2017). The rate-limiting enzyme of adenine nucleotide catabolism is AMP deaminase, and though most AMP is resynthesized to ATP, some enters the pathway of adenine nucleotide degradation (Yamamoto, Moriwaki and Takahashi, 2005)(Figure 3.1.)(Liu *et al.*, 2021).

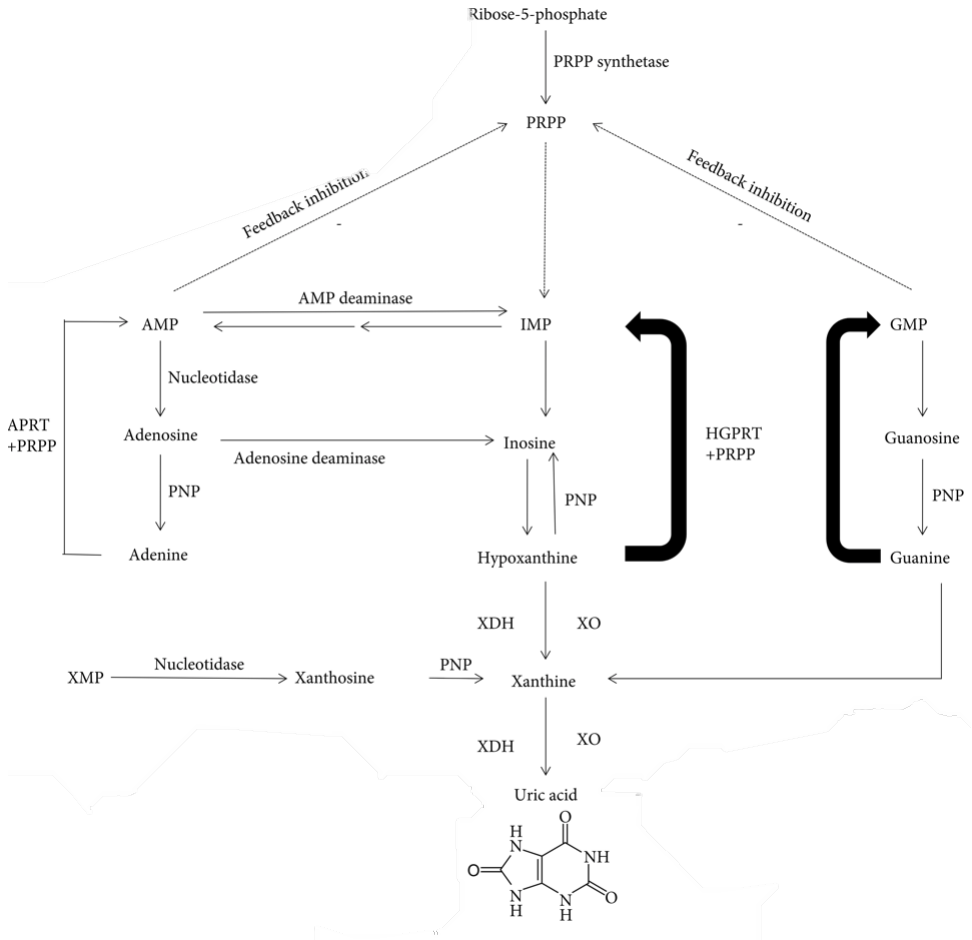

Figure 3.1.
Purine metabolism of adenosine monophosphate to uric acid. Liu *et al.*, 2021.

a) Direct detection approaches

Unlike choline there are a few electrodes that electrochemically detect xanthine (Dervisevic, Dervisevic and Şenel, 2019). As these do not employ the use of an enzyme, the electrode natively detects other electroactive components such as hypoxanthine and uric acid (Wang and Tong, 2010; Luo *et al.*, 2015; Zhu *et al.*, 2019). These types of electrode would not be fit for our purpose due to the levels of uric acid found in urine. Furthermore, the response of these electrodes has been shown to shift depending on pH, which would be an issue in a matrix such as urine (Zhu *et al.*, 2019).

Therefore, it would be preferable to employ the use of an electrode surface tailored for the electrochemical detection of peroxide and ensure selectivity through the use of xanthine oxidase.

b) Xanthine biosensors

Xanthine oxidase (XOD) catalyses xanthine to produce hydrogen peroxide and uric acid (below) (Pundir and Devi, 2014).

$$\boldsymbol{Xanthine + O_2 + H_2O \xrightarrow{Xanthine\ Oxidase} Uric\ acid + H_2O_2} \quad (5)$$
$$\boldsymbol{H_2O_2 \xrightarrow{V\ vs\ (Ag/AgCl)} 2H^+ + O_2 + 2e^-}$$

Some biosensors use xanthine dehydrogenase (XDH) in place of XOD, but then require a mediator to shuttle the electron to the electrode surface (Kalimuthu, Leimkühler and Bernhardt, 2012). As with glucose biosensors the key difference in biosensors is the electrode material and the entrapment of XOD onto the electrode surface. The main compromise being the stability of the enzyme on the electrode surface and the sensitivity and response time of the biosensor. This is because the film used or entrapment method affects enzyme orientation and active site availability. The xanthine biosensors in the

literature are usually developed as to detect xanthine in meat or fish as a measure of freshness measuring xanthine concentration in the micromolar range (Dervisevic *et al.*, 2016; Dervisevic, Dervisevic, Çevik, *et al.*, 2017; Dervisevic, Dervisevic, Senel, *et al.*, 2017).

3.1.3 Electrochemical detection of nitrite

a) Direct detection

Nitrite is found in blood plasma and urine, and is now thought to be a storage of NO due to the ability for it to be reduced at cardiac tissues (Webb *et al.*, 2004) through mammalian nitrite reductases (Kapil *et al.*, 2020).

Nitrite is often detected using Griess reagent and spectrophotometry (Griess, 1879). This method is the most common due to its low detection limit, simple protocols, and use of standard scientific equipment (Iverson, Hofferber and Stapleton, 2018; Gill, Zajda and Meyerhoff, 2019). However, this method suffers from interference from antioxidants and as well as coloured compounds found in the biological matrix (Gill, Zajda and Meyerhoff, 2019). Another method of determining changes in NO concentration is by measuring nitric oxide synthase (NOS) activity. There are three different forms of the enzyme based on their location; endothelial, inducible, and neuronal (eNOS, iNOS and nNOS respectively). Their presence can be detected with immunohistochemistry (Vizzard, Erdman and de Groat, 1996) but levels between cells have high variation making comparisons difficult (Winder *et al.*, 2014).

Nitrite is electrochemically detected at carbon and metal electrodes according to the oxidation equation (below) (Kozub, Rees and Compton, 2010).

$$\boldsymbol{NO_2^- - e^- \rightarrow NO_2} \quad (6)$$

Unlike NO, nitrite calibrations can be easily generated due to the stability of the molecule and the facility of its detection. It also provides the fastest response time and can be used in complex biological matrix. Even though carbon electrodes can detect both nitrite and NO at similar voltages, the half-life of nitric oxide makes it unlikely to be present in a

urinary matrix. However, for *in-vivo* detection a Nafion coating can be used to exclude nitrite (Bedioui and Griveau, 2013). Nafion is a sulfonated tetrafluoroethylene polymer that acts as a perm-selective film which prevents large biological molecules from reaching the electrode surface, thus increasing selectivity (Navera *et al.*, 1993; Kang, Park and Ha, 2019).

3.1.4 Electrochemical advantages of measuring from urinary matrix

The main advantage of measuring urinary metabolites is the non-invasive nature of collection. Provided that the metabolites relate to the signalling molecules being measured and functional data, the use of these metabolites could be explored for a diagnostic purpose.

The electrochemical measurement of metabolites is advantageous as it can be done cheaply and quickly. Due to the low cost of electrode production it can be tailored to the analyte and validated so that interferences are either known or minimised. Tailoring the surface allows the lowest voltage to be used so that other electroactive interferences are unlikely to be oxidised.

If a high voltage is required for detection, a second electrode can be poised at a lower voltage that doesn't oxidise the analyte. In the case of urine, uric acid is a known interferent that oxidises on carbon electrodes at around 0.30 V (vs Ag|AgCl) (Ren, Luo and Li, 2006; Hu *et al.*, 2008; Thiagarajan, Tsai and Chen, 2009). One electrode can be held at a voltage above that required for the detection of nitrite, and another can be held at a voltage above that required to fully oxidise uric acid (and other interferences) but below the oxidation of nitrite. This allows for a simple subtraction of the smaller current from the larger current to isolate the nitrite component (Li *et al.*, 2014).

3.1.5 Aims and objectives

The aim of this chapter is to develop electrochemical sensor suitable for the detection of choline, xanthine, and nitrite in urine

The following objectives will be met to reach this aim:

1. Develop simple and robust fabrication methods for the development of xanthine, choline and nitrite electrochemical sensors.
2. To characterise the performance of the electrochemical sensors for detection of analytes within artificial urine.

3.2 Experimental

3.2.1 Composite electrode fabrication

Electrodes were fabricated as previously described in Chapter 2. Electrode casings were designed using SolidWorks (SOLID Applications Ltd.) to produce a cylindrical casing with a 2.0 mm diameter and 1.1 mm recess to produce a flat disc electrode. The design was sliced using Simplify 3DA coiled wire of 30 awg steel plated copper (R.S components Ltd.) was fed into the casing onto which composite material could be packed.

Composite electrodes consisted of 10% platinum black (PtB) dispersed in 15% w/w multi-walled carbon nanotubes (MWCNTs, 30-50 nm inner diameter 60 m^2/g, Cheap Tubes Inc., VT, USA) were mixed with epoxy resin (Robnor Resin Ltd, Swindon, UK). Composite paste was packed into the recess and after curing for 48 hours was sanded for at least 20 cycles with P400 silicon carbide in figures of eight.

3.2.2 Fabrication of choline biosensors

To produce a batch of eight biosensors 1 mg of 10 unit choline oxidase (ChOx) was dispersed in 100 µL 0.01 M PBS, followed by 10% w/v BSA. The enzyme solution was mixed with 2% glutaraldehyde (Grade II, 25% in H_2O) and 10 µL was rapidly pipetted onto the electrode surface. Biosensors were left to crosslink for 2 hours at 4 °C and then stored in 0.1 M PBS in the fridge until required.

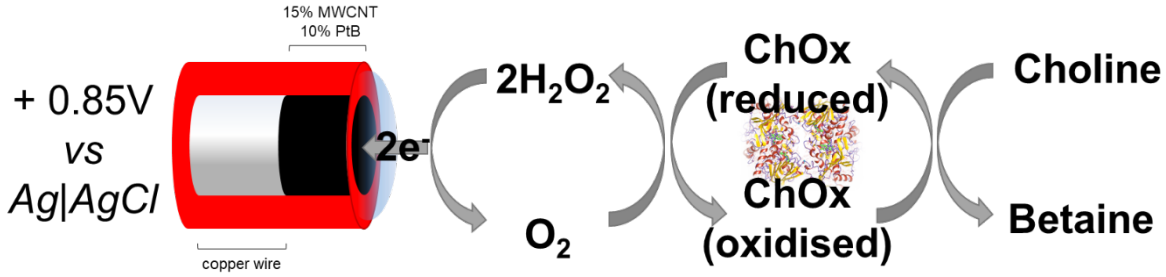

Figure 3.2.
Diagram of choline biosensor.

3.2.3 Fabrication of xanthine biosensors

To produce a batch of eight biosensors 1 mg of 10 unit xanthine oxidase (XOD) was dispersed in 100 µL 0.01 M PBS, followed by 10% w/v BSA. The enzyme solution was mixed with 2% glutaraldehyde (Grade II, 25% in H_2O) and 10 µL was rapidly pipetted onto the electrode surface. Biosensors were left to crosslink for 2 hours at 4 °C and then stored in 0.1 M PBS in the fridge until required.

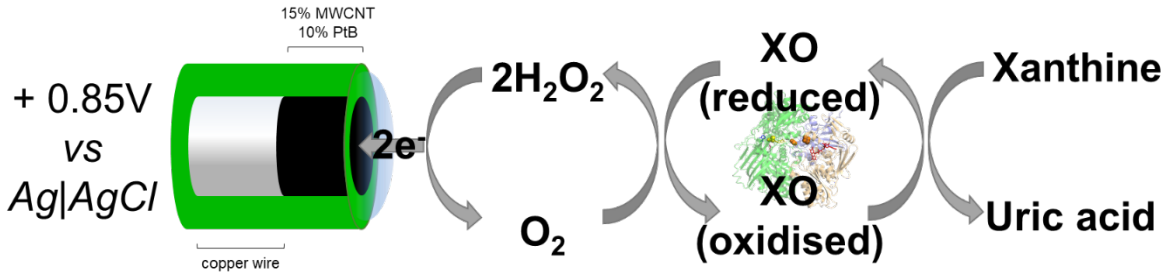

Figure 3.3.
Diagram of xanthine biosensor.

3.2.4 Fabrication of null sensors for background subtraction and nitrite detection

Fabrication of the null sensors was identical to that of both biosensors apart from omitting dispersion of an enzyme in the protein layer. The electrode surface was coated with 10 µL of 10% BSA in 0.01 PBS with 2% glutaraldehyde to crosslink at 4 °C for a minimum of 2 hours.

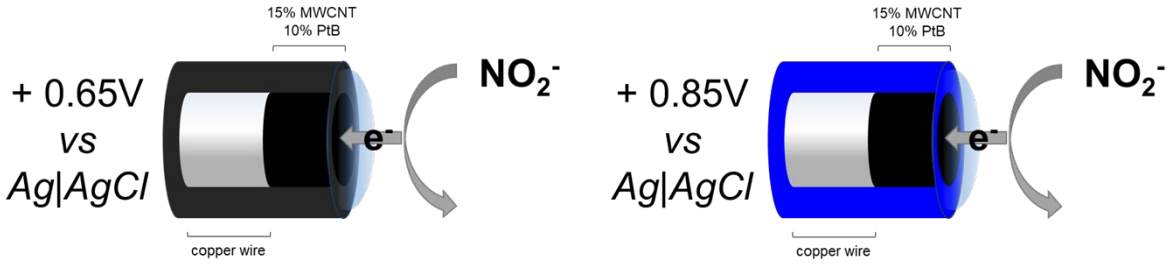

Figure 3.4.
Diagram for background sensor (left) and nitrite/null sensor (right).

3.2.5 Biosensor characterisation

Biosensor activity was explored using amperometric calibrations in stirred 0.1 M PBS, pH 7.2.

Investigations in artificial urine were performed under stirred conditions at pH 6.0. Composition of artificial urine consists of 7.5 mM $CaCl_2.2H_2O$, 50 mM NaCl, 16 mM Na_2SO_4, 10 mM KH_2PO_4, 21 mM KCl, 18 mM NH_4Cl, 415 mM urea, 10 mM creatinine (Griffith, Musher and Itin, 1976; Laube, Mohr and Hesse, 2001; Parra *et al.*, 2016).

Artificial urine with faradaic interferences contained 0.4 µM dopamine (El-Beqqali, Kussak and Abdel-Rehim, 2007), 100 µM adrenaline (Thomas *et al.*, 2006), 54 µM homovanilic acid (Lionetto *et al.*, 2008), 40 µM 5-HIAA (Sirén and Karjalainen, 1999), 100 µM noradrenaline (Thomas *et al.*, 2006), 6 µM peroxide (Yuen and Benzie, 2010), 0.4 µM serotonin (De Irazu *et al.*, 2001), 400 µM uric acid (Brooks and Keevil, 1997).

3.2.6 Statistical analysis

Data was exported to graphpad prism 9 for statistical analysis. Comparisons between calibrations were analysed using two-way ANOVA due to the two variables (concentration and either fabrication method, voltage, day etc.). Multiple comparisons were used to compare between means at different concentrations, using appropriate correction depending on whether the same electrodes were used (Bonferoni or Šídák) or not (Tukey's).

3.3 Results and discussion

3.3.1 Optimisation and characterisation of xanthine biosensor

a) Optimisation of glutaraldehyde concentration

Maximising the sensitivity and stability of the biosensor is important as the ability to store and use the sensor when required ensures it can be used in the lab and as a consumer product. The sensitivity and stability of the sensor depend on the method used to immobilise the enzyme on the electrode surface and its optimisation. The chosen method of immobilisation is the entrapment of the enzyme within a protein matrix (bovine serum albumin) which is crosslinked with glutaraldehyde (GA). Optimisation of the proportion of BSA, GA and XOD affect the sensor's performance and stability (Pravda *et al.*, 1995). Insufficient GA results in less crosslinking and loss of enzyme from the matrix, whilst excess GA can result in crosslinking to the enzyme active site and reduce activity of the biosensor (Migneault *et al.*, 2004). Therefore the effect of the concentration of glutaraldehyde on biosensor sensitivity was tested. This was done by producing batches of xanthine biosensors using different quantities of glutaraldehyde.

Figure 3.5A shows representative traces for biosensors made with concentrations 0.5%, 1%, and 2.0% of glutaraldehyde respectively. Figure 3.5B shows the mean response for each batch of biosensors ($n = 5$, $n = 8$, $n = 6$ respectively) plotted with standard deviations.

Analysis using a two-way ANOVA with multiple comparisons and Tukey correction show a significant increase for 2% GA above 100 µM concentrations against both other GA concentrations.

The concentration of glutaraldehyde has a huge impact on the speed at which the BSA layer sets, consequently affecting the number of electrodes that can be produced from a batch of 100µL of XOD solution. Furthermore, glutaraldehyde concentration affects the amount of cross-linking that occurs between the enzyme and the BSA. If the concentration is too low there is not enough cross-linking resulting in reduced response. The amount of cross-linking also affects porosity of the film and number of available enzyme active sites (Migneault *et al.*, 2004). This suggests that the ratio of enzyme to BSA is as important as the concentration of glutaraldehyde, as a higher BSA to enzyme ratio would reduce the amount of enzymatic cross-linking whilst still allowing sufficient adhesion (Pravda *et al.*, 1995).

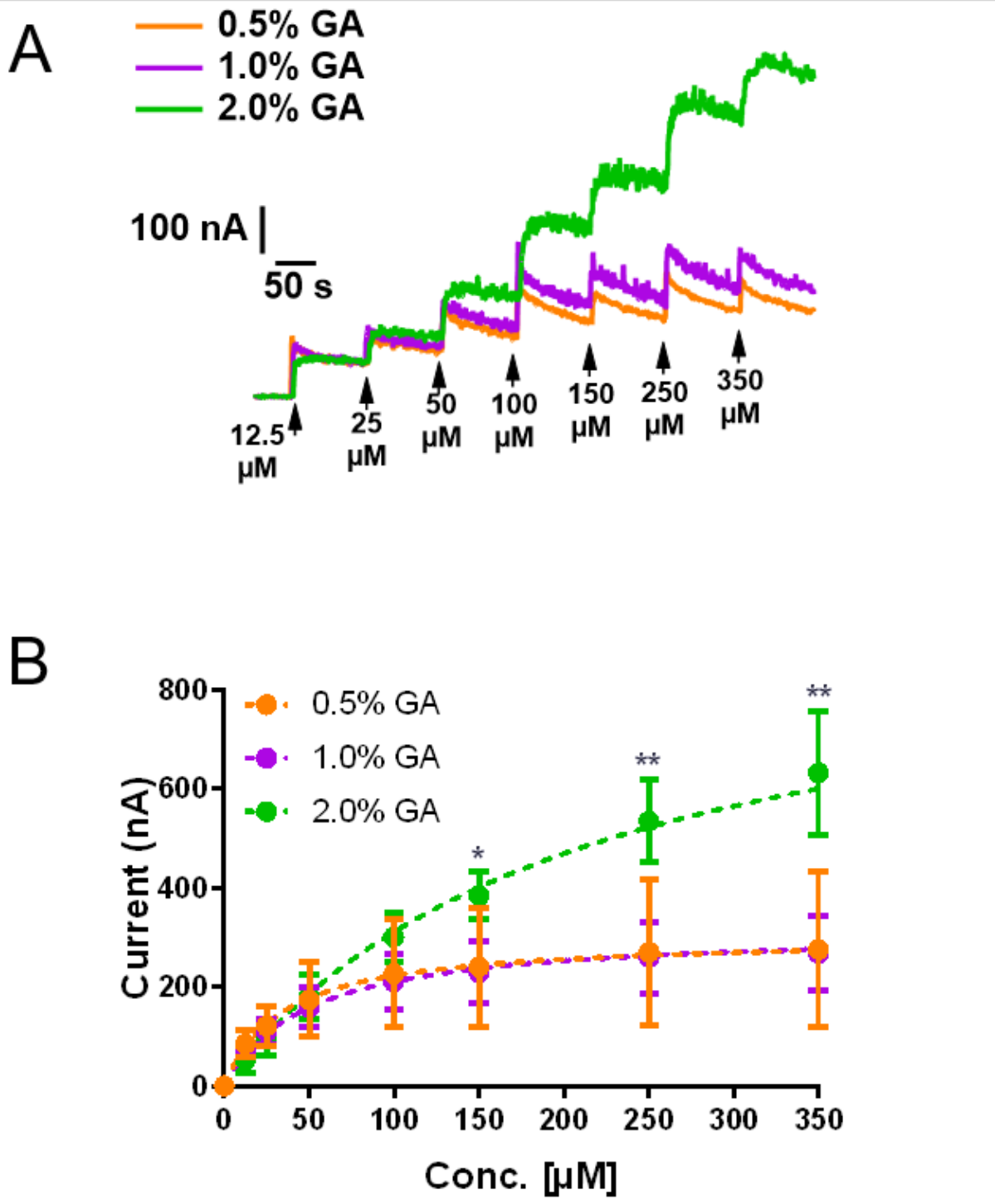

Figure 3.5.
Amperometric calibrations for xanthine biosensors affected by glutaraldehyde concentration. Batches containing 0.5% GA *n* = *5*, 1% GA *n* = *8*, 2% GA *n* = *6*. Measurements generated at +0.85 V vs Ag|AgCl in stirred 0.1 M PBS pH 7.2. (A) Representative trace for each glutaraldehyde concentration. (B) Mean response for each batch ± S.D. Statistical analysis performed using 2-way ANOVA with multiple comparisons and Tukey correction, * $p < 0.05$, ** $p < 0.001$.

b) Composite biosensor amperometric detection of xanthine

As the calibrations in Figure 3.5 showed that the batch of 2% GA xanthine biosensors had not saturated at 350 µM the concentration range was extended further. This was performed in artificial urine as to determine biosensor performance and sensitivity.

Figure 3.6A shows a representative trace for xanthine in artificial urine. Figure 3.6B shows the mean response for a batch of xanthine biosensors with standard deviation (*n* = *8*).

To calculate the limit of detection the standard deviation of the blank noise was used, the Michaelis-Menten equation was used to calculate this as a concentration, then multiplied by 3. This was 7.818 µM for the xanthine biosensors. This is comparable to most of the similar xanthine biosensors which have a detection limit between 0.8-6 µM (Dervisevic, Dervisevic, Çevik, *et al.*, 2017). The Vmax obtained was 518 µM, and the Km was 119.4 µM. Biosensor stability was the same as the glucose biosensor, showing no statistical decrease in response after over a month.

The extended calibration range shows that after an initial plateau another linear range can be obtained. This has not been seen in the literature as biosensors with similar constructions only show calibration ranges that reach 200 µM (Kalimuthu, Leimkühler and Bernhardt, 2012; Çevik, 2016; Dalkıran, Erden and Kılıç, 2016; Dervisevic, Dervisevic, Çevik, *et al.*, 2017). There could be various explanations for this behaviour. The composite electrode used does not detect xanthine natively at the electrode surface, suggesting that the behaviour is to do with the XOD film layer. As shown in the equation (below) the enzyme produces uric acid and peroxide which are both electroactive.

$$\boldsymbol{Xanthine + O_2 + H_2O \xrightarrow{Xanthine\ Oxidase} Uric\ acid + H_2O_2} \quad (7)$$

This should be advantageous as this means that the xanthine signal is amplified if the voltage is sufficient to oxidise both molecules. As both molecules are being produced in equimolar amounts there are other factors that could be affecting their detection. Once produced in the enzymatic film both molecules need to diffuse to the electrode surface for electron transfer to occur. It could be possible that the production of uric acid is affecting the stability of peroxide, such that it is unable to make it to the electrode surface.

Both of these seem unlikely as uric acid is biosensors that incorporate a scavenging enzymatic layer have not significantly reduced UA from reaching the electrode surface (Lielpetere *et al.*, 2023). There are been many biosensors produced for the detection of uric acid which use urate oxidase to catalyse uric acid into peroxide (below). If peroxide and uric acid affected each other these sensors would also exhibit the same interaction, and they do not (Aafria *et al.*, 2022).

$$\boldsymbol{UA + O_2 + H_2O \xrightarrow{Urate\ oxidase} Allantoin + H_2O_2 + CO_2} \quad (8)$$

To investigate this further differential pulse voltammetry can be performed to identify at what voltage uric acid and peroxide are being detected.

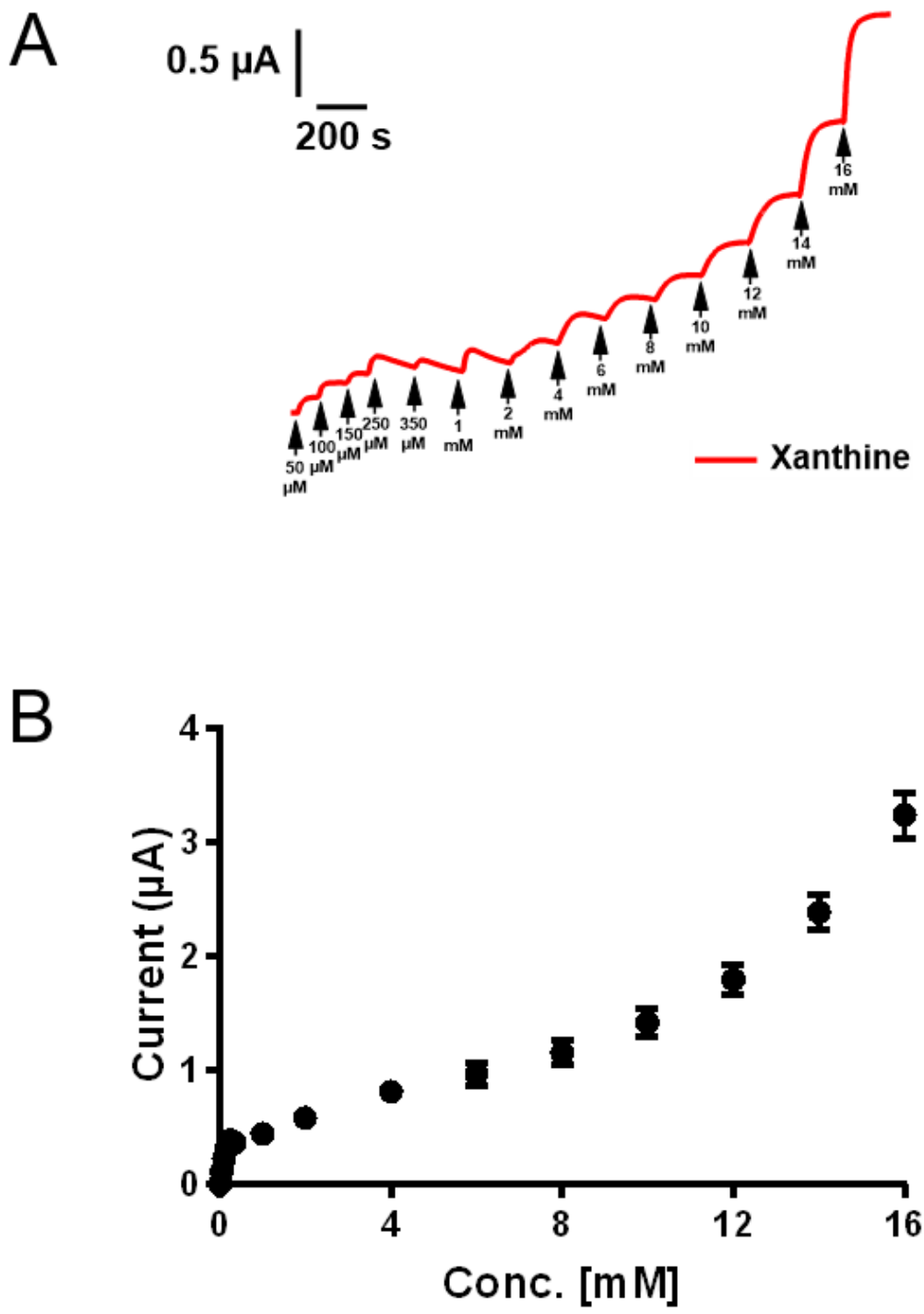

Figure 3.6.
Amperometric xanthine calibrations for xanthine biosensors. Measurements generated at +0.85 V vs Ag|AgCl in stirred artificial urine pH 6.0. (A) Representative trace for xanthine calibration. (B) Mean response for batch ± S.D. (*n* = *8*).

c) Detection of peroxide, uric acid, and xanthine using DPV

Differential pulse voltammetry allows the identification of different molecules based on their peak voltage. This would help determine if peroxide and uric acid were being detected at different amounts or at different voltages, resulting in the extended calibration curve.

Figure 3.7A shows the DPV performed at 0.35 mM and 4 mM of xanthine, in the middle and after a calibration. The reading at 0.35 mM shows a peak at +0.6 V, whilst 4 mM shows a peak at around +0.4 V. This is interesting as it shows how increasing the concentration has changed the detection at the electrode. To explore further DPV was performed on a high concentration of uric acid and peroxide.

Figure 3.7B shows a representative trace for analytes hydrogen peroxide, uric acid, and xanthine. The trace for peroxide displays a peak at just over +0.2 V which is in concordance with values in the literature (Li *et al.*, 2013; Fagan-Murphy *et al.*, 2016; Abdalla *et al.*, 2021). The peak for UA is also at around 0.3 V as seen on other carbon electrodes (Shi and Shiu, 2001; Li and Lin, 2006; Thiagarajan, Tsai and Chen, 2009).

This experiment shows that the peaks obtained from xanthine are not a clear combination of both uric acid and peroxide, and shift depending on concentration. This possibly suggests that the diffusion through the film layer could be affecting the detection of one of the analytes. As the peak at a higher voltage than both peroxide and uric acid this experiment is unable to determine which is being detected. This could be explored further by quenching either peroxide or UA mid measurement to see which one is being preferentially detected. This could be done through the addition of catalase or uricase into the solution, or the BSA film (O'Brien *et al.*, 2007; Zhang *et al.*, 2007).

Based off these results the biosensor will need to be held at +0.85 V as to ensure that the electrode detects the analyte produced at the electrode surface regardless of any shift in the peak. If the peak shifts to a lower voltage this will not affect the calibration data. The quantity of xanthine expected in human urine is in the micromolar range, and the biosensor should be able to detect this in its linear range (Boulieu *et al.*, 1983).

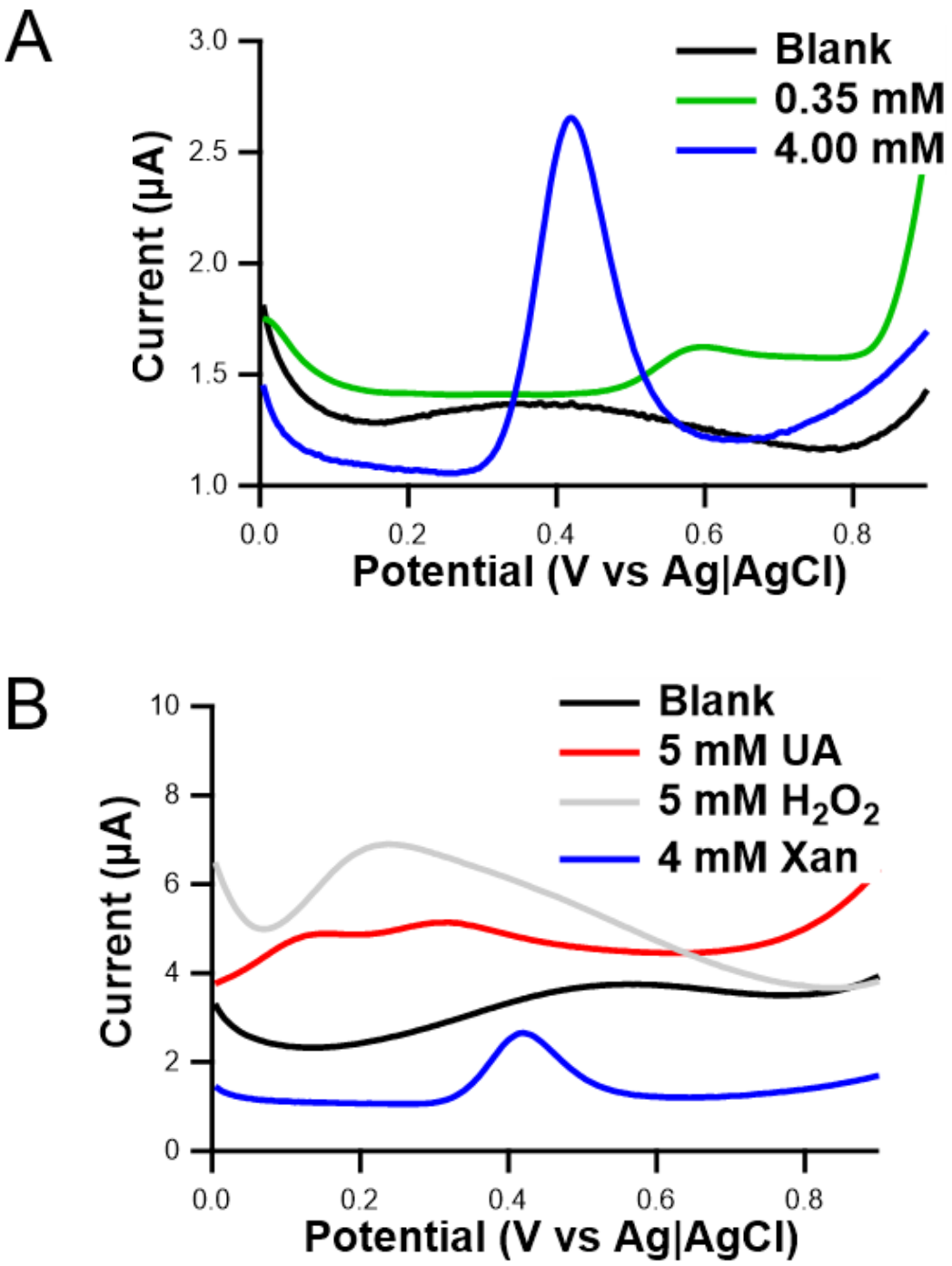

Figure 3.7.
Differential pulse voltammograms for electroactive molecules related to XO catalysis using xanthine biosensors. Measurements generated vs Ag|AgCl in artificial urine pH 6.0. (A) Responses for xanthine biosensor generated midway through xanthine calibration (0.35 mM) and at the end of the calibration (4 mM). (B) Representative traces for peroxide, uric acid and xanthine.

3.3.2 Optimisation and characterisation of choline biosensor

a) Effect of glutaraldehyde concentration

Similar to the xanthine biosensor, the effect of glutaraldehyde concentration on biosensor sensitivity was tested.

Figure 3.8A shows representative traces for biosensors fabricated with concentrations of 1%, 2% and 3% GA. The data is displayed in Figure 3.8B as the mean response for the batch of each GA concentration (1% GA $n = 4$, 2% GA $n = 7$, 3% GA $n = 5$) with error bars denoting standard deviation. Statistical analysis with a two-way ANOVA and Tukey's multiple comparisons correction shows no significant difference in GA concentration.

At this concentration range GA concentration did not impact enzyme activity and consequently biosensor sensitivity. This is likely due to the high intra-batch variation seen with biosensors due to random enzyme orientation (Sassolas, Blum and Leca-Bouvier, 2012). Potentially the effect of GA may be seen at higher choline concentrations where higher GA concentration may result in lower Vmax due to increased cross linking affecting the amount of functional enzyme. However, this was not investigated due to the physiological range of choline in biological samples expected to be in the micromolar range (Jin *et al.*, 2010; Kirsch *et al.*, 2010).

The concentration chosen for crosslinking was 2% due to the ease of fabrication compared to 3% which set too fast resulting in smaller batch sizes. Not only did this maximise the number of electrodes that could be fabricated per 100µL of enzymatic solution, but it would also allow the same null electrode to be used for both the choline and the xanthine biosensors. By using the same fabrication method for the null the background current at +0.85 V should be the same across all three sensors.

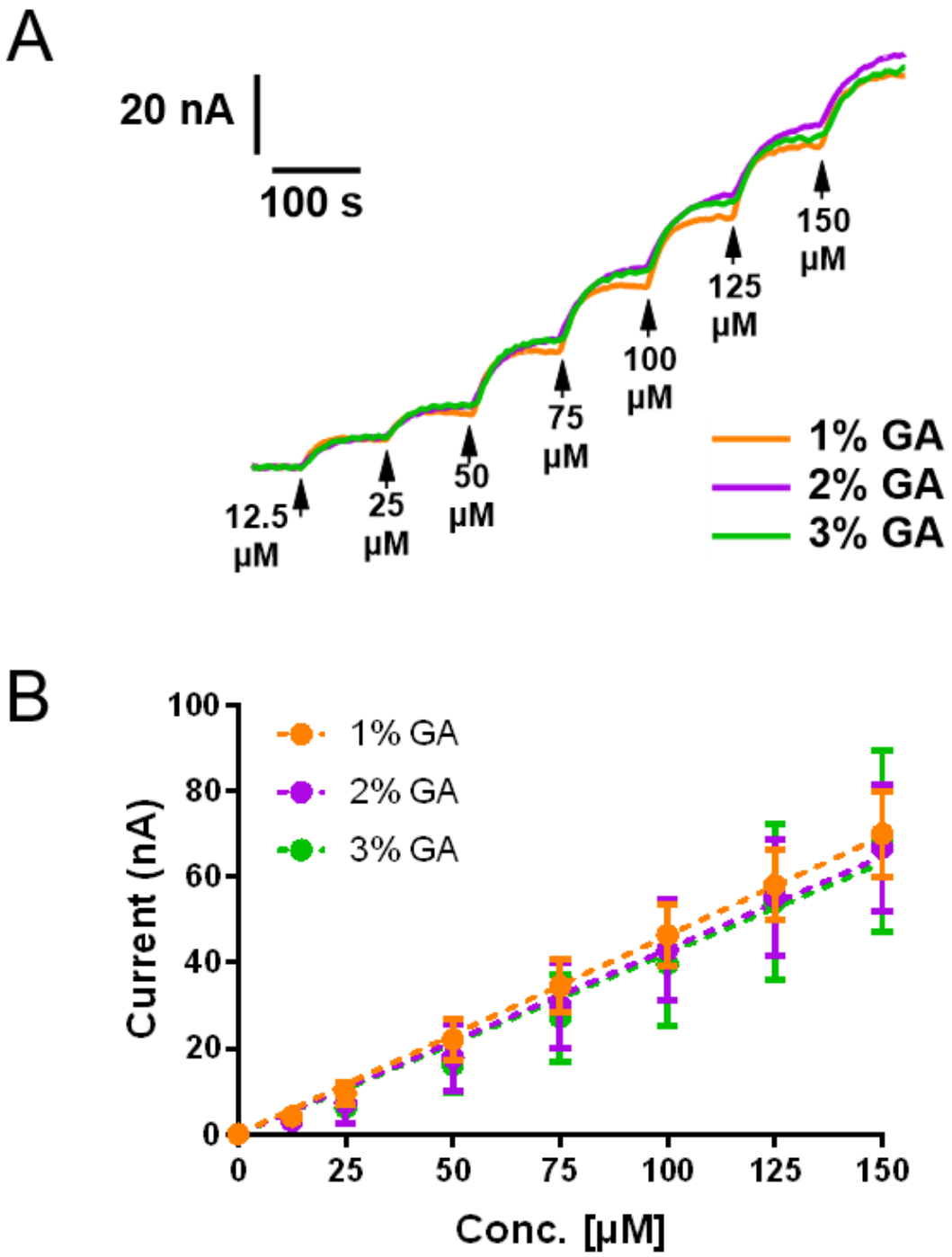

Figure 3.8.
Amperometric choline calibrations for choline biosensors fabricated with varying concentrations of glutaraldehyde (GA). Batches containing 1% GA *n* = *4*, 2% GA *n* = *7*, 3% GA *n* = *5*. Measurements generated at +0.85 V vs Ag|AgCl in stirred 0.1 M PBS pH 7.2. (A) Representative trace for each GA concentration. (B) Mean response for each batch ± S.D. analysed with two-way repeated measures ANOVA with Tukey's correction for multiple comparisons. Concentration of glutaraldehyde had no significant effect at any concentration ($p = 0.7637$).

b) Optimisation of applied voltage for detection

When measuring amperometrically in a complex matrix a lower voltage is usually preferred as the higher the voltage the higher the number of interferents that can be oxidised as well as the analyte. To investigate the effect of voltage a batch of choline biosensors was fabricated and subjected to choline calibrations at increasing voltages.

Figure 3.9A shows a representative trace for the batch of choline biosensors (n = 3) subject to choline calibrations at +0.20, +0.30 V, +0.60 V, and 0.85 V vs Ag|AgCl. Figure 3.9B shows the mean response at each voltage (n = *3*) with standard deviation.

Data was analysed using two-way ANOVA with multiple comparisons Statistical analysis reveals that there is no statistical difference between calibrations at +0.60 V compared to +0.85 V. There is a statistically significant decrease between +0.60 V (and 0.85 V) and +0.30 V and +0.20 V.

Even though +0.6 V gives a response equal to that of +0.85 V, +0.85 V was chosen for experiments. This would ensure maximum response when used in biological samples even if biosensors become subject to signal drift (Vadgama, Desai and Crump, 1991; Myszka, 1999). Furthermore, the use of the same voltage as that of the xanthine biosensor allows the same null sensor to be used to subtract from both biosensors.

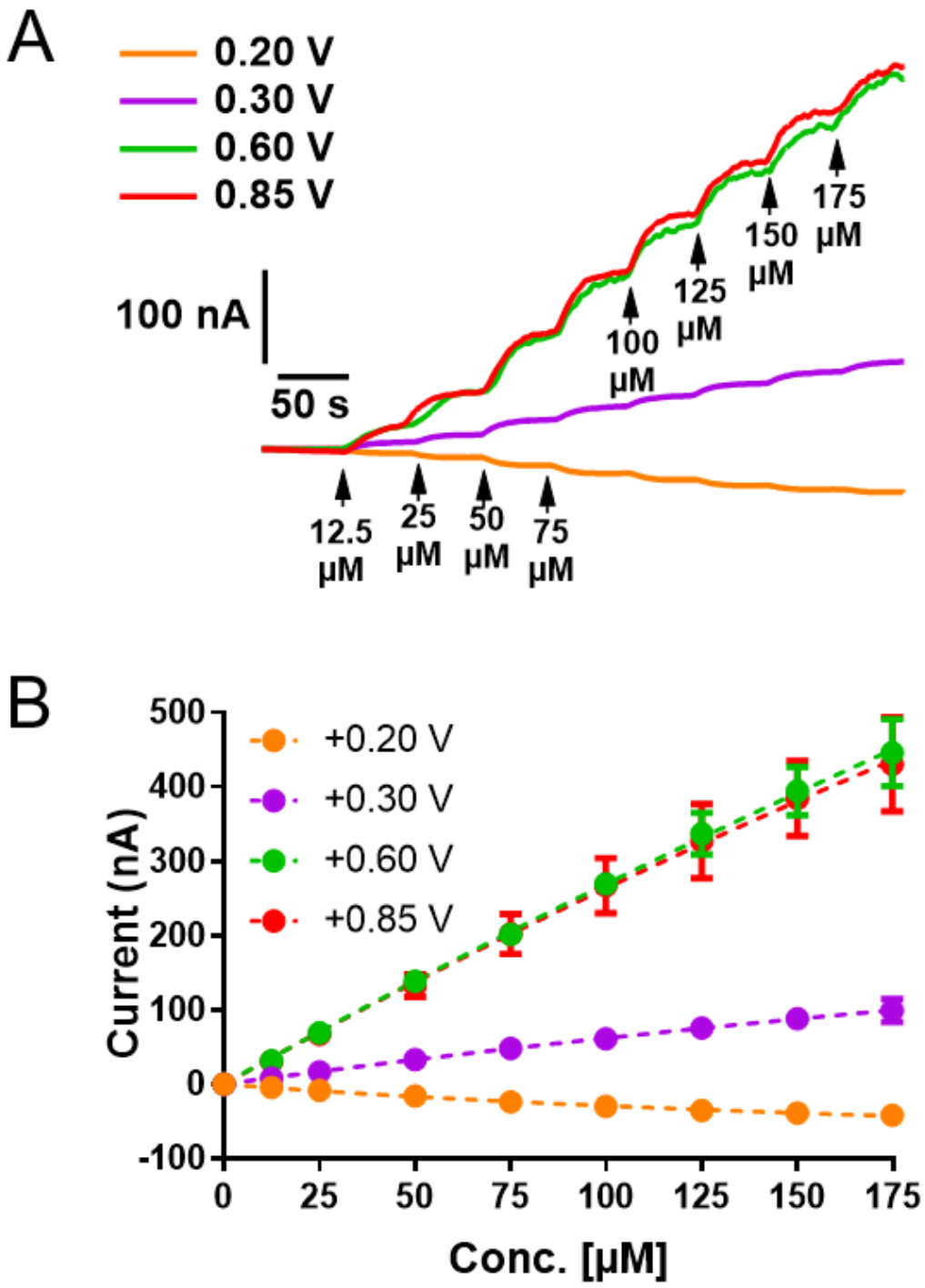

Figure 3.9.
Effect of voltage on choline biosensor response in stirred 0.1 M PBS pH 7.2 (*n* = *3*). (A) Representative traces for choline biosensors at +0.20 V, +0.30 V, +0.60 V, and 0.85 V vs Ag|AgCl. (B) Mean response ± S.D for choline biosensor batch at different voltages.

c) Stability testing

Quantifying the stability of the choline biosensor is important to determine if the biosensors can be stored for later use.

Figure 3.10.A shows the response of a batch of choline biosensors on day 1, day 10, and day 25, after being stored in 0.1 M PBS at 4°C. Figure 3.10.B shows the mean batch responses of the biosensors over time with standard deviation. Analysis with two-way ANOVA with multiple comparison and Tukey correction reveals no significant difference between the time points at any concentration.

This stability is similar to the previous glucose biosensors, and allows the ability to fabricate the sensors and store them until required. In the literature most choline biosensors exhibit a decrease in response over time, decreasing by 65% (Özdemir and Arslan, 2014), 50% (Song *et al.*, 2006) or not reporting long term stability at all. The best sensors showed a 7% reduction after a month (Magar *et al.*, 2017), a 10% decrease after 30 weeks (Ricci *et al.*, 2002), and a 5.4% decrease after 90 (Zhang *et al.*, 2014).

The stability obtained for our sensors far exceeded what was required for our use case. But it does confirm the rugged nature of the electrode and biosensor layer despite its low cost.

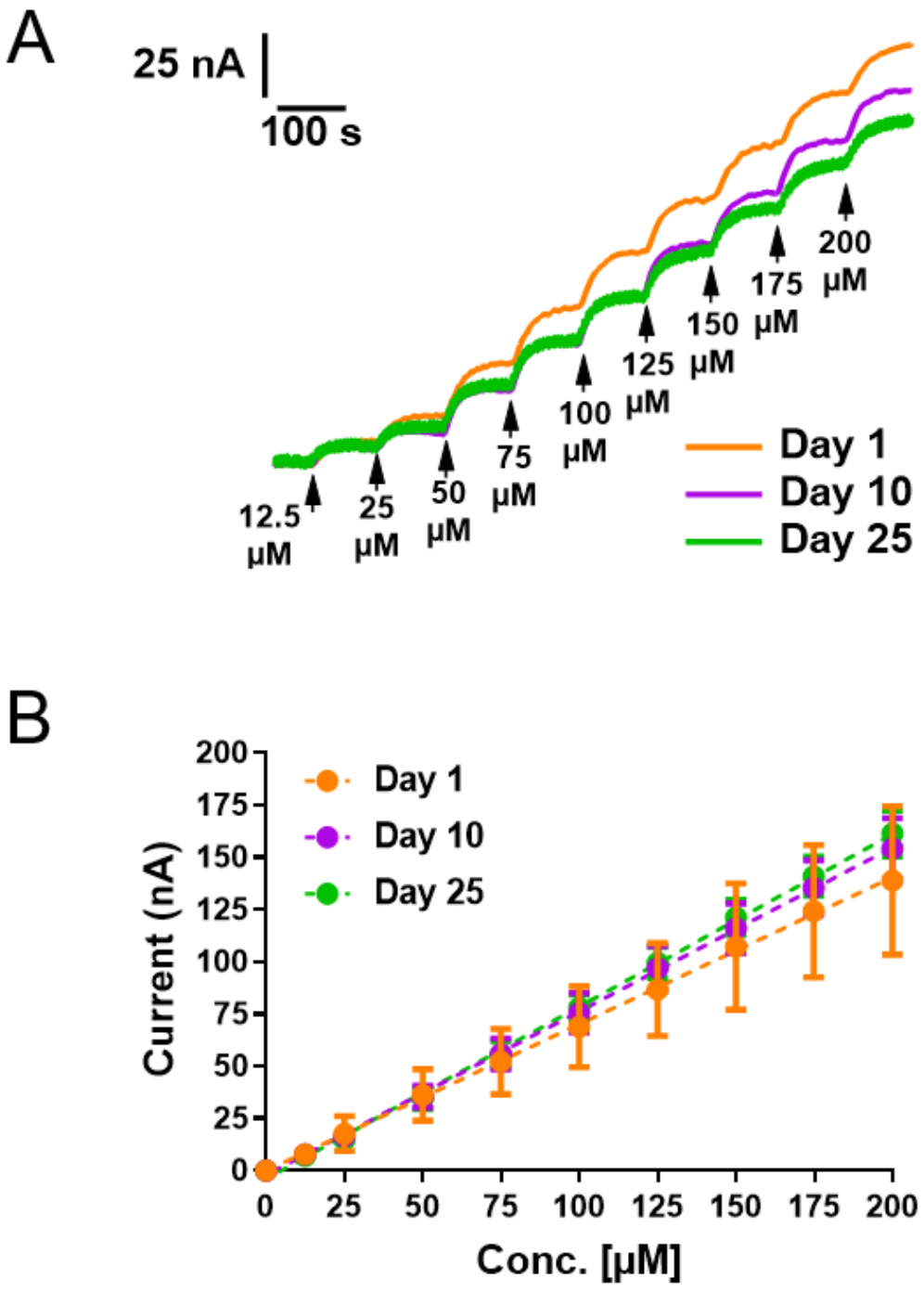

Figure 3.10.
Amperometric choline calibrations of choline biosensors at +0.85 V over time. Measurements taken in 0.1 M PBS pH 7.2 at days 1, 10, and 25 (*n* = 6, *n* = 5, and *n* = 5 respectively). (A) Representative traces for choline biosensor on days 1, 10, and 25. (B) Mean response ± S.D for batch of choline biosensors over time.

d) Response in artificial urine

Calibrations in buffers such as PBS may not reflect biosensor performance in the biological matrix. Though the composition of human urine is complex and variable, the general components have been established. The artificial urine tested is described in 3.2.5 and was chosen as it has been previously used to measure electrochemical analytes.

A batch of biosensors was tested in PBS buffer and then in artificial urine (AU). The representative traces in Figure 3.11A show that despite the biosensors detecting choline in PBS, current was not generated in artificial urine. This data is shown in Figure 3.11B as mean response with standard deviation.

The absence of response in AU could be due to one of the components interfering with the normal operation of the biosensor. To investigate this, different batches of AU were produced each with a different component omitted. This investigation revealed that it was urea affecting the response. This was confirmed by testing choline biosensors in urea-free artificial urine (UF-AU) and after a choline response had been established, urea was introduced to the solution and the current decreased, as shown in Figure 3.11C.

The literature does not contain any similar choline biosensors that have detected in urine. Jin et al detected choline in human urine using ECL and choline oxidase, measuring low micromolar amounts of choline (3.4-8.6 μM) (Jin *et al.*, 2010). However their setup used dilution (1:10), filtration (0.22μm pore) and HPLC to separate out any interferences (Jin *et al.*, 2010). Therefore there is no information regarding interactions of choline oxidase and urea.

Commercial kits for choline detection in urine use the same enzyme (ChOx) so it is unlikely that the molecule directly interacts with the enzyme. Even though urea can be used to denature proteins through solvation (Bennion and Daggett, 2003; Hua *et al.*, 2008), this is done at much higher concentrations (molar, compared to physiological 250 mM) (Guinn *et al.*, 2011). The rapid timescale with which the decrease occurs points towards urea hindering the electrode response. Urea is known to be low molecular weight, low toxicity, and low reactivity, but it could be blocking the choline oxidase active site due to its similar structure to choline.

Upon excretion, urea is catalysed fast by urea amidohydrolase (Senecal and Vinnerås, 2017), or slowly through uncatalyzed hydrolysis (Jespersen, 1975). This releases ammonia and leaves carbamate (H_2NCOOH) to spontaneously hydrolyse to carbonic acid (H_2CO_3) and release the second molecule of ammonia (Krajewska, 2009). Decomposition of urea therefore leads to the release of ammonia and increase in solution pH. These process need active prevention by researchers (Hellström, Johansson and Grennberg, 1999; Panyachariwat and Steckel, 2014) and thus urea is likely to degrade prior to urinary measurement.

Therefore, to evaluate if urea would interfere in real urine a sample of rat urine was thawed and choline was measured.

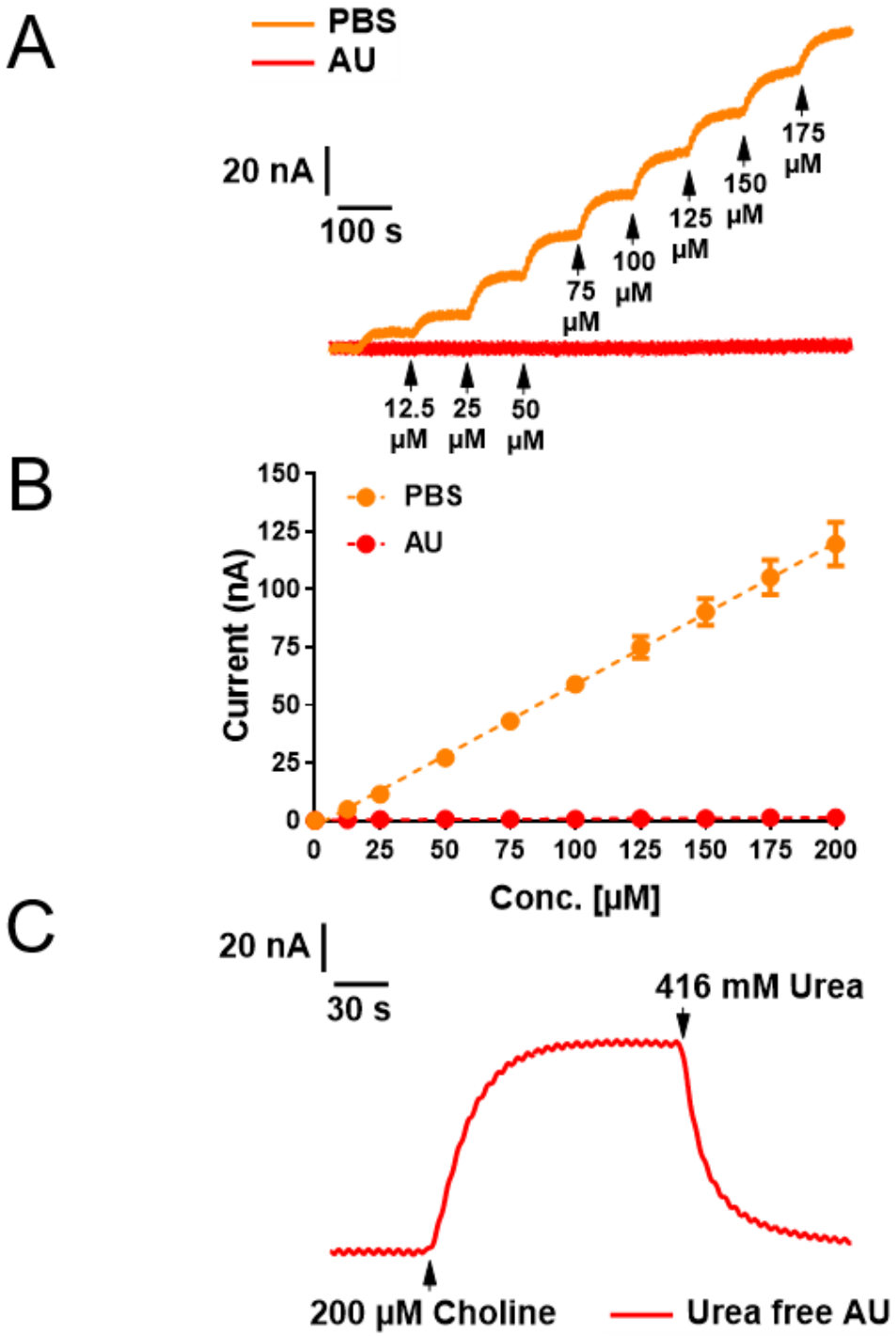

Figure 3.11.
Choline biosensor calibrations at +0.85 V vs Ag|AgCl in stirred 0.1 M PBS pH 7.2 and artificial urine pH 6.0 (*n* = 6). (A) Representative traces for choline biosensors in artificial urine and PBS. (B) Calibration for choline biosensors in PBS and AU shown as mean ± S.D (*n* = 6). (C) Representative trace for choline biosensor in urea free AU with addition of choline followed by addition of urea.

e) Response in real urine

To investigate if urea would impact measurement from real samples, a sample of rat urine was defrosted from the -80C and choline was measured.

Figure 3.12. shows that the choline biosensor measures a higher current than the null sensor held at +0.85 V.

As the only difference between the two sensors is that the null does not contain any choline oxidase in the BSA film, and therefore the change in current is directly attributable to the presence of choline. This suggests that hydrolysis and degradation from ureases is a problem for stored samples of urine (Soliman *et al.*, 1986). It also means that urea should not have a negative impact on our samples that have not been stored with any urea stabilisers for urea.

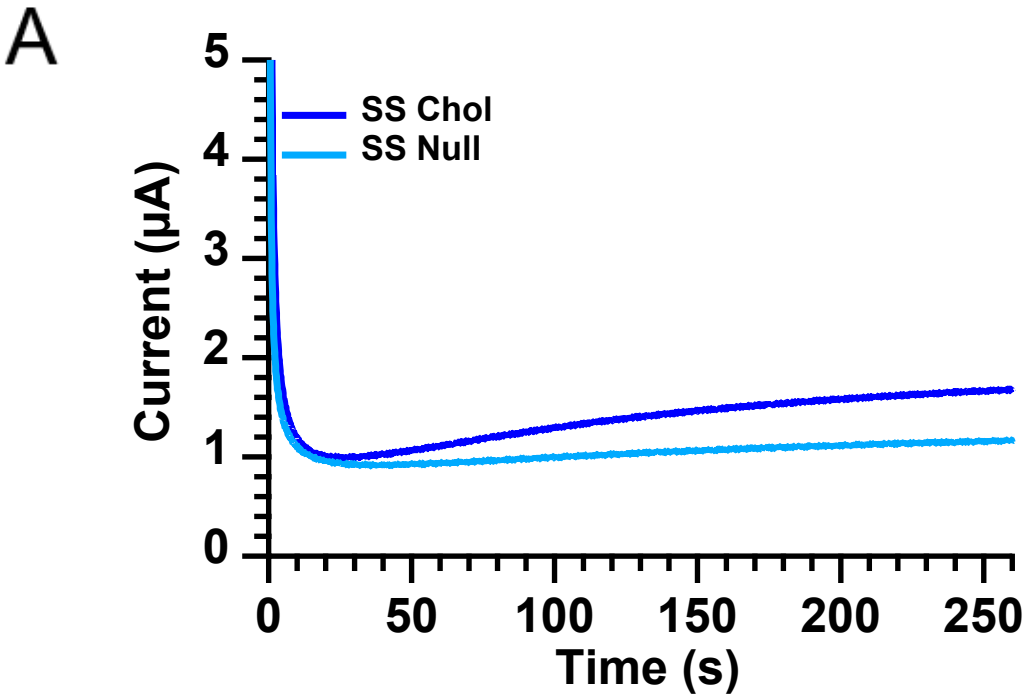

Figure 3.12.
Detection of choline in urine from a healthy Sprague-Dawley rat. Raw traces generated at a choline biosensor and null sensor in urine. SS denotes a healthy control rat.

f) Effect of modified matrix

Having identified established the absence of urea in our rat urine stored samples, future experiments will use urea-free artificial urine (UF-AU). This will allow the biosensors to be tested in a matrix more similar to the one they are expected to measure in. To ensure good function of the biosensors in urine, a batch of sensors was tested in both UF-UA and PBS so that comparisons in enzyme kinetics could be made.

Figure 3.13A shows representative traces for the same batch of biosensors tested first in 0.1 M PBS followed by urea free artificial urine (UF-UA) (*n* = *6*, *n* = *7* respectively). Figure 3.13**Error! Reference source not found.**B shows the mean response for the batch of biosensors in PBS buffer or urea free matrix. Analysis with Šídák multiple comparisons show a significant decrease when biosensors were used in UF-AU compared to when used in PBS.

The limit of detection for the batch of biosensors in PBS was found to be 32.14 µM. Most choline biosensors are constructed for in vivo measurements and so have smaller detection limits (0.01-0.025 µM) (Zhu *et al.*, 2009; Özdemir and Arslan, 2014; Baker *et al.*, 2019) and linear ranges (Baker, Bolger and Lowry, 2015, 2017; Baker *et al.*, 2019). Comparably sized biosensors constructed using glassy carbon and platinum electrodes have limits between 0.1-10 µM (Song *et al.*, 2006; Wang, Liu and Lin, 2006; Ren *et al.*, 2009; Rahimi, Ghourchian and Sajjadi, 2012; Huang *et al.*, 2021).

Despite the statistically significant decrease, the magnitude of the decrease is small. From a practical perspective the biosensors function in the modified matrix almost as well as in the buffer. This decrease could be due to a decrease in enzyme activity due to the lower pH of the matrix, which is at pH 6.0 compared to pH 7.2. The composition of

the modified matrix could be affecting the response, where the reduction in ions relative to analyte concentration could affect migration to the electrode surface.

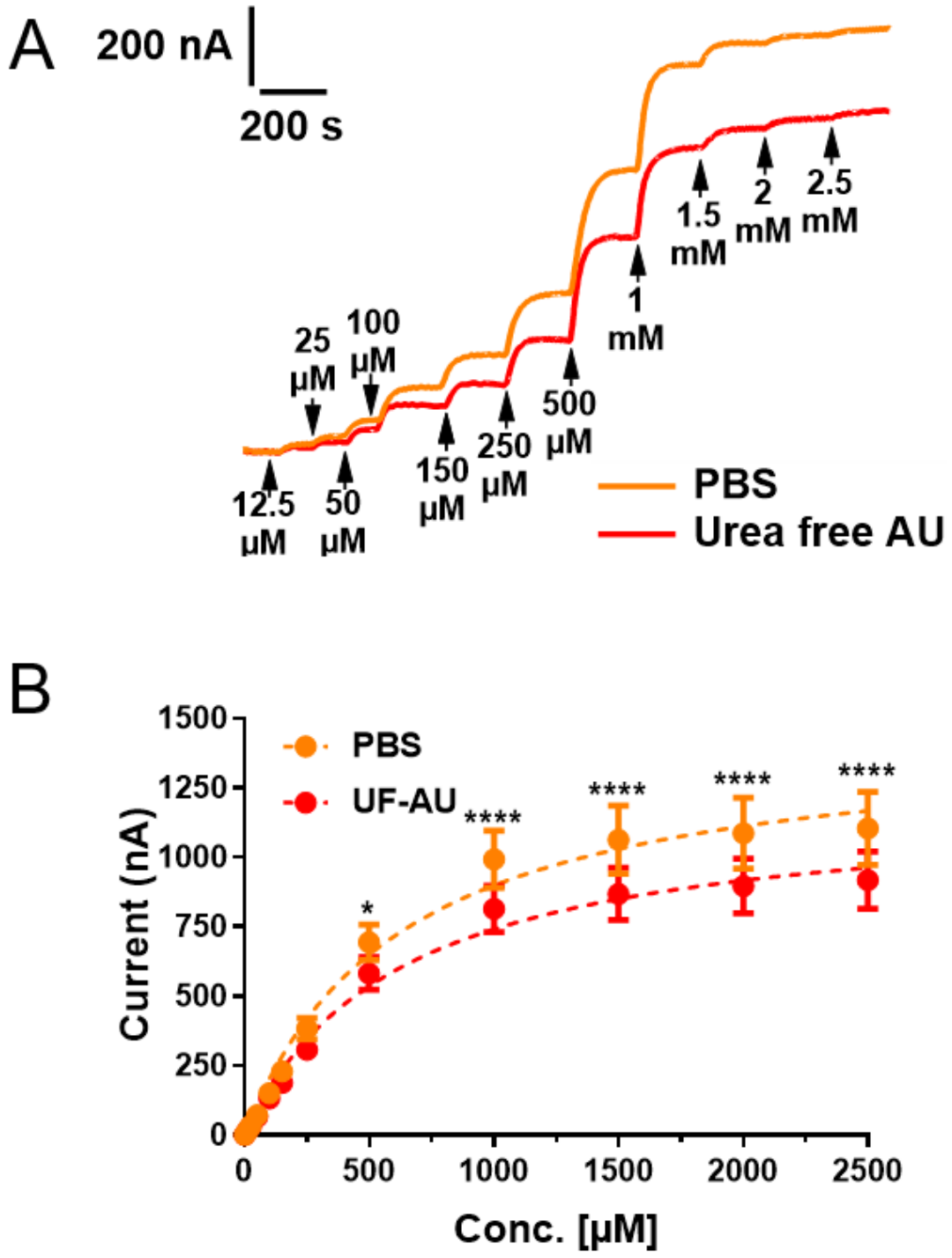

Figure 3.13.
Effect of modified matrix on choline biosensor amperometric calibrations at +0.85 V vs Ag|AgCl in stirred 0.1 M PBS pH 7.2 and urea free artificial urine (UF-AU) pH 6.0. (A) Representative traces for choline biosensors in PBS and UF-AU. (B) Mean responses for choline biosensors in PBS and UF-AU shown as mean ± S.D. (*n* = *6* and *n* = *7*). Data analysed with 2-way ANOVA with Šidák correction for multiple comparisons.

g) Enzyme kinetics and modified matrix

To further explore the effect of the matrix on performance, the enzyme kinetics of the biosensors in PBS and in urea free artificial urine were compared. Each biosensor in the previous figure was individually plotted using graphpad prism and data was fitted using the built-in Michaelis-Menten equation.

Figure 3.14A shows the K_m for the sensors in either PBS or UF-AU, analysed with a paired t-test to reveal no significant difference between the two matrices. Figure 3.14**Error! Reference source not found.**B shows the V_{max} for the sensors in PBS or UF-AU analysed with a paired t-test showing a significant decrease for the modified matrix.

The biosensors follow Michealis-Menten kinetics as increased substrate results in an increase in current that is proportionally smaller.

$$\boldsymbol{Current} = \frac{\boldsymbol{Vmax \times concentration}}{\boldsymbol{Km + concentration}} \quad (9)$$

This model relies on only a small percentage of analyte being catalysed to generate the signal, at a constant rate at a single time point (Cass, Cooper and Cass, 2004). The theoretical maximum current produced at the highest analyte concentration is known as the V_{max}, and it occurs as all enzymes are saturated despite further increases in concentration. The analyte concentration required to achieve half of V_{max} is known as the Michealis constant (K_m), and is unaffected by enzyme purity or concentration.

This experiment shows that despite the decrease in maximum current that can be achieved between the two matrices, the Michealis constant is unchanged. This implies that the choline oxidase is functioning the same in both environments.

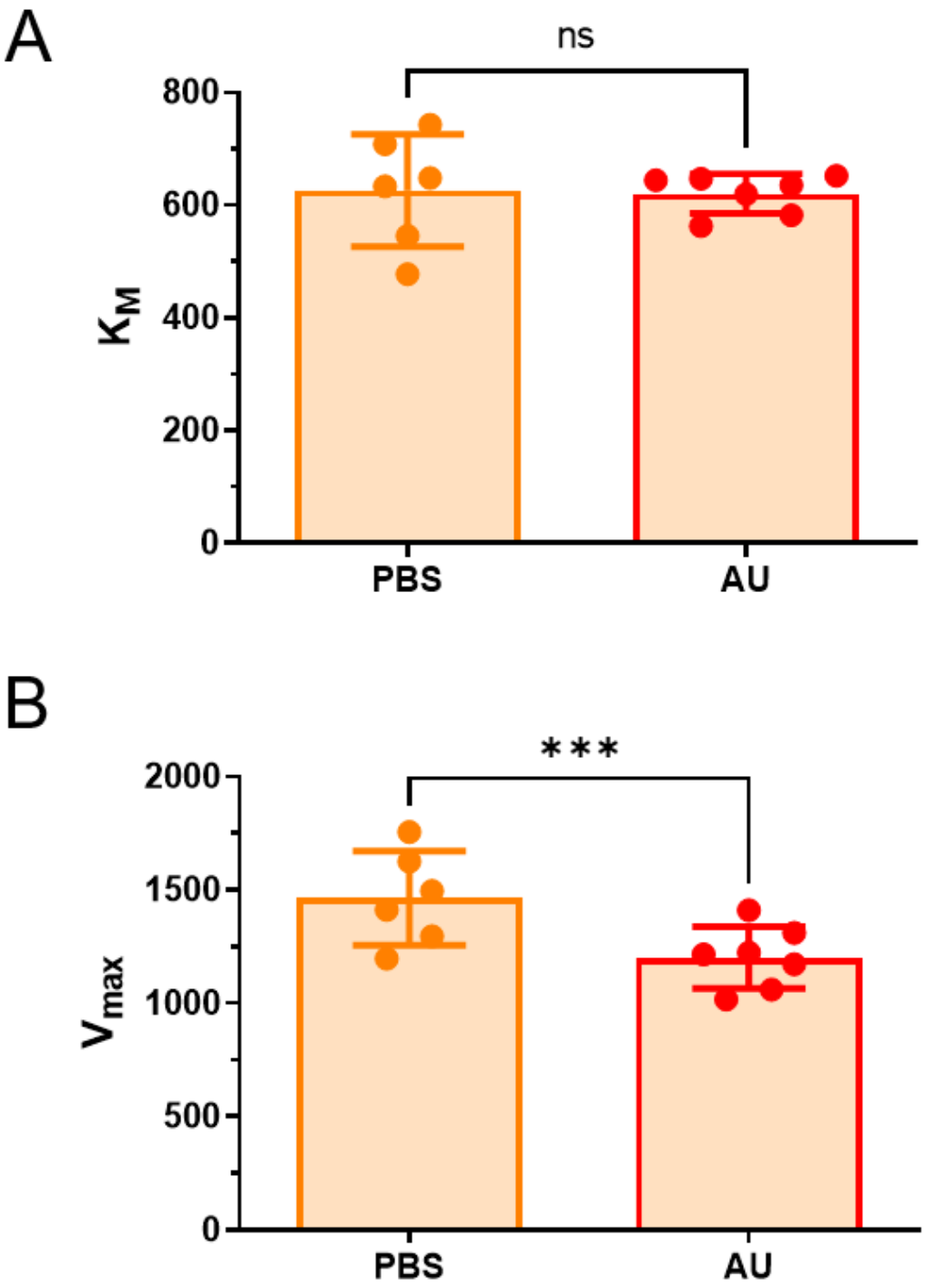

Figure 3.14.
Effect on enzyme kinetics of choline biosensors in either 0.1 M PBS pH 7.2 or urea free artificial urine (UF-AU). (A) Michaelis constant (K_M) for choline biosensors in either PBS or UF-AU. (B) Maximum rate of reaction (V_{MAX}) for choline biosensors in either PBS or UF-AU. Data shown as mean ± S.D. (*n* = 6, *n* = 7).

3.3.3 Nitrite electrode with null electrode functionality

a) Selectivity to nitrite in artificial urine

The composite electrode natively oxidises nitrite (NO_2^-) at positive potentials. Nitrite is considered to be a stable degradation product of nitric oxide (NO) and thus can be used to relate back to physiological levels of NO. Of the known electroactive interferents present in urine nitrite is the most abundant and the easiest to detect at the carbon composite. The current generated at the choline and xanthine biosensors will include the oxidation of other electroactive components in urine, particularly nitrite. Use of a sensor with no oxidase enzyme (null sensor) in the protein layer will allow detection of the total background electroactive components in urine. The subtraction of the current from the null biosensor current leaves the current component solely attributed to xanthine or choline when using the biosensors.

To determine nitrite sensor, measurements were conducted in the presence of commonly present urinary electroactive metabolites at appropriate physiological concentration (Table 4), calibrations were performed in both artificial urine and then artificial urine with electroactive metabolites.

Metabolite	Concentration (μM)
Dopamine	0.4
Peroxide	6
Serotonin	0.4
Uric acid	400
HVA	54
Norepinephrine	0.9
Epinephrine	0.2
5-HIAA	40

Table 4. Overestimation of urinary electroactive metabolites.

Figure 3.15A shows a representative trace for additions of nitrite to null sensor held at 0.85 V in artificial urine containing physiological concentrations of metabolites. The same sensor was then calibrated with nitrite in artificial urine containing no other metabolites.

Figure 3.15B shows the mean nitrite sensitivity for both the calibrations with standard deviation ($n = 6$). Statistical analysis performed with two-way ANOVA and Šídák multiple comparisons showed no significance ($p = 0.1786$) between the two calibrations at any concentration.

The data suggests that nitrite can be detected just as well in artificial urine containing faradaic metabolites as in metabolite free artificial urine.

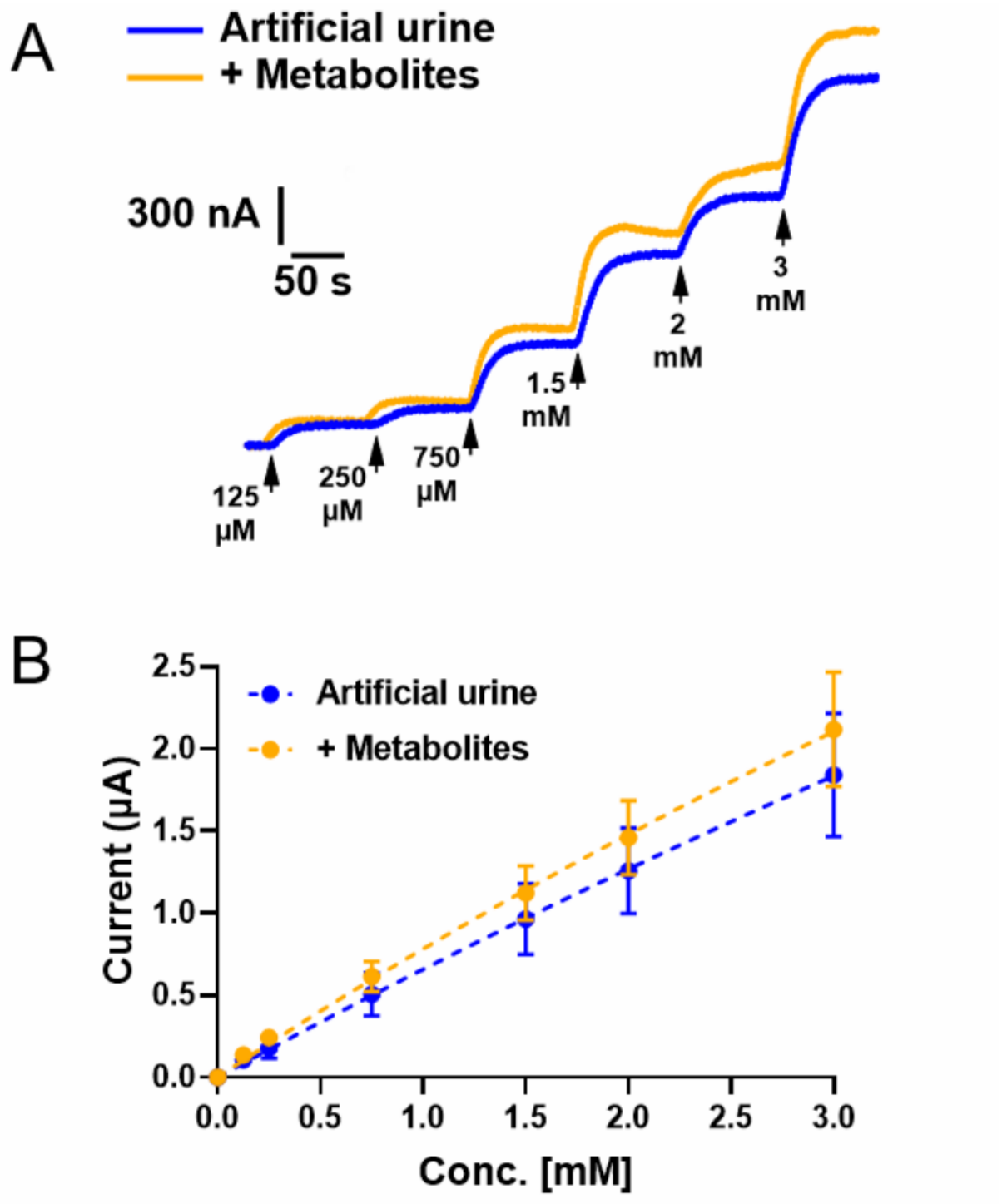

Figure 3.15.
Amperometric nitrite calibrations using nitrite sensors. Measurements generated at +0.85 V vs Ag|AgCl in stirred artificial urine pH 6.0. (A) Representative traces for nitrite in artificial urine without or with electroactive metabolites. (B) Mean batch response ± S.D (*n* = 6). Statistical analysis performed using two-way ANOVA with multiple comparisons and Šídák correction (p = 0.1786).

b) Selective detection of nitrite against urinary metabolites

Although the findings in this study show that commonly present electroactive metabolites do not interfere with the detection of nitrite. However, to ensure selective detection of nitrite within urine where other unknown biological or drug metabolites, the response of nitrite was observed using a null sensor. To isolate the current only produced by nitrite a second null sensor was held at +0.65 V. Subtraction of the currents produced between the two sensors is proportional to the concentration of nitrite.

Figure 3.6A shows representative traces for the two null sensors held at +0.65 V and +0.85 V. Figure 3.6B shows the mean responses for the batch of null sensors ($n = 6$). Data shows minimal response to nitrite at +0.65 V compared to at +0.85 V. This allows the concentration of nitrite to be determined whilst in the presence of other oxidisable compounds. Limit of detection for the sensors in artificial urine were 64 μM as determined by 3 times the blank signal divided by the slope.

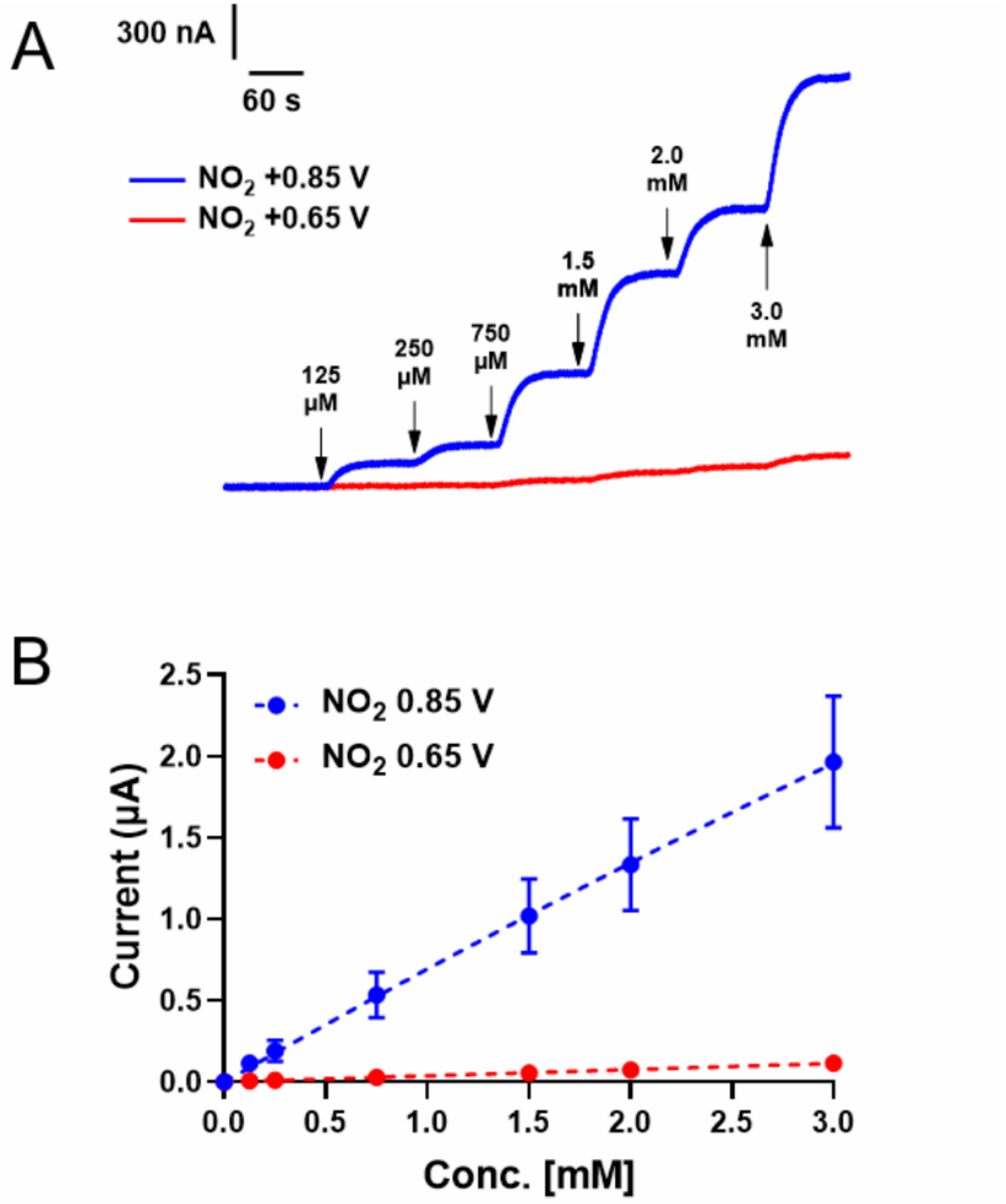

Figure 3.16.
Amperometric nitrite calibrations using nitrite sensors. Measurements generated at +0.85 and +0.65 V vs Ag|AgCl in stirred artificial urine pH 6.0. (A) Representative traces for nitrite in artificial urine. (B) Mean batch response ± S.D (*n* = 6). Statistical analysis performed using two-way ANOVA with multiple comparisons and Šídák correction.

3.4 Conclusion

The fabrication of choline and xanthine biosensors were optimised and characterised for the detection of their respective metabolites in an artificial urinary matrix.

Maximum choline sensitivity was achieved with 2% glutaraldehyde and 10% BSA composition. Choline detection was as sensitive at +0.6 V as at +0.85 V. Biosensor stability was shown to be as good as that of the glucose oxidase biosensor (Chapter 2). Despite interference of urea in an artificial urine matrix, detection of choline in real rat urine sample was successful. This is due to the hydrolysis and degradation of urea likely to be occurring with unestablished samples despite freezing. Measuring choline in artificial urine without containing urea showed sensor performance was satisfactory.

Xanthine biosensors also showed optimal sensitivity using 2% glutaraldehyde and 10% BSA. Differential pulse voltammetry could not identify the electroactive product produced by Xanthine Oxidase (XOD) detected at the electrode surface. Amperometric calibration showed Michaelis-Menten kinetics of the enzyme, and a large linear range.

Nitrite detection of the composite electrode was tested after protein crosslinking on the electrode surface. Sensitivity to nitrite was unaffected when calibrated in artificial urine, and artificial urine containing a plethora of electroactive metabolites. The detection of nitrite was almost completely lost when performed at +0.65 V, in concordance with DPV data. This allows the detection of nitrite at +0.85 V and the current component attributed to electroactive urinary metabolites can be removed through the use of an electrode poised at +0.65 V.

The nitrite electrode poised at +0.85 V can also function as a null electrode for choline and xanthine biosensor currents, allowing the concentrations of both the analytes to be determined without bias from electroactive urinary metabolites.

In conclusion, we have designed and characterised four electrodes; a choline biosensor (+0.85 V), a xanthine biosensor (+0.85 V), a nitrite sensor (+0.85 V) which can also function as a null for the two biosensors, and a background sensor (+0.65 V) to separate the current component due to interferences from the nitrite sensor.

Chapter 4: Understanding how urothelial signalling metabolites change in OAB

4.1 Introduction

4.1.1 Signalling within the bladder

Micturition is controlled through central nervous mechanisms, through the partially understood micturition reflex. Urine storage and voiding is also controlled through peripheral efferent and afferent nerves, which cause and monitor bladder contraction and relaxation respectively. The smooth muscle in the bladder wall is known as the detrusor, and is also controlled by non-neuronal signalling molecules that are released locally by the inner lining of the bladder, known as the urothelium.

Efferent parasympathetic nerves release signalling molecules onto receptors located in the detrusor, urothelium, and afferent nerve terminals (Yoshimura, 2007). These nerves release acetylcholine which can act on muscarinic G protein coupled receptors (GPCR) which can either be excitatory (M1, M3, M5) or inhibitory (M2, M4) (Mansfield *et al.*, 2005; Winder *et al.*, 2014). Excitation occurs through activation of phospholipase C (PLC) then inositol 1,4,5-triphosphate (IP3) and diacylglycerol resulting in increased calcium (Wu *et al.*, 2000) whilst inhibition is through inactivation of adenylyl cyclase which prolongs ion channel opening (Van Koppen and Kaiser, 2003). All five subtypes have been found in the human bladder, and detrusor contraction has been shown to be mediated through the M3 receptor (Tobin and Sjögren, 1995), despite the M2 receptor being the most abundant (Mansfield *et al.*, 2005), at a ratio of about 3:1 (Goepel *et al.*, 1998). Acetylcholine (of neuronal and non-neuronal origin) also acts on nicotinic receptors located in the urothelium that affect the release of ATP (Beckel and Birder, 2012).

Efferent sympathetic nerves release noradrenaline (NA) onto α-adrenergic receptors at the bladder base, and onto β-adrenergic receptors in the main body. The α1 and α2 receptors have a weak contractile effect useful in regulating bladder tone (α1A) by triggering hydrolysis of inositol phosphate and increasing calcium, thus counteracting urine leakage during the storage phase (Chang *et al.*, 2000; Michel and Vrydag, 2006). Furthermore, α1D receptors in the urothelium are thought to facilitate afferent nerve activity necessary for the micturition reflex (Ishihama *et al.*, 2006).

β-adrenergic receptor agonists cause detrusor relaxation through adenylyl cyclase activation, and though all three subtypes are found in the bladder, β3 is the most abundant (Nomiya and Yamaguchi, 2003). This means that overall NA mediates detrusor relaxation during the filling phase as well as contraction of the urethra and bladder neck (Caine, Raz and Zeigler, 1975).

The existence of a contractile parasympathetic response of about 30% (Luheshi and Zar, 1990) despite the use of the muscarinic antagonist atropine hinted at a 'non-adrenergic, non-cholinergic' (NANC) response (Langley and Anderson, 1896). After further investigation these NANC transmitters consisted of adenosine (Dunning-Davies *et al.*, 2013; Pakzad *et al.*, 2016), adenosine triphosphate (ATP) (Burnstock, 1972), neuropeptides (Arms and Vizzard, 2011), nitric oxide (NO) (Andersson and Persson, 1994), prostanoids (Anderson, 1993; Martínez-Saénz *et al.*, 2011), and transient receptor potential (TRP) channels (Franken *et al.*, 2014; Deruyver *et al.*, 2018).

Of the NANC transmitters ATP is thought to be responsible for most of this atropine-resistant bladder response (Burnstock, Dumsday and Smythe, 1972; Burnstock *et al.*, 1978; Moro and Chess-Williams, 2012). ATP is known for its use as a source of

intracellular energy, and has now been shown to act as an important co-transmitter in various nerve types (Burnstock, 2009). Synthesis of ATP requires energy to add a phosphate group to adenosine diphosphate (ADP) via oxidative phosphorylation or glycolysis and then a transporter to allow storage in vesicles (Dowdall, Boyne and Whittaker, 1974; Pankratov *et al.*, 2006; Hasuzawa *et al.*, 2020). Stimulation of parasympathetic nerves results in a release of neuronal ATP which causes non-cholinergic contractions (de Groat, Griffiths and Yoshimura, 2015). This contraction occurs through activation of $P2X_1$ receptors (Sjogren *et al.*, 1982; Aronsson *et al.*, 2010), that seem less important in healthy human bladder physiology (de Groat, Griffiths and Yoshimura, 2015) but could be involved in pathology (Palea *et al.*, 1993).

The more important release of ATP is locally after mechanical deformation that results in urothelial ATP release after bladder stretching or swelling. This non-neuronal ATP is thought to provide sensory information of bladder filling through purinergic receptors on bladder afferent nerves (Andersson, 2015). There are seven types of P2X receptors ($P2X_{1-7}$) that are ligand gated ion channels permeable to sodium or calcium, present in human (Moore, Ray and Barden, 2001) and rat bladder tissue (Creed, Loxley and Phillips, 2010). Of these, $P2X_1$ activation is thought to initiate human detrusor contraction, whilst $P2X_2$ and $P2X_3$ located on afferent nerves to mediate sensation of bladder filling. This can initiate the voiding reflex, or ATP can act on interstitial cells and myofibroblasts so that a calcium signal can travel to the detrusor. Recent studies have shown that $P2X_1$ and $P2X_3$ activation on urothelial cells can trigger the release of local acetylcholine (Stenqvist, Carlsson, *et al.*, 2020).

There are eight P2Y receptors, which are GPRC and can be activated by ATP and ADP, then affecting PLC or adenylyl cyclase activity. In the urothelium the subtypes $P2Y_1$, $P2Y_2$, $P2Y_4$, $P2Y_6$, $P2Y_{11}$ have been identified (Chopra *et al.*, 2008; Shabir *et al.*, 2013; Timóteo *et al.*, 2014), with $P2Y_2$ thought to affect afferent activity (Chen, Molliver and Gebhart, 2010).

The breakdown of ATP by ectonucleotidases results in extracellular adenosine, which also has some pharmacological effects through P1 receptors. There are four P1 receptors ($P1A_1$, $P1A_{2A}$, $P1A_{2B}$ and $P1A_3$) which have been all found in the bladder, with $P1A_1$ in control of efferent signalling (Ikeda *et al.*, 2012). Adenosine reduces neuronal detrusor contractions acting at $P1A_1$ located presynaptically at the neuroeffector junction. Activation of $P1A_{2b}$ located on the detrusor blocks P2X1 contractions causing relaxation for the next filling cycle.

Nitric oxide (NO) is a NANC transmitter which activated guanylyl cyclase, increasing cGMP and thus activating protein-kinase. This results in smooth muscle relaxation when released from parasympathetic nerves mostly affecting urethral relaxation. Activation of M5 receptors cause NO release, as well as through noradrenaline activation of β3 receptors causing Ca dependent release. This release is not vesicular and instead relies on formation through three nitric oxide synthase enzymes. This occurs using L-arginine and one of three forms of nitric oxide synthase; endothelial (eNOS), inducible (iNOS), and neuronal (nNOS). The forms eNOS and nNOS require the presence of calcium, unlike iNOS. The urothelium expresses eNOS and iNOS and expression is affected by disease.

4.1.2 Changes in signalling with overactive bladder (OAB)

Overactive bladder (OAB) is characterised by increased urinary frequency, urgency, and nocturia (Haylen *et al.*, 2010). The combination of these symptoms in absence of a UTI is used to establish a diagnosis, yet the underlying pathophysiology is unknown. This is because detrusor overactivity is only present in 50% of females with OAB (Hashim and Abrams, 2006), and pharmacological treatment of symptoms often provide an insufficient effect or intolerable side effects resulting in a high rate of discontinuation (Peeker *et al.*, 2010; Sexton *et al.*, 2011). This has led to multiple theories to explain the dysfunction behind OAB.

The main theories proposed involve changes in signalling which would then affect bladder function. The positive improvements found with antimuscarinic therapy during the filling phase without improving detrusor contraction (Finney *et al.*, 2006) points towards abnormal afferent sensory activity. Acetylcholine is released neuronally and non-neuronally on different cells with excitatory or inhibitory muscarinic receptors, with downstream release of ATP, NO and prostanoids thus making it hard to identify where dysfunction occurs.

The main theories put forward are dysfunction in afferent signalling, myogenic hypersensitivity (Brading, 1997), and altered sensory function. Each theory has some merit and OAB could be a collection of some or all of these factors. In a study ice water cystometry was used to show c-fibre upregulation, indicating dysfunction in afferent signalling. OAB sufferers have been shown to have increased stretch-induced ATP release (Contreras-Sanz *et al.*, 2016). This has recently been shown to be reflected with increased urinary ATP.

4.1.3 Models for overactive bladder (OAB)

The usual method of investigating bladder function is through *ex-vivo* preparations which explore the response to agonists and antagonists. The advantage of this is that it is a robust setup that can shed light on the signalling molecules necessary for detrusor contraction and relaxation. This experimental design can isolate the effect of a molecule from other factors that are present *in-vivo* such as metabolism and other downstream pathways. This is further explored through the use of agonists and antagonists selective to a receptor subtype. However, this neglects the effect of the nervous system and reflexes that are severed upon excision, which in the case of OAB could be a key player in dysfunction (4.1.2). This has been addressed through more complex *in-situ* preparations which leave these nerves intact to allow a realistic model to be built.

Comparison between animal bladder tissue and human bladder tissue can be made using the *in-vitro* setup with biopsied tissue. The translation between the two can be strengthened using techniques to quantify receptor quantity and location through qtPCR, IHC, and western blot. However, the *in-situ* method is too destructive and invasive for use in healthy human subjects let alone patients suffering from OAB. Methods that have been used in humans include urodynamics, where catheterisation and filling of the bladder with warm water can be used to record changes in intravesical pressure during filling and voiding (Colhoun *et al.*, 2017). This has also been done with internal electrodes that detect micromotion to see if OAB presented with more detrusor activity (Drake *et al.*, 2005). These methods re-enforce the need for a non-invasive method that can diagnose OAB.

There are disadvantages to using an animal model for OAB. There can be functional and structural differences between species so it is important to validate the model based on its limitations and how it relates to human physiology and pathophysiology (Brading, 2006). There are some specific differences in humans that have been noted, such as minimal component of purinergic contraction (Palea *et al.*, 1993; Hashitani, Bramich and Hirst, 2000), parasympathetic ganglia in the bladder wall (McMurray, Casey and Naylor, 2006), and potentially differences in muscarinic receptor subtype density (Wang, Luthin and Ruggieri, 1995). However, the most difficult problem in modelling OAB is the ability to quantify and incorporate the subjective perception of urgency, which is the key symptom of OAB (Parsons and Drake, 2011). This has led to other markers serving as a surrogate for urgency, namely urinary frequency, void volume, and changes in micturition habit (Parsons and Drake, 2011).

Development of a urinary biomarker for OAB could be possible by exploring these functional changes in a rodent OAB model. Functional changes can be induced either through central or peripheral damage. Research on human subjects suffering from injuries or diseases of the central nervous system present with distinct voiding disturbances that appear separate to OAB (Andersson, 2004; Peyronnet *et al.*, 2018; Partin *et al.*, 2020). This indicates a peripheral model would be more representative of the condition. Peripheral damage can be induced with a noxious substance that stimulates afferent C-fibres and induces their upregulation (Kanai and Andersson, 2010). These include acetic acid (Choudhary *et al.*, 2015), capsaicin, citric acid (Dasgupta, Elliott and Tincello, 2009), hydrochloric acid, protamine sulphate (Tyagi *et al.*, 2017), xylene, and turpentine (Parsons and Drake, 2011). The most successful and well characterised is cyclophosphamide (Andersson, Tobin and Giglio, 2008; Andersson *et*

al., 2011; Aronsson *et al.*, 2015), which when excreted as the metabolite acrolein produces an aseptic inflammation of the bladder (Cox, 1979). Cyclophosphamide induced cystitis is a good mimic for OAB as it shares the same characteristics such as increased urinary frequency, urgency, and decreased micturition volume (Augé *et al.*, 2013; Aronsson *et al.*, 2014, 2015).

Other useful models for OAB are receptor knock-out mice. The removal of a specific receptor allows to evaluate functional effects and receptor contribution without affecting nerves. Knocking out $P2X_2$ or $P2X_3$ results in decreased voiding frequency and increased bladder capacity without affecting bladder pressure (Cockayne *et al.*, 2005). Whilst removal of nNOS causes increased urinary frequency without affecting volume (Burnett *et al.*, 1997), which is mirrored by reduced bladder capacity and increased detrusor contractions when NO scavengers or NO inhibitors are given (Masuda, 2008).

4.1.4 Aims and objectives

The aim of this study is to explore changes in signalling molecule urinary metabolites with OAB.

The following objectives will be explored to achieve this aim:

1. Measure choline, xanthine, and nitrite in urine from a rat model used to explore symptoms of OAB.
2. Correlate these metabolites with the pathophysiological symptoms of overactive bladder.

4.2 Experimental

4.2.1 Materials

Bovine serum albumin (BSA microbiological grade powder fraction v), glutaraldehyde (Grade II, 25% in H_2O), sodium chloride, potassium phosphate monobasic, disodium hydrogen phosphate, potassium chloride were obtained from Merck and used as described.

4.2.2 Biosensor fabrication

Biosensors were fabricated using composite electrodes containing 10% w/w PtB and 15% w/w MWCNT dispersed in epoxy resin (Chapter 2). Electrodes were coated with 10 µL solution containing either choline or xanthine oxidase with 10% w/v BSA crosslinked with 2% glutaraldehyde (Chapter 3).

4.2.3 Nitrite/null sensor fabrication

Sensors for the detection of nitrite contained the same mixture of 10% w/w PtB and 15% w/w MWCNT dispersed in epoxy resin (Chapter 2). Sensors were coated with 10% w/v BSA crosslinked with 2% glutaraldehyde (Chapter 3) as to mimic biosensor composition to then act as null sensors and allow current subtraction. The difference in current between a null sensor held at +0.85 V and another null sensor at +0.65 V allows determination of the proportion of current solely attributed to nitrite concentration.

4.2.4 Electrochemical setup

Measurements were obtained using a 1009A potentiostat (CH instruments, Texas) a Ag|AgCl (3 M KCl) reference electrode, a platinum wire auxiliary electrode (IJ Cambria Scientific Ltd, Wales). Each sample was measured using four working electrodes;

choline biosensor held at +0.85 V, xanthine biosensor at +0.85 V, a +0.85 V null electrode, and a second null at +0.65 V.

4.2.5 Animal study design

The study was undertaken at the University of Gothenburg after approval by the local ethical committee. Male Sprague-Dawley rats of similar age (10-16 weeks) and weight (285-495g) were randomly allocated between the two groups, with eight rats in each group. Animals were subject to an intraperitoneal injection of either saline (4mL/Kg) or cyclophosphamide (100mg/Kg). Urine samples were obtained 48 hours post injection, for a total of 16 hours using a metabolic cage. A WFL30-40B416 laser Doppler (SICK) recorded the quantity and frequency of urine, allowing for micturition parameters to be calculated.

Total urine volume was recorded and used to normalise metabolite concentration. Functional data was also collected in the form of volume per micturition and micturition per hour.

4.2.6 Electrochemical measurements of urine samples

Prior to analysis urine samples were thawed at room temperature and vortexed for two minutes. Four millilitres of sample were decanted into the electrochemical cell (A). Measurements of choline and xanthine were obtained through subtraction of the null current from the associated biosensor current. Subtraction of the current from the +0.65 V null sensor from the +0.85 V null sensor would give a current related to nitrite concentration.

4.2.7 Evaluation of bladder inflammation

To evaluate bladder inflammation the tissue was stained with haematoxylin and eosin. This was performed by Histocentre (Mölndal, Sweden). Bladders were cross sectioned as to show the urothelium, suburothelium and the detrusor. Pictures were evaluated blind using an inflammatory grading system. Each sample was graded according to the following system:

1. No inflammatory signs,
2. Few signs of interstitial oedema
3. Signs of interstitial oedema, inflammatory cells, thinner transitional epithelium and ulceration
4. Serious interstitial oedema, signs of inflammatory cells, thinner transitional epithelium and ulceration

4.2.8 Statistical analysis

DPV data was processed using CHI software by manually detecting peaks generated by the sample. Data was normalised using total urine volume produced over 16 hours. Amperometric data after subtraction was interpolated using calibrations for the biosensor and normalised to total urine volume.

4.3 Results and discussion

4.3.1 Setup for simultaneous measurement of urinary metabolites

To detect the metabolites simultaneously biosensors were produced in batches and arranged in the electrochemical cell as shown in Figure 4.1A. The cell containing 4 mL of stirred rat urine used a Ag|AgCl reference and platinum counter to hold the working electrodes at their required voltage. As per the validation in chapter 3, the choline (red) and xanthine (green) biosensors were held at +0.85 V so that the composite electrode can detect the peroxide produced by the oxidase enzymes trapped on the electrode surface when in the presence of the analyte. The composite null electrode (blue) coated with BSA and no enzyme that is also held at +0.85 V can be used to measure the concentration of the oxidisable components of the matrix such as uric acid (El Ridi and Tallima, 2017; Kulyk *et al.*, 2022) and nitrite (Patel *et al.*, 2020). This current can then be subtracted from the currents produced at both biosensors as to ensure that the metabolite concentration is measured accurately. This is important as there is variation in matrix composition between samples (Rose *et al.*, 2015), biasing the current detected at the biosensors.

To separate the nitrite component from the other oxidisable compounds in the biological matrix, another null electrode (black) is held at +0.65 V and the current measured is subtracted from that at the +0.85 V null(Patel *et al.*, 2011; Price *et al.*, 2020).

Figure 4.1B shows a measurement of the three analytes in a sample of rat urine. During the first few seconds of applying voltage a charging current is seen, decaying off as the double layer is established at the surface of the sensors(Bard and Faulkner, 2001). Within twenty seconds the current stabilises, representing the faradaic current related

to the concentration of analyte at the electrode surface. The stability of the current at the choline biosensor and both nulls suggests minimal fouling however this would be better tested with post measurement calibrations.

Figure 4.1C shows the current at the three sensors in B after subtracting the current from the appropriate null. The +0.85 V null current was subtracted from the current at the choline and xanthine biosensors, whilst the +0.65 V current was subtracted from the +0.85 V null to obtain the nitrite response. The figure still shows the decrease in current as the double layer forms, followed by stabilisation. Stabilisation occurs at different time points depending on the sample due to different urinary composition, compared to the consistent biosensor response times seen in Chapter 3. Therefore, measurements for all samples were taken at 200 seconds.

Current was used to calculate concentration using the calibration data of the biosensor in artificial urine. This was normalised by the amount of urine produced over 16 hours.

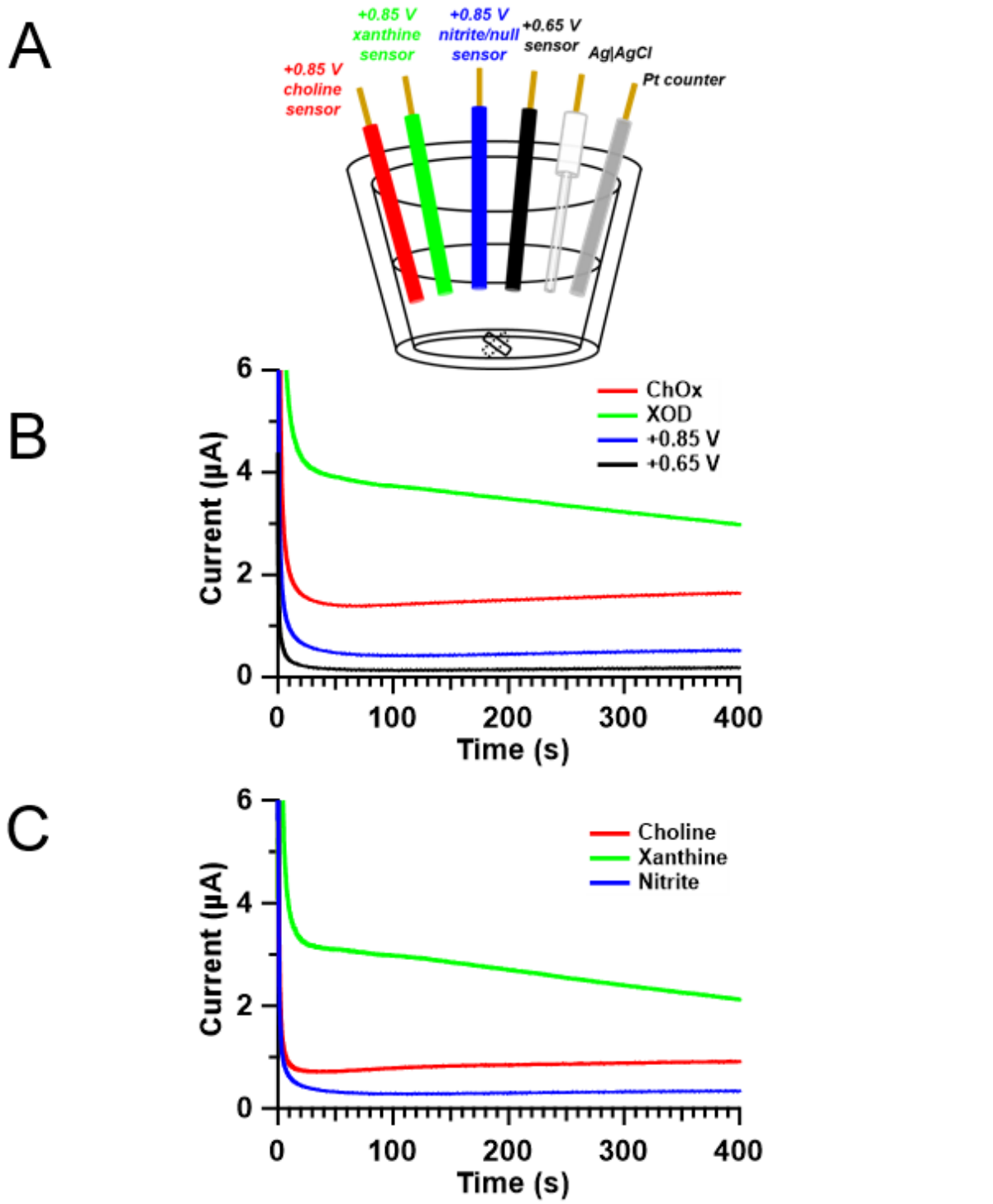

Figure 4.1.
Experimental setup for simultaneous detection of multiple urinary metabolites. (A) Diagram of electrode configuration for the detection of choline, nitrite, and xanthine using choline biosensor (+0.85 V), xanthine biosensor (+0.85 V), nitrite/null sensor (+0.85 V) and nitrite exclusion sensor (+0.65 V). (B) Raw traces for data generated from urine obtained from saline injected Sprague-Dawley rat. (C) Response for choline and xanthine determined through subtraction of +0.85 V null from biosensor currents. Current for nitrite determined through subtraction of +0.65 V from +0.85 V current.

4.3.2 Detection of choline in OAB rat urine

Choline biosensors were used to determine the difference in choline between samples from healthy control rats injected with saline (SS) and those subject to an injection of cyclophosphamide to induce OAB symptoms (CS).

Figure 4.2A shows raw current detected from a choline biosensor and null sensor both held at +0.85 V. Sensors measured currents in control rat urine (SS Chol and SS Null), and from OAB urine (CS Chol and CS Null). The slight difference in null current between the two samples indicates differences in the urine matrix between the treated and untreated rat, justifying the use of a null sensor.

To generate choline quantity in urine seen in Figure 4.2B the raw traces were processed by subtracting the null current from the biosensor current. Average current was determined using a timepoint after all biosensors had reached stability so that the results would be comparable. Current was converted to concentration using calibration data of the individual choline biosensor calibration and related back to the original quantity in the urine sample using micturition volume. Figure 4.2B shows the quantity of choline in each sample was not significantly different between the control and OAB urine ($p = 0.35$ using unpaired two-tailed t test).

The relationship between urinary choline and OAB symptoms has not been fully explored. One paper reports a decrease in median choline level in women with OAB, finding choline levels drop to 2.66 µM from 4.08 µM (Sheyn *et al.*, 2020). Our data shows a non-significant decrease in means, which could be limited by our small sample size. On the other hand, a more recent study by the same authors reported an increase in urinary choline with OAB (15.2 µmoles to 29.0 µmoles, median) which they argued to be

due to different patient demographics, namely increased age and post-menopause (Sheyn *et al.*, 2022). If this is correct it instead highlights high variability in choline levels within the control group, and a correlation between choline and age which should be studied first.

The study also differs by being able to measure urinary acetylcholine levels that for the previous cohort were below detectable levels, but this time were found to be higher in OAB (82.1 nmoles, median) than in the control group (50.3 nmoles, median) (Sheyn *et al.*, 2022).

This in conjunction with the absence of significant difference in urinary acetylcholinesterase supports the hypothesis that dysfunction is related to excess acetylcholine release, but does not take into account the other signalling molecules involved in controlling bladder function.

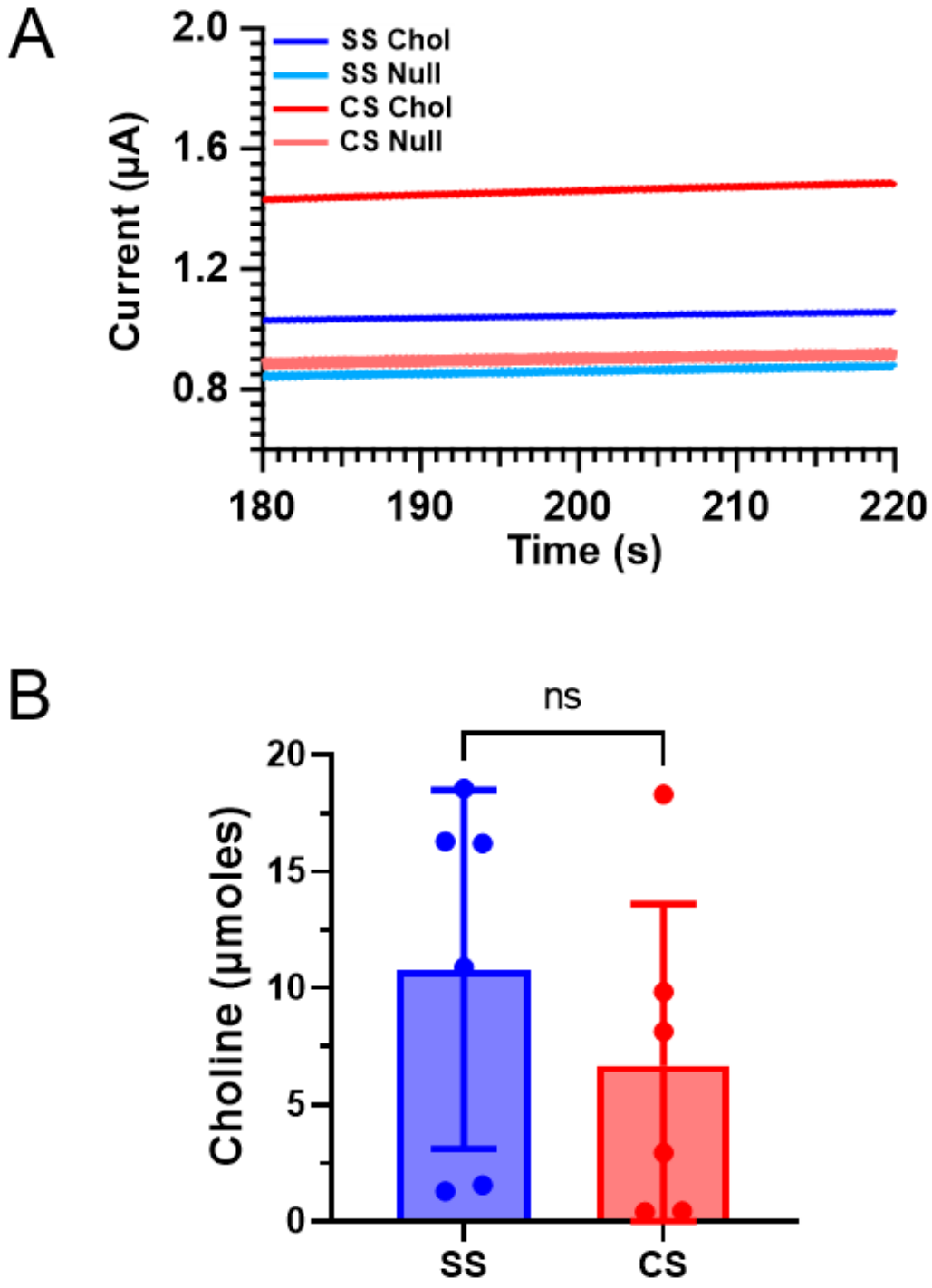

Figure 4.2.
Detection of choline in urine samples from saline injected rats (SS) and cyclophosphamide injected rats (CS). (A) Representative traces for choline biosensors and null sensors in urine from control or OAB induced Sprague-Dawley rats. (B) Total quantity of choline in urine sample for control (SS) *n* = *6* or OAB (CS) *n* = *6* rats. Data analysed using unpaired two-tailed t test, p = 0.3523.

4.3.3 Detection of xanthine in OAB

Xanthine was detected similarly to choline through the use of xanthine biosensors and associated null electrodes in control rat urine (SS) OAB urine (CS). Figure 4.3A shows the raw currents detected from the xanthine biosensors in both samples (SS Xanthine and CS xanthine) and their associated nulls (SS Null and CS Null). The null currents appear stable thus indicating a lack of biological fouling, whilst there is a stable decrease in the current of the xanthine biosensors in both samples. Despite the presence of this decrease in both treated and untreated samples the relative decrease is the same and can still allow comparison of xanthine content between samples.

The xanthine oxidase current was taken at a stable time point and the null current was subtracted from it and then concentration was calculated using the xanthine calibration. This concentration was normalised to total quantity released using total micturition volume. This is shown in Figure 4.3B where the OAB urine has significantly less xanthine compared to the control urine ($p = 0.025$ using unpaired two-tailed t test).

Urinary detection of xanthine has been of interest due to it being a precursor to uric acid, which can cause an accumulation of urate crystals in joints resulting in inflammation and pain (Seegmiller *et al.*, 1961). This has led to measurements in serum and urine using gas chromatography-mass spectrometry (Lartigue-Mattei *et al.*, 1990), high performance liquid chromatography (Boulieu *et al.*, 1983; Kurtz *et al.*, 1986; Kock, Delvoux and Greiling, 1993; Czauderna and Kowalczyk, 2000; Samanidou, Metaxa and Papadoyannis, 2002; Cooper *et al.*, 2006), tandem mass spectrometry (Clariana *et al.*, 2010), and enzymatic methods (Berti *et al.*, 1988; Jabs *et al.*, 1990; Agarwal and Banerjee, 2009). These methods necessitate expensive laboratory equipment operated by skilled

personnel as well as complex sample preparation for a slow reading. Electrochemical biosensors have also been developed as they are comparatively cheap, require little to no sample preparation to provide instantaneous measurement. Despite the numerous enzymatic biosensors developed none have been applied to the detection of xanthine in urine.

The large current measured by the xanthine biosensors confirms the expected larger quantity of xanthine that is expected in urine (up to 161 µmoles per 24 hours in healthy human urine (Boulieu *et al.*, 1983)) as part of normal purine excretion. Urothelial ATP is known to be released during stretching (Vlaskovska *et al.*, 2001; Lewis and Lewis, 2006; Kumar *et al.*, 2010; Young *et al.*, 2012; Dunning-Davies *et al.*, 2013) and then cause local release of acetylcholine to stimulate detrusor contraction (Stenqvist *et al.*, 2017; Stenqvist, Aronsson, *et al.*, 2020), whilst also stimulating contraction via P2X receptors (Ford *et al.*, 2006). This suggests that the increase in urothelial ATP present in OAB would relate to an increase in urinary ATP (Silva-Ramos *et al.*, 2013; Firouzmand, Ajori and Young, 2020). This has been explored in a few papers where urinary ATP has been shown to be affected by age (Silva-Ramos *et al.*, 2013; Sugaya *et al.*, 2018), nucleotidases (Gutierrez Cruz *et al.*, 2023), urine production rate (McLatchie *et al.*, 2021), biological sex (Sugaya *et al.*, 2018), and water intake (Silva-Ramos *et al.*, 2013). ATP measurements are often corrected to creatinine or total urine volume for comparison between subjects. ATP is not derived from plasma, instead released locally into urine such that the amount accumulating in the bladder is expected to be fairly constant and the concentration is likely to decrease as urine production increases (McLatchie *et al.*, 2021). Though normalisation to urine volume for a specific time should give a more accurate

measurement of ATP, the same cannot be said for xanthine. The total quantity of xanthine will have a component of normal purine excretion, plus the locally released ATP.

The potential for ATP to be a marker for OAB is very compelling. The variability in urinary ATP and lack of correlation with volume found by Silva-Ramos et al points towards its instability and degradation. This is further confirmed by McLatchie et al that suggest that ATP increases over time and that concentration varies based off urine production rate. Considering the poor stability of ATP it is unlikely that the assay being used is going to give an accurate measurement of urothelial release. Detection of a stable metabolite like xanthine is more accurate than measuring ATP. Therefore the decrease in xanthine seen in our OAB data could be due to a compensatory mechanism whereby increased local ATP release then needs to be replenished so the salvage pathways are upregulated, resulting in reduced xanthine excretion.

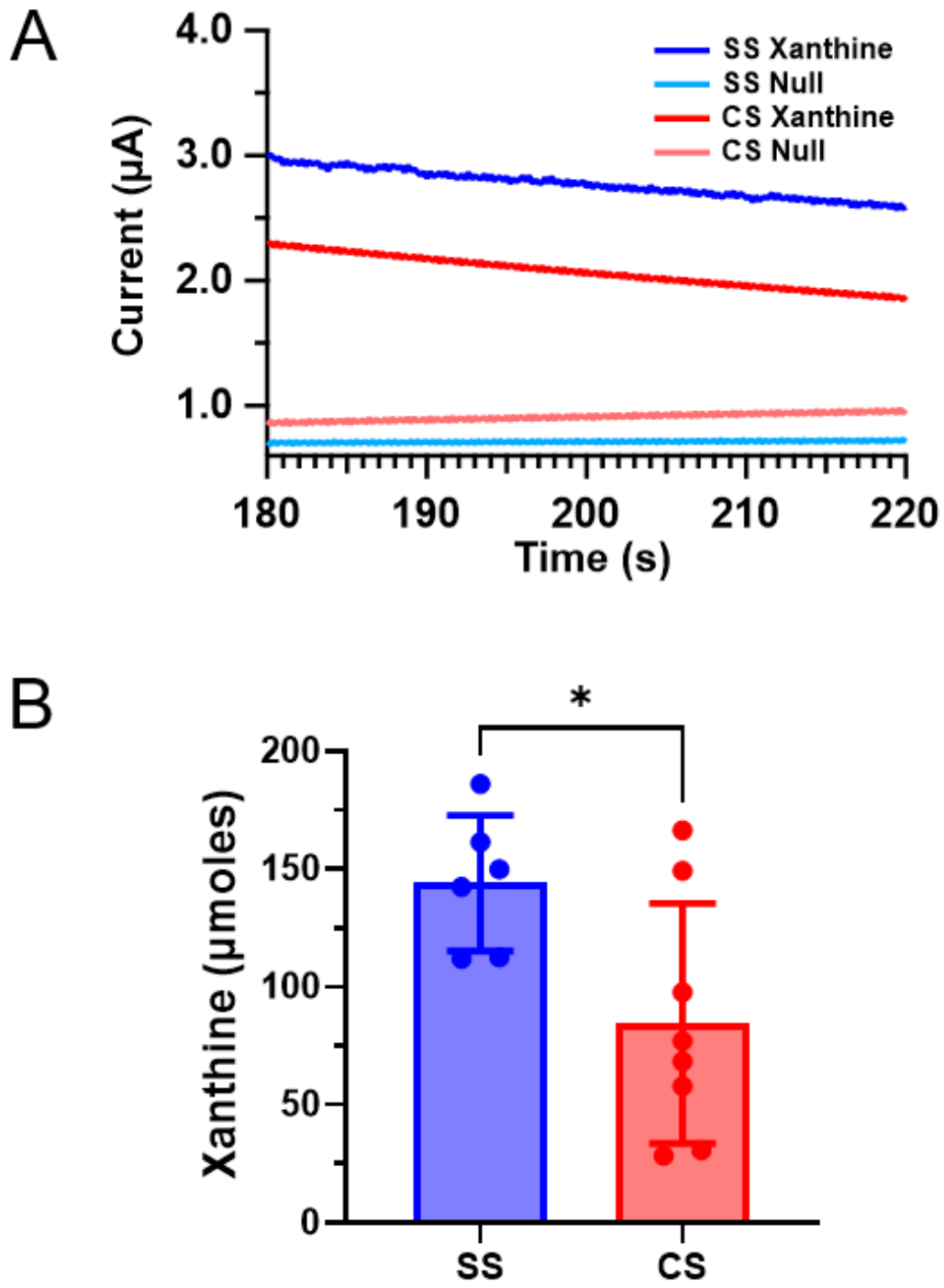

Figure 4.3.
Detection of xanthine in urine samples from saline injected rats (SS) and cyclophosphamide injected rats (CS). (A) Representative traces for xanthine biosensors and null sensors in urine from control or OAB induced Sprague-Dawley rats. (B) Total quantity of xanthine in urine sample for control (SS) *n = 6* or OAB (CS) *n =8* rats. Data analysed using unpaired two-tailed t test, p = 0.0250

4.3.4 Amperometric detection of nitrite in OAB

The null electrodes have been shown to detect nitrite at +0.85 V but not at +0.65 V (Chapter 3) allowing nitrite concentration to be measured in a complex matrix. Figure 4.4A shows the raw traces from nulls in either healthy rat urine (SS +0.85 V and SS +0.65 V) or rat OAB urine (CS +0.85 V and +0.65 V).

The current from the low voltage null (+ 0.65V) was subtracted from the high voltage null (+0.85 V) and the delta was converted to concentration using the nitrite calibration. This was then normalised using total micturition volume and shown in Figure 4.4B. The nitrite released was significantly increased in the OAB urine samples (unpaired two-tailed t test, p = 0. 0.0029).

Nitrite is regarded as a measure of nitric oxide (NO) due to it being a stable degradation product (Feelisch and Stamler, 1996; Gladwin *et al.*, 2005; Lundberg, Weitzberg and Gladwin, 2008). An indirect measurement of NO is necessary due to its short half-life of a few seconds (Andersson and Persson, 1994). NO is known to directly cause smooth muscle cell relaxation in the bladder (Fathian-Sabet *et al.*, 2001), as well as act on afferent nerve receptors to regulate relaxation (Bennett *et al.*, 1995; Masuda *et al.*, 2007; Kullmann *et al.*, 2008; Daly *et al.*, 2011). As OAB is thought to be due to increased involuntary bladder contractions it was hypothesised that local nitric oxide levels would decrease with symptom severity, and consequently urinary levels of nitrite would fall. Our nitrite electrodes show increased current in OAB, and this was confirmed to be nitrite in a separate experiment using a commercial platinum electrode (Patel *et al.*, 2020). This increase could be explained by the cholinergic release of NO from the inflamed bladder (Andersson, Tobin and Giglio, 2008). A study using human urine confirms elevated nitrite

with increased urinary frequency, as well as increased ATP/NO with OAB symptom severity (Firouzmand and Young, 2020). This supports the hypothesis that ATP is linked to bladder overactivity through activation of P2X3 receptors indirectly triggering NO release, which feeds back to reduce ATP release (Shen *et al.*, 2005; Munoz *et al.*, 2011). Therefore the ratio of xanthine to nitrite in urine could be a more stable marker for OAB than ATP/NO.

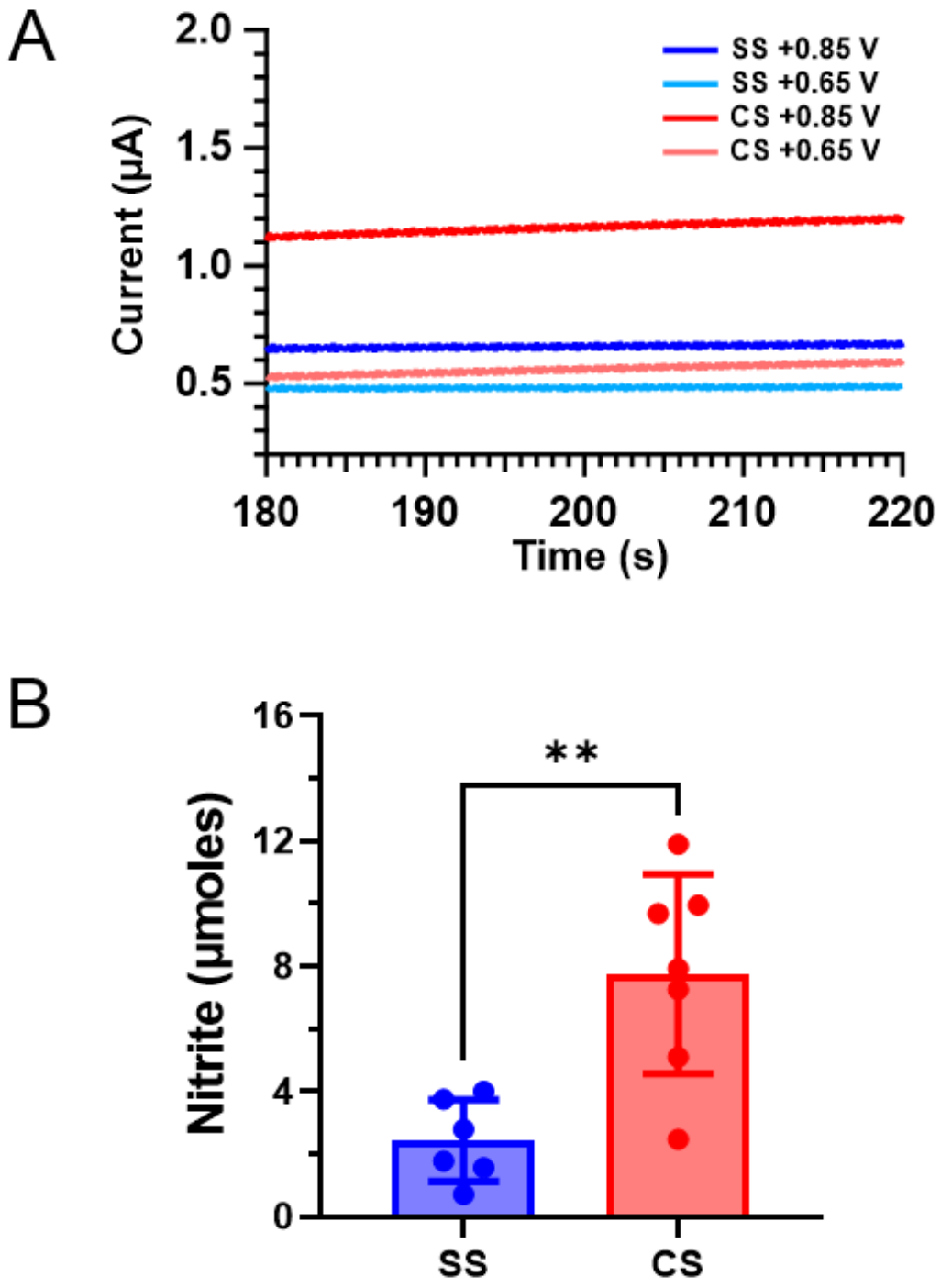

Figure 4.4.
Detection of nitrite in urine samples from Sprague-Dawley rats injected with saline (SS) or cyclophosphamide (CS). (A) Representative traces for nitrite sensors (+0.85 V) and background sensors (+0.65 V) in urine from control or OAB induced Sprague-Dawley rats. (B) Total quantity of nitrite in urine sample for control (SS) *n* = *6* or OAB (CS) *n* = *7* rats. Data analysed using unpaired two-tailed t test, p = 0. 0.0029.

4.3.5 Effect of OAB on physiological symptoms

The use of cyclophosphamide induced cystitis works as a model for OAB due to exhibiting the same clinical signs of patients with the disease. These are an increase in voiding events, increased detrusor activity, and pain (Giglio *et al.*, 2005; Boudes *et al.*, 2011). The model has also evaluated changes in bladder function through electrophysiology, histology, and pharmacology (Giglio *et al.*, 2005; Augé *et al.*, 2013; Stenqvist *et al.*, 2018). To confirm the effectiveness of the model functional data was collected, namely urine volume per micturition event (Figure 4.5A), micturition events per hour (Figure 4.5B), and inflammatory grade (Figure 4.5C).

Figure 4.5A shows how the use of cyclophosphamide statistically decreases the volume of urine per micturition event ($p = 0.0025$), whilst Figure 4.5B shows a statistical increase in micturitions per hour ($p = 0.0197$). Figure 4.5C shows a clear distinction in inflammatory grade between control and cyclophosphamide treated rats ($p = 0.0006$). This data aligns with the studies that confirmed the use of cyclophosphamide to induce OAB symptoms (Andersson *et al.*, 2011; Augé *et al.*, 2020).

This method of inducing OAB has allowed the exploration of the mechanisms behind the worsening symptoms. Cyclophosphamide causes bladder changes such as oedema, redness, and wall thickening(Giglio *et al.*, 2005). This correlates with evidence in the literature that inflammatory markers such as prostaglandin E2, BDNF (Frias *et al.*, 2013), NGF (Antunes-Lopes *et al.*, 2011), are elevated with OAB (McLatchie *et al.*, 2021). The disruption caused to the urothelium and smooth muscle layers seems responsible for the increased voiding of smaller micturition volumes (Giglio *et al.*, 2005). The treatment decreases sensitivity of urothelial muscarinic receptors, upregulates M1 and M5, and

affects purinergic afferent signalling (Giglio *et al.*, 2007; Burnstock, 2014; Aronsson *et al.*, 2015).

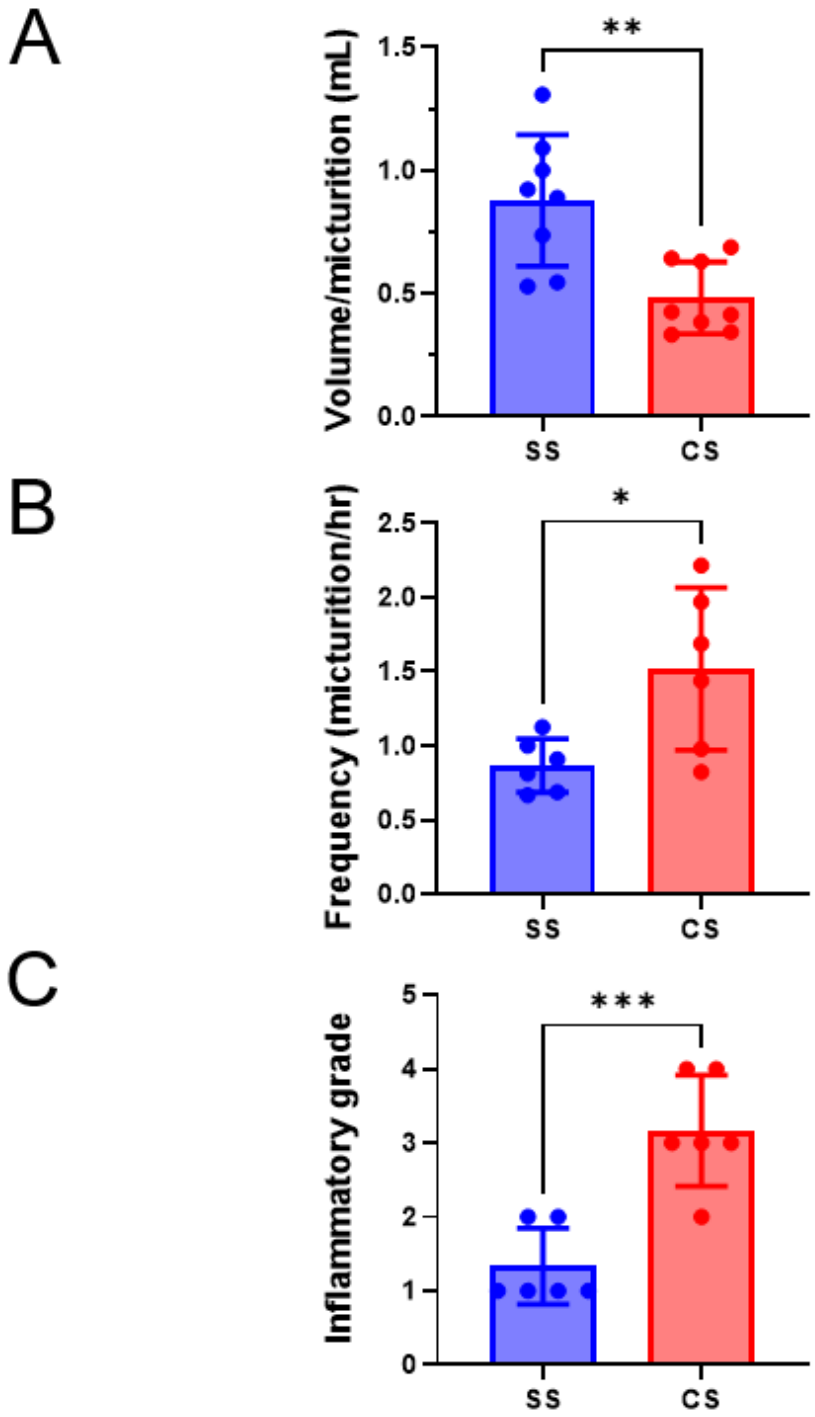

Figure 4.5.
Effect of cyclophosphamide injection on physiological parameters of Sprague-Dawley rats. (A) Urine volume per micturition between control and OAB (p = 0.0025) *n* = *8*. (B) Micturition per hour between control and OAB (p = 0.0197) *n* = *6*. (C) Level of bladder inflammation between control and OAB (p = 0.0006) *n* = *6*. All data analysed using unpaired two-tailed t test.

4.3.6 Relationship between urinary metabolites and volume per micturition

The functional data was then related to the quantity of signalling metabolites released in either healthy or OAB urine to see if a relationship could be determined.

Figure 4.6A shows no relationship between the choline quantity and volume per micturition. This is shown by the low Pearson r value of 0.067, which in conjunction with the non-significant difference in choline in OAB suggests it is not diagnostically useful.

Figure 4.6B shows a positive correlation between xanthine and volume per micturition, with an r value of 0.57. From a functional point of view, increased ATP would act locally via P2X receptors to increase contractions, or through afferent nerves to stimulate involuntary contractions. This would decrease volume per micturition. However, the methods used to detect this increased urinary ATP are affected by its fast degradation (Swennen *et al.*, 2008) and dilution effects (McLatchie *et al.*, 2021). Therefore a decrease in urinary xanthine could be due to increased local contractions induced by ATP, which then is re-up taken at a higher rate in OAB.

Figure 4.6C shows a strong negative correlation between nitrite and volume per micturition. The r value of -0.78 shows nitrite decreases as volume per micturition increases. This increase in nitrite suggests an increase in local nitric oxide, which induces smooth muscle relaxation. However, treatment with antimuscarinics and β3 agonists have shown to reduce this release of nitric oxide (Patel *et al.*, 2020). Therefore this increased urothelial NO is likely to be due to the increased inflammation of the bladder (Aronsson *et al.*, 2015). The release of NO regulates spontaneous detrusor contractions and the use of NO donors has been shown to slow these down (Moro, Leeds and Chess-Williams, 2012).

In summary, bladder dysfunction can be related to low urinary xanthine and high urinary nitrite.

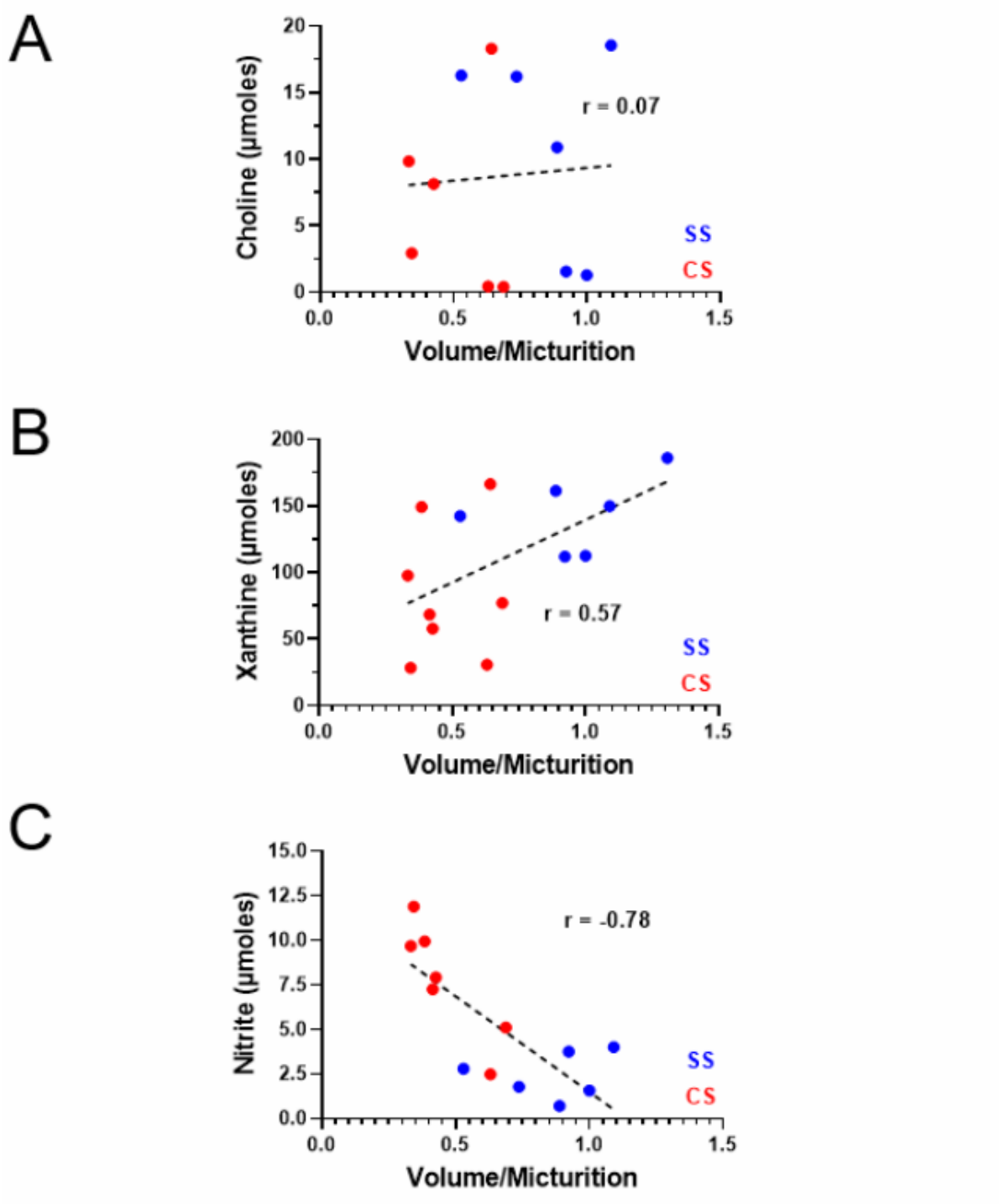

Figure 4.6.
Relationship between urinary metabolites and volume per micturition between control and OAB Sprague-Dawley rats. (A) Correlation between choline and volume per micturition. (B) Correlation between xanthine and volume per micturition (C) Correlation between nitrite and volume per micturition. All data analysed by calculating Pearson's correlation coefficient.

4.3.7 Relationship between urinary metabolites and urinary frequency

The relationship between urinary frequency and signalling molecules metabolites could be used to detect OAB, so correlations were determined between these variables.

Figure 4.7A shows the relationship between choline and urinary frequency. The slight negative correlation (r = -0.32) could indicate lower choline is associated with OAB and increased urinary frequency. As with Figure 4.6A the lack of significance between the choline data in Figure 4.2 weakens the association of urinary choline in OAB. From a functional point of view, increased urinary frequency would be controlled by increased cholinergic contractions (Kanai and Andersson, 2010).. A lower urinary choline with OAB could be due to increased re-uptake of choline to provide the acetylcholine to drive increased contractions.

Figure 4.7B shows a negative correlation between xanthine and urinary frequency (r = -0.58). As with decreased volume per micturition, the increase in urinary frequency is associated with OAB. The increase in frequency could be due to increased ATP release during filling, stimulating afferent nerves to send the impulse to void (Andersson, Tobin and Giglio, 2008). This increased ATP release would then require more ATP production and a decrease in xanthine excretion (Furuhashi, 2020).

Figure 4.7C shows a positive correlation between nitrite and urinary frequency in OAB. The strong correlation of 0.80 supports a relationship between increased nitrite and increased urinary frequency in OAB. Nitric oxide could also be stimulating afferent nerves and acting directly on detrusor smooth muscle. Furthermore, there is evidence that NO is linked to urothelial damage and inflammation, such that treatment with a NOS inhibitor decreases subsequent inflammation (Souza-Filho *et al.*, 1997). This would the

similarity in symptoms with UTI, where increased nitrite and increased urinary frequency is also present. Increased urinary nitrite in both conditions causing the same increase in urinary frequency confirms the involvement of NO causing OAB symptoms. This nitric oxide is then regulated upon treatment with antimuscarinics and β3 agonists.

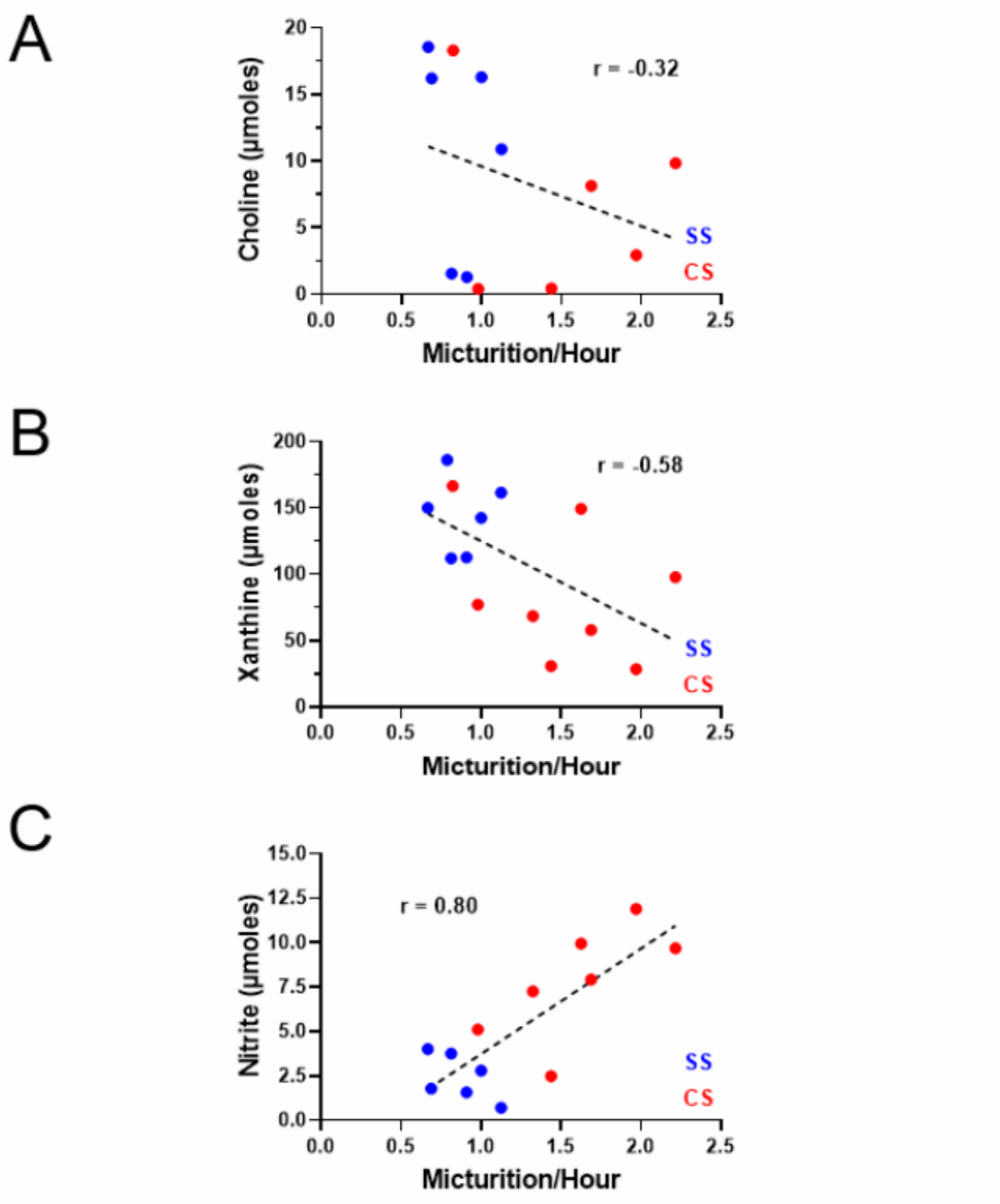

Figure 4.7.
Relationship between urinary metabolites and urinary frequency (micturition per hour) between control and OAB Sprague-Dawley rats. (A) Correlation between choline and micturition per hour. (B) Correlation between xanthine and micturition per hour. (C) Correlation between nitrite and micturition per hour. All data analysed by calculating Pearson's correlation coefficient.

4.3.8 Relationship between urinary metabolites and inflammation

The level of inflammation was related to the three urinary metabolites to see if correlations could be derived.

Figure 4.8A shows the inflammation related to the level of choline in control and OAB urine. There is a slight negative correlation of -0.22, which is weak in showing a relationship between choline and inflammation.

Figure 4.8B shows a negative correlation of -0.34 between xanthine and inflammation in OAB. Compared to frequency and volume this is the weakest correlation. Despite this the literature highlights ATP as a marker of inflammation (Gill *et al.*, 2015).

Figure 4.8C shows a positive correlation of 0.76 between inflammation nitrite in OAB. This is further supported by the statistical increase in nitrite in OAB and increase in inflammation with OAB. Increased nitric oxide signalling has clear relations to OAB and inflammation.

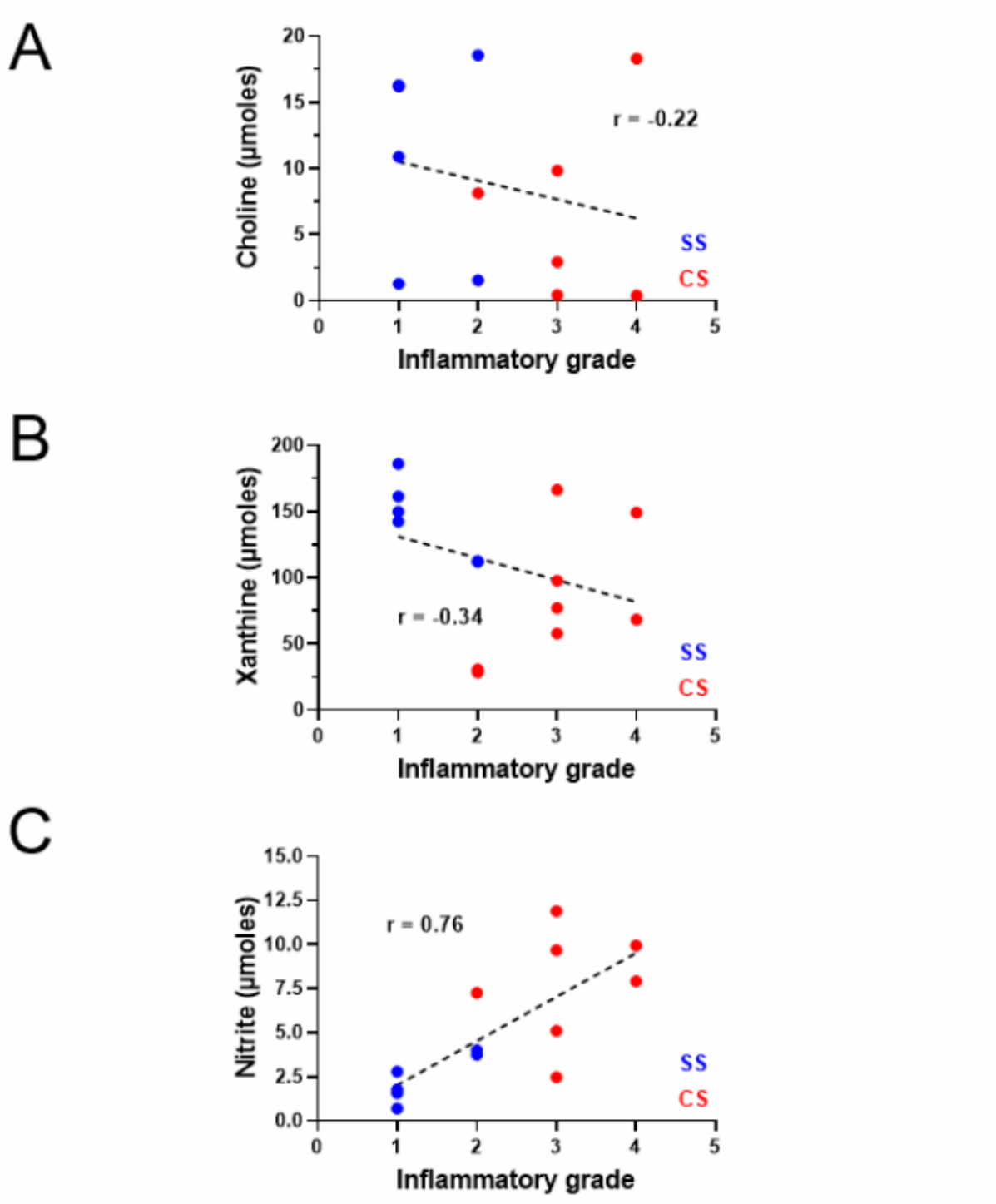

Figure 4.8.
Relationship between urinary metabolites and bladder inflammation between control and OAB Sprague-Dawley rats. (A) Correlation between choline and inflammatory grade. (B) Correlation between xanthine and inflammatory grade. (C) Correlation between nitrite and inflammatory grade. All data analysed by calculating Pearson's correlation coefficient.

4.4 Conclusion

The multi-analyte biosensor developed was tested in normal rat urine and OAB rat model urine. Results show no change in urinary choline, a statistical decrease in urinary xanthine, and an increase in urinary nitrite.

Increased nitrite in OAB urine has been confirmed with a commercial platinum electrode (Patel *et al.*, 2020), and is related to increased NO (Aronsson *et al.*, 2014). This increase shows positive correlation with symptom severity, specifically decreased micturition volume and increased urinary frequency. A lack of increase in choline could be due to slow breakdown of acetylcholine to choline in conjunction with large biological variation. The decrease in xanthine could be due to the diurnal changes in ATP (Silva-Ramos *et al.*, 2013) or background changes on purine metabolism (Antunes-Lopes and Cruz, 2019).

Chapter 5: Conclusions and Future work

5.1 Conclusions

The aim was to understand how urothelial signalling molecules are altered with OAB, and investigate their potential for use in a point of care diagnostic test. To achieve this goal sensors and biosensors were produced to detect these metabolites.

The urothelial molecules acetylcholine (ACh) (Yoshida *et al.*, 2004; McLatchie *et al.*, 2021), adenosine triphosphate (ATP) (Silva-Ramos *et al.*, 2013; Antunes-Lopes and Cruz, 2019), and nitric oxide (NO) (Munoz *et al.*, 2011) have links to OAB but their detection in urine can only be done using expensive assays or specialised lab equipment (Kirsch *et al.*, 2010; Firouzmand, Ajori and Young, 2020). Furthermore, the deterioration (Gill *et al.*, 2015; McLatchie *et al.*, 2021) or metabolism (Gutierrez Cruz *et al.*, 2023) of the molecules becomes a factor and changes in their metabolites may be easier to detect. As these signalling molecules are known to cause detrusor contraction or relaxation, the absolute concentration may be less important than the relative concentrations between them (Firouzmand, Ajori and Young, 2020; McLatchie *et al.*, 2021), further adding complexity to the diagnostic test.

Of the three signalling molecules, only NO and its metabolite nitrite are easily oxidisable at sensible voltages of electrodes of carbon and metal (Patel *et al.*, 2006; Amatore *et al.*, 2008; Fagan-Murphy *et al.*, 2016). The metabolites of ACh and ATP are not easily electroactive using conventional electrodes or electrochemical techniques (Xu and Venton, 2010; Baker, Bolger and Lowry, 2017; Pinyou *et al.*, 2022). The cheapest and most reliable method of detection is through the use of oxidase enzymes that generate peroxide proportional to the concentration of choline or xanthine for ACh and ATP

respectively. Peroxide is easily detected at metal electrodes (Hall, Khudaish and Hart, 1998), but can be detected cheaper and with geometrically tuneable electrodes using carbon composites (Abdalla *et al.*, 2021).

The carbon composite electrodes explored contained multi-walled carbon nanotubes (MWCNT) and had their detection to peroxide enhanced using transition metals, of which platinum black showed the most reliable and robust response. Composite paste was packed into 3D printed casings to highlight the concept that CAD could be used to create a urine sample pot with the different electrodes built in. Oxidase entrapment was prototyped using glucose oxidase, such that desirable features of the biosensor like reliability, stability, and sensitivity were explored.

The electrodes were then converted into biosensors through the entrapment of choline oxidase or xanthine oxidase within the BSA layer (Pundir and Devi, 2014; Baker, Bolger and Lowry, 2015). The reproducibility, sensitivity, and stability of both were tested in artificial urine. As to maximally detect peroxide a high voltage was required, and this would cause a problem as high concentrations of uric acid are present in urine samples and require a lower voltage. Nitrite was able to be detected at a voltage above uric acid, similar to that of peroxide. Therefore, to eliminate interference from easily oxidisable species the nitrite sensor was used to take a measurement of the background faradaic molecules (including nitrite) at a voltage of +0.85 V. This nitrite sensor was constructed identical to the biosensors but omitting the enzyme such that it would detect a current that could be subtracted from either biosensor to calculate the component solely due to the analyte. Then to calculate the nitrite component another sensor of the same

construction held at +0.65 V can have its current subtracted from the +0.85 V sensor to isolate the concentration of nitrite.

This allowed the choline oxidase (ChOx) and xanthine oxidase (XO) sensors to both use the same nitrite (+0.85 V null) sensor, maximising stability and minimising variation. Biosensors were tailored such that their sensitivity would match the expected physiological ranges of the analyte. The choline biosensor followed Michaelis Menten kinetics, whilst the xanthine biosensor showed two linear ranges, potentially due to the enzyme generating peroxide and uric acid. The nitrite sensor in artificial urine after subtraction had a linear range within the physiological measurements to be measured.

To validate the simultaneous detection of the three analytes for OAB a rat model was used. Measurements were taken for blinded samples of either control or OAB induced rat urine. The values were normalised for total urine volume over 16 hours and analysed. OAB showed no statistical difference for choline, a statistical decrease for xanthine, and a statistical increase for nitrite. The increased levels of nitrite have been confirmed using a commercial platinum electrode (Patel *et al.*, 2020), and match other groups findings in the field.

There is conflicting data regarding urinary choline in OAB (Firouzmand, Ajori and Young, 2020; Sheyn *et al.*, 2020, 2022), supporting the hypothesis that the quantity is less important than the relationship between choline and the other metabolites (Firouzmand, Ajori and Young, 2020; McLatchie *et al.*, 2021). The decrease in urinary xanthine seems counter to the expected increase in urothelial ATP seen with disease (Silva-Ramos *et al.*, 2013), but purine excretion is affected by many factors that could be altered in a diseased state (Sugaya *et al.*, 2018; Gutierrez Cruz *et al.*, 2023).

To investigate these metabolites further they were related to functional data of the rat. The model accurately produces symptoms of OAB as seen by the decrease in urine per void, and increase in urinary frequency (Andersson *et al.*, 2011). Urgency cannot be evaluated in the rat model, but the inflammation of the bladder can be (Augé *et al.*, 2020), and could be used as a proxy for severity. Each metabolite data point was matched to the functional data and correlations were plotted to see if there was a relationship between quantity and symptom severity.

Choline showed no change in volume, a mild increase in frequency and a mild increase with inflammation. As choline did not show a statistical decrease, and these functional changes are slight, a relationship could not be confirmed. However, xanthine showed a strong decrease in volume, increase in frequency, and increase in inflammation. The correlations with r values above 0.5 could suggest predictive power for lower xanthine to be linked with symptom severity. This is further supported by the increased inflammation seen with the urinary symptoms. Nitrite also showed clear relationships with r values above 0.7 for decreased volume and increased frequency, supporting the use of nitrite as a marker for disease (Firouzmand and Young, 2020).

In conclusion, xanthine and nitrite show relationships with OAB symptom severity that could allow them to be used for diagnosis. However choline requires more validation to see if a relationship exists.

5.2 Future work

The work that has produced this multi-analyte biosensing platform for OAB diagnosis shows potential in multiple directions.

The work in Chapter 2 focused on producing composite electrodes suitable for the detection of peroxide for subsequent use in oxidase biosensors. The fabrication of the composite for the working electrode is the most labour intensive and time-consuming step. This could be improved by dispersing the carbon nanotubes and platinum black in a different non-conductive binder. Other research groups have used beeswax as a binder, which although greener and more sustainable, still requires a drying time of 24 hours (de Oliveira *et al.*, 2021). Thermosetting plastics like PLA would make an ideal binder for the components, and a dual nozzle 3D printer can easily print the working electrode within a non-conductive design (Shergill *et al.*, 2022; Hussain *et al.*, 2023). This method is advantageous as the electrode fabrication is automated, reproducible, quick, and can be used almost instantly after being produced (Singh Shergill *et al.*, 2022). This method retains the advantages of the epoxy composite such as complex geometry, low cost, rugged electrodes.

The latter half of Chapter 2 focuses on the entrapment of the oxidase enzyme on the electrode surface, which also has scope for improvement. Firstly, optimisation of layer thickness on the electrode could improve sensitivity by reducing the distance the analyte needs to diffuse. Further improvements could be made by switching the BSA layer for a different polymer such as Nafion (Wahono *et al.*, 2012), PEDOT (Peteu *et al.*, 2021), polyaniline (PANI)(Osuna *et al.*, 2022), polymethylmethacrylate (PMMA), polyphenol (Patel *et al.*, 2011), polypyrrole (ppy) (Wang and Musameh, 2005; Karunakaran *et al.*,

2020; Mentana *et al.*, 2020), polyvinylidene fluoride (PVDF) (Ghorbani Zamani *et al.*, 2019). Furthermore, other methods of attaching the enzyme to the electrode surface may increase sensitivity at the expense of stability (Nöll and Nöll, 2011).

Chapter 3 focuses on the tailoring of the biosensors for detection in urine. The main limitation is the voltage to detect peroxide being above that for uric acid. Though this was overcome using a null sensor, a better way would be to use a material that oxidises peroxide preferentially to uric acid, or to use a permselective layer. The use of Nafion could reduce the interference from uric acid as well as nitrite (Wang, Musameh and Lin, 2003; Yuan *et al.*, 2005), allowing only the analyte to generate current. However, increasing layers decreases response time and increases variability.

Chapter 4 focuses on the urinary metabolites and their relation to OAB. Urothelial acetylcholine is implicated in OAB (Yoshida *et al.*, 2004, 2006) but urinary acetylcholine alone has not been fully explored as a biomarker (Firouzmand, Ajori and Young, 2020). There are contradictory studies for urinary choline (Sheyn *et al.*, 2020, 2022), indicating the need to fully explore the effect of age on choline levels.

There is evidence supporting urinary ATP is elevated in OAB (Sugaya *et al.*, 2009, 2018; Silva-Ramos *et al.*, 2013; Firouzmand and Young, 2020; Firouzmand, Ajori and Young, 2020; McLatchie *et al.*, 2021) and one study showing a decrease (Cheng *et al.*, 2013). The release of ATP doesn't relate to creatinine and can be stimulated with bladder distension from drinking (McLatchie *et al.*, 2021). Using ATP/NO seems to be more predictive than ATP alone, potentially indicating a method of normalising that doesn't rely on creatinine (Firouzmand and Young, 2020). It would be useful to tease out how urinary ATP relates to xanthine, as xanthine levels may be stable through normal purine excretion.

There is some evidence for urinary nitric oxide in OAB (Firouzmand and Young, 2020; Mossa *et al.*, 2020) despite its purportedly short half-life (Winder *et al.*, 2014). The evidence for increased urinary nitrite in OAB animal models is clear (Patel *et al.*, 2020), but would seem contradictory in human urine as nitrite is used to diagnose UTIs. Therefore the electrochemical detection of nitrite in human urine could potentially differentiate between OAB or UTI due to the increased sensitivity of the technique compared to the colorimetric test strips.

For all three of these biomarkers, the effect of urine volume on biomarker concentration needs exploration, as well as their stability in the urinary matrix (Gill *et al.*, 2015). This would be part of the effort of normalising the biomarker such that urine volume does not bias the measurement. Perhaps osmolality instead of creatinine should be used, as it would be a measure of urine concentration as biomarker release is not due to glomerular filtration rate (Wu and Li, 2016).

There are other urinary biomarkers in the recent literature that could help in the diagnosis of OAB such as BDNF (Bhide *et al.*, 2013; Wang *et al.*, 2014; Alkis *et al.*, 2017), NGF (Kuo, 2012; Seth *et al.*, 2013; Alkis *et al.*, 2017), malondialdehyde (Rada *et al.*, 2020), and h8-OHdG (Dokumacioglu *et al.*, 2018), but the construction of a cheap point-of-care device for these needs much more research.

References

Aafria, S. *et al.* (2022) 'Electrochemical biosensing of uric acid: A review', *Microchemical Journal*. Elsevier B.V., 182(June), p. 107945. doi: 10.1016/j.microc.2022.107945.

Abdalla, A. *et al.* (2021) 'Bicomponent composite electrochemical sensors for sustained monitoring of hydrogen peroxide in breast cancer cells', *Electrochimica Acta*. Elsevier Ltd, 398, p. 139314. doi: 10.1016/j.electacta.2021.139314.

Agarwal, A. *et al.* (2014) 'What is the most bothersome lower urinary tract symptom? Individual- and population-level perspectives for both men and women', *European Urology*. European Association of Urology, 65(6), pp. 1211–1217. doi: 10.1016/j.eururo.2014.01.019.

Agarwal, A. and Banerjee, U. C. (2009) 'Screening of Xanthine Oxidase Producing Microorganisms Using Nitroblue Tetrazolium Based Colorimetric Assay Method', *The Open Biotechnology Journal*, 3(1), pp. 46–49. doi: 10.2174/1874070700903010046.

Ahlawat, J., Sharma, M. and Shekhar Pundir, C. (2023) 'Advances in biosensor development for detection of acetylcholine', *Microchemical Journal*. Elsevier B.V., 190(September 2022), p. 108620. doi: 10.1016/j.microc.2023.108620.

Ahmad, R. *et al.* (2018) 'Deposition of nanomaterials: A crucial step in biosensor fabrication', *Materials Today Communications*, 17(July), pp. 289–321. doi: 10.1016/j.mtcomm.2018.09.024.

Alhajj, M., Zubair, M. and Farhana, A. (2023) 'Enzyme linked immunosorbent assay', *StatPearls*.

Alkis, O. *et al.* (2017) 'The use of biomarkers in the diagnosis and treatment of overactive bladder: Can we predict the patients who will be resistant to treatment?', *Neurourology and Urodynamics*, 36(2), pp. 390–393. doi: 10.1002/nau.22939.

Amatore, C. *et al.* (2008) 'Real-time amperometric analysis of reactive oxygen and nitrogen species released by single immunostimulated macrophages', *ChemBioChem*, 9(9), pp. 1472–1480. doi: 10.1002/cbic.200700746.

Anderson, K. E. (1993) 'Pharmacology of lower urinary tract smooth muscles and penile erectile tissues', *Pharmacological Reviews*, 45(3), pp. 253–308.

Andersson, K.-E. (2004) 'Mechanisms of Disease: central nervous system involvement in overactive bladder syndrome', *Nature Clinical Practice Urology*, 1(2), pp. 103–108. doi: 10.1038/ncpuro0021.

Andersson, K. E. (2015) 'Purinergic signalling in the urinary bladder', *Autonomic Neuroscience: Basic and Clinical*. Elsevier B.V., 191, pp. 78–81. doi: 10.1016/j.autneu.2015.04.012.

Andersson, K. E. and Persson, K. (1994) 'Nitric oxide synthase and nitric oxide-mediated effects in lower urinary tract smooth muscles', *World Journal of Urology*, 12(5), pp. 274–280. doi: 10.1007/BF00191207.

Andersson, M. *et al.* (2011) 'Pharmacological modulation of the micturition pattern in normal and cyclophosphamide pre-treated conscious rats', *Autonomic Neuroscience: Basic and Clinical*, 159(1–2), pp. 77–83. doi: 10.1016/j.autneu.2010.08.008.

Andersson, M. C., Tobin, G. and Giglio, D. (2008) 'Cholinergic nitric oxide release from the urinary bladder mucosa in cyclophosphamide-induced cystitis of the anaesthetized rat', *British Journal of Pharmacology*. John Wiley & Sons, Ltd, 153(7), pp. 1438–1444. doi: 10.1038/BJP.2008.6.

Antunes-Lopes, T. *et al.* (2011) 'Biomarkers in overactive bladder: A new objective and noninvasive tool?', *Advances in Urology*, 2011. doi: 10.1155/2011/382431.

Antunes-Lopes, T. and Cruz, F. (2019) 'Urinary Biomarkers in Overactive Bladder: Revisiting the Evidence in 2019', *European Urology Focus*. European Association of Urology, 5(3), pp. 329–336. doi: 10.1016/j.euf.2019.06.006.

Aoki, Y. *et al.* (2017) 'Urinary incontinence in women', *Nature Reviews Disease Primers*, 3(9), pp. 661–671. doi: 10.1038/nrdp.2017.42.

Apodaca, G. (2004) 'The uroepithelium: Not just a passive barrier', *Traffic*, 5(3), pp. 117–128. doi: 10.1046/j.1600-0854.2003.00156.x.

Arms, L. and Vizzard, M. A. (2011) 'Neuropeptides in Lower Urinary Tract Function', in Andersson, K.-E. and Michel, M. C. (eds) *Urinary Tract*. Berlin, Heidelberg: Springer Berlin Heidelberg, pp. 395–423. doi: 10.1007/978-3-642-16499-6_19.

Aronsson, P. *et al.* (2010) 'Assessment and characterization of purinergic contractions and relaxations in the rat urinary bladder', *Basic and Clinical Pharmacology and Toxicology*, 107(1), pp. 603–613. doi: 10.1111/j.1742-7843.2010.00554.x.

Aronsson, P. *et al.* (2014) 'Inhibition of nitric oxide synthase prevents muscarinic and purinergic functional changes and development of cyclophosphamide-induced cystitis in the rat', *BioMed Research International*, 2014. doi: 10.1155/2014/359179.

Aronsson, P. *et al.* (2015) 'Cyclophosphamide-induced alterations of the micturition reflex in a novel in situ urinary bladder model in the anesthetized rat', *Neurourology and Urodynamics*, 34(4), pp. 375–380. doi: 10.1002/nau.22562.

Augé, C. *et al.* (2013) 'Relevance of the cyclophosphamide-induced cystitis model for pharmacological studies targeting inflammation and pain of the bladder', *European Journal of Pharmacology*. Elsevier, 707(1–3), pp. 32–40. doi: 10.1016/j.ejphar.2013.03.008.

Augé, C. *et al.* (2020) 'Characterization and Validation of a Chronic Model of Cyclophosphamide-Induced Interstitial Cystitis/Bladder Pain Syndrome in Rats', *Frontiers in Pharmacology*, 11(August), pp. 1–11. doi: 10.3389/fphar.2020.01305.

Aydin, S. (2015) 'A short history, principles, and types of ELISA, and our laboratory experience with peptide/protein analyses using ELISA', *Peptides*. Elsevier Inc., 72, pp. 4–15. doi: 10.1016/j.peptides.2015.04.012.

Baker, K. L. *et al.* (2019) 'Characterisation of a Platinum-based Electrochemical Biosensor for Real-time Neurochemical Analysis of Choline', *Electroanalysis*, 31(1), pp.

129–136. doi: 10.1002/elan.201800642.

Baker, K. L., Bolger, F. B. and Lowry, J. P. (2015) 'A microelectrochemical biosensor for real-time in vivo monitoring of brain extracellular choline', *Analyst*. Royal Society of Chemistry, 140(11), pp. 3738–3745. doi: 10.1039/c4an02027h.

Baker, K. L., Bolger, F. B. and Lowry, J. P. (2017) 'Development of a microelectrochemical biosensor for the real-time detection of choline', *Sensors and Actuators, B: Chemical*. Elsevier B.V., 243, pp. 412–420. doi: 10.1016/j.snb.2016.11.110.

Balasubramanian, P. *et al.* (2019) 'Rational Design of Cu@Cu2O Nanospheres Anchored B, N Co-doped Mesoporous Carbon: A Sustainable Electrocatalyst to Assay Eminent Neurotransmitters Acetylcholine and Dopamine', *ACS Sustainable Chemistry and Engineering*. American Chemical Society, 7(6), pp. 5669–5680. doi: 10.1021/acssuschemeng.8b04473.

Ballarin, B. *et al.* (2007) 'Enzyme electrodes based on sono-gel containing ferrocenyl compounds', *Biosensors and Bioelectronics*, 22(7), pp. 1317–1322. doi: 10.1016/j.bios.2006.05.034.

Bard, A. J. and Faulkner, L. R. (2001) *Electrochemical methods, fundamentals and applications*. Second, *Journal of Chemical Education*. Second. John Wiley & Sons.

Beale, D. J. *et al.* (2018) *Review of recent developments in GC–MS approaches to metabolomics-based research*, *Metabolomics*. Springer US. doi: 10.1007/s11306-018-1449-2.

Beckel, J. M. and Birder, L. A. (2012) 'Differential expression and function of nicotinic acetylcholine receptors in the urinary bladder epithelium of the rat', *Journal of Physiology*, 590(6), pp. 1465–1480. doi: 10.1113/jphysiol.2011.226860.

Bedioui, F. and Griveau, S. (2013) 'Electrochemical Detection of Nitric Oxide: Assessement of Twenty Years of Strategies', *Electroanalysis*, 25(3), pp. 587–600. doi: 10.1002/elan.201200306.

Bedretdinova, D. *et al.* (2016) 'Prevalence of Female Urinary Incontinence in the General Population According to Different Definitions and Study Designs', *European Urology*. European Association of Urology, 69(2), pp. 256–264. doi: 10.1016/j.eururo.2015.07.043.

Bennett, B. C. *et al.* (1995) 'Neural Control of Urethral Outlet Activity in Vivo: Role of Nitric Oxide', *The Journal of Urology*, 153(6), pp. 2004–2009. doi: 10.1016/S0022-5347(01)67391-9.

Bennion, B. J. and Daggett, V. (2003) 'The molecular basis for the chemical denaturation of proteins by urea', *Proceedings of the National Academy of Sciences of the United States of America*, 100(9), pp. 5142–5147. doi: 10.1073/pnas.0930122100.

Berti, G. *et al.* (1988) 'Enzymatic Colorimetric Method for the Determination of Inorganic Phosphorus in Serum and Urine', *Clinical Chemistry and Laboratory Medicine*, 26(6), pp. 399–404. doi: 10.1515/cclm.1988.26.6.399.

Bhalla, N. *et al.* (2016) 'Introduction to biosensors', *Essays in Biochemistry*, 60(June), pp. 1–8. doi: 10.1042/EBC20150001.

Bhide, A. A. *et al.* (2013) 'Biomarkers in overactive bladder', *International Urogynecology Journal*, 24(7), pp. 1065–1072. doi: 10.1007/s00192-012-2027-1.

Boguszewska, K. *et al.* (2019) 'Review: immunoassays in DNA damage and instability detection', *Cellular and Molecular Life Sciences*. Springer International Publishing, 76(23), pp. 4689–4704. doi: 10.1007/s00018-019-03239-6.

Borges, L., Dermargos, A. and Hatanaka, E. (2022) 'Technical bioanalytical considerations for detection and quantification of cytokines in ELISA assays', *Cytokine*. Elsevier Ltd, 151(May 2021), p. 155615. doi: 10.1016/j.cyto.2021.155615.

Boudes, M. *et al.* (2011) 'Functional characterization of a chronic cyclophosphamide-induced overactive bladder model in mice', *Neurourology and Urodynamics*, 30(8), pp. 1659–1665. doi: 10.1002/nau.21180.

Boulieu, R. *et al.* (1983) 'Hypoxanthine and xanthine levels determined by high-performance liquid chromatography in plasma, erythrocyte, and urine samples from healthy subjects: The problem of hypoxanthine level evolution as a function of time', *Analytical Biochemistry*, 129(2), pp. 398–404. doi: 10.1016/0003-2697(83)90568-7.

Brading, A. F. (1997) 'A myogenic basis for the overactive bladder', *Urology*, 50(6, Supplement 1), pp. 57–67. doi: https://doi.org/10.1016/S0090-4295(97)00591-8.

Brading, A. F. (2006) 'Spontaneous activity of lower urinary tract smooth muscles: correlation between ion channels and tissue function', *The Journal of Physiology*, 570(1), pp. 13–22. doi: 10.1113/jphysiol.2005.097311.

Bright, E. *et al.* (2014) 'Developing and Validating the International Consultation on Incontinence Questionnaire Bladder Diary', *European Urology*, 66(2), pp. 294–300. doi: 10.1016/j.eururo.2014.02.057.

Brooks, T. and Keevil, C. W. (1997) 'A simple artificial urine for the growth of urinary pathogens', *Letters in Applied Microbiology*, 24(3), pp. 203–206. doi: 10.1046/j.1472-765X.1997.00378.x.

Burnett, A. L. *et al.* (1997) 'Urinary bladder-urethral sphincter dysfunction in mice with targeted disruption of neuronal nitric oxide synthase models idiopathic voiding disorders in humans', *Nature Medicine*, 3(5), pp. 571–574. doi: 10.1038/nm0597-571.

Burnstock, G. (1972) 'Purinergic nerves', *Pharmacological Reviews*, 24(3).

Burnstock, G. *et al.* (1978) 'Direct evidence for ATP release from non-adrenergic, non-cholinergic ("purinergic") nerves in the guinea-pig taenia coli and bladder', *European Journal of Pharmacology*, 49(2), pp. 145–149. doi: 10.1016/0014-2999(78)90070-5.

Burnstock, G. (2009) 'Purinergic cotransmission', *Experimental Physiology*, 94(1), pp. 20–24. doi: 10.1113/expphysiol.2008.043620.

Burnstock, G. (2013) 'Chapter 3 - Cotransmission in the autonomic nervous system', in Buijs, R. M. and Swaab, D. F. (eds) *Autonomic Nervous System*. Elsevier (Handbook of Clinical Neurology), pp. 23–35. doi: https://doi.org/10.1016/B978-0-444-53491-0.00003-1.

Burnstock, G. (2014) ‘Purinergic signalling in the urinary tract in health and disease’, *Purinergic Signalling*, 10(1), pp. 103–155. doi: 10.1007/s11302-013-9395-y.

Burnstock, G., Dumsday, B. and Smythe, A. (1972) ‘Atropine resistant excitation of the urinary bladder: the possibility of transmission via nerves releasing a purine nucleotide’, *British Journal of Pharmacology*, 44(3), pp. 451–461. doi: 10.1111/j.1476-5381.1972.tb07283.x.

Caine, M., Raz, S. and Zeigler, M. (1975) ‘Adrenergic and Cholinergic Receptors in the Human Prostate, Prostatic Capsule and Bladder Neck’, *British Journal of Urology*, 47(2), pp. 193–202. doi: 10.1111/j.1464-410X.1975.tb03947.x.

Cass, T., Cooper, J. M. and Cass, A. E. G. (2004) *Biosensors*. 2nd edn. Oxford University Press (Practical approach series). Available at: https://books.google.co.uk/books?id=nQQFvgAACAAJ.

Çevik, S. (2016) ‘Xanthine biosensor based on XO/AuNP/PtNP/MWCNT hybrid nanocomposite modified GCPE’, *Biotechnology and Bioprocess Engineering*, 21(2), pp. 314–320. doi: 10.1007/s12257-016-0014-y.

Chang, R. S. L. *et al.* (2000) ‘In vitro studies on L-771,688 (SNAP 6383), a new potent and selective α(1A)-adrenoceptor antagonist’, *European Journal of Pharmacology*, 409(3), pp. 301–312. doi: 10.1016/S0014-2999(00)00854-2.

Chapple, C. R., Steers, W. D. and Evans, C. P. (2020) *Urologic Principles and Practice*. 2nd edn. Edited by C. R. Chapple, W. D. Steers, and C. P. Evans. Springer International Publishing. doi: 10.1007/978-3-030-28599-9.

Chatziharalambous, D. *et al.* (2016) ‘Analytical performance of ELISA assays in Urine: One more bottleneck towards biomarker validation and clinical implementation’, *PLoS ONE*, 11(2), pp. 1–12. doi: 10.1371/journal.pone.0149471.

Chen, X., Molliver, D. C. and Gebhart, G. F. (2010) ‘The P2Y2 receptor sensitizes mouse bladder sensory neurons and facilitates purinergic currents’, *Journal of Neuroscience*, 30(6), pp. 2365–2372. doi: 10.1523/JNEUROSCI.5462-09.2010.

Cheng, Y. *et al.* (2013) ‘Correlation between cystometric volumes, ATP release, and pH in women with overactive bladder versus controls’, *Neurourology and Urodynamics*, 32(7), pp. 969–973. doi: 10.1002/nau.22344.

Chopra, B. *et al.* (2008) ‘Expression and function of rat urothelial P2Y receptors’, *American Journal of Physiology - Renal Physiology*, 294(4), pp. 821–829. doi: 10.1152/ajprenal.00321.2006.

Choudhary, M. *et al.* (2015) ‘Neurophysiological modeling of bladder afferent activity in the rat overactive bladder model’, *Journal of Physiological Sciences*. Springer Japan, 65(4), pp. 329–338. doi: 10.1007/s12576-015-0370-y.

Clariana, M. *et al.* (2010) ‘Analysis of seven purines and pyrimidines in pork meat products by ultra high performance liquid chromatography-tandem mass spectrometry’, *Journal of Chromatography A*, 1217(26), pp. 4294–4299. doi: 10.1016/j.chroma.2010.04.033.

Clark, M. F., Lister, R. M. and Bar-Joseph, M. (1986) ‘ELISA techniques’, in, pp. 742–766. doi: 10.1016/0076-6879(86)18114-6.

Clay, M. and Monbouquette, H. G. (2018) ‘A Detailed Model of Electroenzymatic Glutamate Biosensors to Aid in Sensor Optimization and in Applications in Vivo’, *ACS Chemical Neuroscience*, 9(2), pp. 241–251. doi: 10.1021/acschemneuro.7b00262.

Cockayne, D. A. *et al.* (2005) ‘P2X2 knockout mice and P2X2/P2X3 double knockout mice reveal a role for the P2X2 receptor subunit in mediating multiple sensory effects of ATP’, *Journal of Physiology*, 567(2), pp. 621–639. doi: 10.1113/jphysiol.2005.088435.

Colhoun, A. F. *et al.* (2017) ‘A pilot study to measure dynamic elasticity of the bladder during urodynamics’, *Neurourology and Urodynamics*, 36(4), pp. 1086–1090. doi: 10.1002/nau.23043.

Colley, A. L. *et al.* (2006) ‘Examination of the spatially heterogeneous electroactivity of boron-doped diamond microarray electrodes’, *Analytical Chemistry*, 78(8), pp. 2539–2548. doi: 10.1021/ac0520994.

Contreras-Sanz, A. *et al.* (2016) ‘Altered urothelial ATP signaling in a major subset of human overactive bladder patients with pyuria’, *American Journal of Physiology-Renal Physiology*, 311(4), pp. F805–F816. doi: 10.1152/ajprenal.00339.2015.

Cooper, N. *et al.* (2006) ‘Quantification of uric acid, xanthine and hypoxanthine in human serum by HPLC for pharmacodynamic studies’, *Journal of Chromatography B: Analytical Technologies in the Biomedical and Life Sciences*, 837(1–2), pp. 1–10. doi: 10.1016/j.jchromb.2006.02.060.

Corcos, J. (2001) *The Urinary Sphincter*. CRC Press. doi: 10.3109/9780203904510.

Corcos, J., Ginsberg, D. and Karsenty, G. (2015) *Textbook of the Neurogenic Bladder*. 3rd edn. CRC Press. Available at: https://www.crcpress.com/Textbook-of-the-Neurogenic-Bladder/c-Ginsberg-Karsenty/p/book/9781482215540#googlePreviewContainer.

Cox, L. and Rovner, E. S. (2018) *Contemporary Pharmacotherapy of Overactive Bladder*, *Contemporary Pharmacotherapy of Overactive Bladder*. doi: 10.1007/978-3-319-97265-7.

Cox, P. J. (1979) ‘Cyclophosphamide cystitis-Identification of acrolein as the causative agent’, *Biochemical Pharmacology*, 28(13), pp. 2045–2049. doi: 10.1016/0006-2952(79)90222-3.

Coyne, K. S. *et al.* (2012) ‘Racial differences in the prevalence of overactive bladder in the United States from the Epidemiology of LUTS (EpiLUTS) study’, *Urology*. Elsevier Inc., 79(1), pp. 95–101. doi: 10.1016/j.urology.2011.09.010.

Coyne, K. S. *et al.* (2013) ‘The prevalence of lower urinary tract symptoms (LUTS) and overactive bladder (OAB) by racial/ethnic group and age: Results from OAB-POLL’, *Neurourology and Urodynamics*, 32(3), pp. 230–237. doi: 10.1002/nau.22295.

Creed, K. E., Loxley, R. A. and Phillips, J. K. (2010) ‘Functional expression of muscarinic and purinoceptors in the urinary bladder of male and female rats and guinea pigs’, *Journal of Smooth Muscle Research*, 46(4), pp. 201–215. doi: 10.1540/jsmr.46.201.

Cruz, P. M. R. *et al.* (2015) 'Clinical features and diagnostic usefulness of antibodies to clustered acetylcholine receptors in the diagnosis of seronegative myasthenia gravis', *JAMA Neurology*, 72(6), pp. 642–649. doi: 10.1001/jamaneurol.2015.0203.

Czauderna, M. and Kowalczyk, J. (2000) 'Quantification of allantoin, uric acid, xanthine and hypoxanthine in ovine urine by high-performance liquid chromatography and photodiode array detection', *Journal of Chromatography B: Biomedical Sciences and Applications*, 744(1), pp. 129–138. doi: 10.1016/S0378-4347(00)00239-5.

Dale, H. (1914) 'The action of certain esters and ethers of choline, and their relation to muscarine', *Journal of Pharmacology and Experimental Therapeutics*. American Society for Pharmacology and Experimental Therapeutics, 6(2), pp. 147–190. Available at: https://jpet.aspetjournals.org/content/6/2/147.

Dale, H. (1934) 'Chemical transmission of the effects of nerve impulses', *British Medical Journal*, 1(3827), pp. 835–841. doi: 10.1136/bmj.1.3827.835.

Dalkıran, B., Erden, P. E. and Kılıç, E. (2016) 'Construction of an Electrochemical Xanthine Biosensor Based on Graphene/Cobalt Oxide Nanoparticles/Chitosan Composite for Fish Freshness Detection', *Journal of the Turkish Chemical Society, Section A: Chemistry*, 3(3), pp. 23–44. doi: 10.18596/jotcsa.54485.

Dallosso, H. M. *et al.* (2004) 'Nutrient composition of the diet and the development of overactive bladder: A longitudinal study in women', *Neurourology and Urodynamics*, 23(3), pp. 204–210. doi: 10.1002/nau.20028.

Daly, D. M. *et al.* (2011) 'The afferent system and its role in lower urinary tract dysfunction', *Current Opinion in Urology*, 21(4), pp. 268–274. doi: 10.1097/MOU.0b013e3283476ea2.

Dasgupta, J., Elliott, R. A. and Tincello, D. G. (2009) 'Modification of rat detrusor muscle contraction by ascorbic acid and citric acid involving enhanced neurotransmitter release and Ca2+ influx', *Neurourology and Urodynamics*, 28(6), pp. 542–548. doi: https://doi.org/10.1002/nau.20701.

Deruyver, Y. *et al.* (2018) 'Intravesical Activation of the Cation Channel TRPV4 Improves Bladder Function in a Rat Model for Detrusor Underactivity', *European Urology*. The Author(s), 74(3), pp. 336–345. doi: 10.1016/j.eururo.2018.05.020.

Dervisevic, M. *et al.* (2016) 'Novel amperometric xanthine biosensor based on xanthine oxidase immobilized on electrochemically polymerized 10-[4H-dithieno(3,2-b:2',3'-d)pyrrole-4-yl]decane-1-amine film', *Sensors and Actuators, B: Chemical*, 225, pp. 181–187. doi: 10.1016/j.snb.2015.11.043.

Dervisevic, M., Dervisevic, E., Senel, M., *et al.* (2017) 'Construction of ferrocene modified conducting polymer based amperometric urea biosensor', *Enzyme and Microbial Technology*, 102(January), pp. 53–59. doi: 10.1016/j.enzmictec.2017.04.002.

Dervisevic, M., Dervisevic, E., Çevik, E., *et al.* (2017) 'Novel electrochemical xanthine biosensor based on chitosan–polypyrrole–gold nanoparticles hybrid bio-nanocomposite platform', *Journal of Food and Drug Analysis*, 25(3), pp. 510–519. doi: 10.1016/j.jfda.2016.12.005.

Dervisevic, M., Dervisevic, E. and Şenel, M. (2019) 'Recent progress in nanomaterial-based electrochemical and optical sensors for hypoxanthine and xanthine. A review', *Microchimica Acta*, 186(12). doi: 10.1007/s00604-019-3842-6.

Dokumacioglu, E. *et al.* (2018) 'Measuring urinary 8-hydroxy-2'-deoxyguanosine and malondialdehyde levels in women with overactive bladder', *Investigative and Clinical Urology*, 59(4), p. 252. doi: 10.4111/icu.2018.59.4.252.

Dowdall, M. J., Boyne, A. F. and Whittaker, V. P. (1974) 'Adenosine triphosphate. A constituent of cholinergic synaptic vesicles.', *The Biochemical journal*, 140(1), pp. 1–12. doi: 10.1042/bj1400001.

Drake, M. J. *et al.* (2005) 'Localized contractions in the normal human bladder and in urinary urgency', *BJU International*, 95(7), pp. 1002–1005. doi: 10.1111/j.1464-410X.2005.05455.x.

Drake, R. L. (Richard L. *et al.* (2020) *Gray's anatomy for students, Fourth edition*. Philadelphia, PA: Elsevier. Available at: http://prism.librarymanagementcloud.co.uk/brighton-ac/items/1501071.

Dunning-Davies, B. M. *et al.* (2013) 'The regulation of ATP release from the urothelium by adenosine and transepithelial potential', *BJU International*, 111(3), pp. 505–513. doi: 10.1111/j.1464-410X.2012.11421.x.

El-Beqqali, A., Kussak, A. and Abdel-Rehim, M. (2007) 'Determination of dopamine and serotonin in human urine samples utilizing microextraction online with liquid chromatography/electrospray tandem mass spectrometry', *Journal of Separation Science*, 30(3), pp. 421–424. doi: 10.1002/jssc.200600369.

Elbadawi, A. (1996) 'Functional anatomy of the organs of micturition', *Urologic Clinics of North America*, 23(2), pp. 177–210. doi: 10.1016/S0094-0143(05)70304-9.

Elgrishi, N. *et al.* (2018) 'A Practical Beginner's Guide to Cyclic Voltammetry', *Journal of Chemical Education*, 95(2), pp. 197–206. doi: 10.1021/acs.jchemed.7b00361.

Engvall, E. (2010) 'The ELISA, enzyme-linked immunosorbent assay', *Clinical Chemistry*, 56(2), pp. 319–320. doi: 10.1373/clinchem.2009.127803.

Engvall, E., Jonsson, K. and Perlmann, P. (1971) 'Antiserum , immunoglobulin fraction , and specific antibodies Iodinated proteins', *Biochim. Biophys. Acta.*, 251, pp. 427–434.

Engvall, E. and Perlmann, P. (1972) 'Enzyme-Linked Immunosorbent Assay, Elisa: III. Quantitation of Specific Antibodies by Enzyme-Labeled Anti-Immunoglobulin in Antigen-Coated Tubes1', *The Journal of Immunology*, 109(1), pp. 129–135. doi: 10.4049/jimmunol.109.1.129.

Fagan-Murphy, A. *et al.* (2016) 'Electrochemical sensor for the detection of multiple reactive oxygen and nitrogen species from ageing central nervous system homogenates', *Mechanisms of Ageing and Development*. Elsevier Ireland Ltd, 160(2), pp. 28–31. doi: 10.1016/j.mad.2016.10.002.

Fathian-Sabet, B. *et al.* (2001) 'Localization of constitutive nitric oxide synthase isoforms and the nitric oxide target enzyme soluble guanylyl cyclase in the human bladder',

Journal of Urology, 165(5 I), pp. 1724–1729. doi: 10.1016/s0022-5347(05)66402-6.

Feelisch, M. and Stamler, J. S. (1996) *Methods in nitric oxide research*. Edited by M. Feelisch and J. Stamler. Wiley-Blackwell.

Feldman, B. *et al.* (2000) 'Freestyle(TM): A small-volume electrochemical glucose sensor for home blood glucose testing', *Diabetes Technology and Therapeutics*, 2(2), pp. 221–229. doi: 10.1089/15209150050025177.

Finney, S. M. *et al.* (2006) 'Antimuscarinic drugs in detrusor overactivity and the overactive bladder syndrome: Motor or sensory actions?', *BJU International*, 98(3), pp. 503–507. doi: 10.1111/j.1464-410X.2006.06258.x.

Firouzmand, S., Ajori, L. and Young, J. S. (2020) 'New participant stratification and combination of urinary biomarkers and confounders could improve diagnostic accuracy for overactive bladder', *Scientific Reports*, 10(3085), pp. 1–10. doi: 10.1038/s41598-020-59973-6.

Firouzmand, S. and Young, J. S. (2020) 'A pilot study to investigate the associations of urinary concentrations of NO, ATP and derivatives with overactive bladder symptom severity', *Experimental Physiology*, 105(6), pp. 932–939. doi: 10.1113/EP088450.

Fisher, A. C. (1998) *Electrode Dynamics*. Second. Bath: University Oxford Press.

Ford, A. P. D. W. *et al.* (2006) 'Purinoceptors as therapeutic targets for lower urinary tract dysfunction', *British Journal of Pharmacology*, 147(SUPPL. 2), pp. 132–143. doi: 10.1038/sj.bjp.0706637.

Fowler, C. J., Griffiths, D. and De Groat, W. C. (2008) 'The neural control of micturition', *Nature Reviews Neuroscience*, 9(6), pp. 453–466. doi: 10.1038/nrn2401.

Franken, J. *et al.* (2014) 'TRP channels in lower urinary tract dysfunction', *British Journal of Pharmacology*, 171(10), pp. 2537–2551. doi: 10.1111/bph.12502.

Frias, B. *et al.* (2013) 'Brain-derived neurotrophic factor, acting at the spinal cord level, participates in bladder hyperactivity and referred pain during chronic bladder inflammation', *Neuroscience*, 234, pp. 88–102. doi: 10.1016/j.neuroscience.2012.12.044.

Fry, C. H. *et al.* (2007) 'The function of suburothelial myofibroblasts in the bladder', *Neurourology and Urodynamics*, 26(S6), pp. 914–919. doi: 10.1002/nau.20483.

Furchgott, R. and Zawadski, J. V (1980) 'The obligatory role of endothelial cells in the relaxation of atrial smooth muscle.', *Nature*, 288(November), pp. 373–376.

Furuhashi, M. (2020) 'New insights into purine metabolism in metabolic diseases: Role of xanthine oxidoreductase activity', *American Journal of Physiology - Endocrinology and Metabolism*, 319(5), pp. E827–E834. doi: 10.1152/ajpendo.00378.2020.

Gao, X. *et al.* (2021) 'Rapid Fabrication of Superhydrophilic Micro/Nanostructured Nickel Foam Toward High-Performance Glucose Sensor', *Advanced Materials Interfaces*, 8(7), pp. 1–8. doi: 10.1002/admi.202002133.

Ghorbani Zamani, F. *et al.* (2019) 'Current trends in the development of conducting

polymers-based biosensors', *TrAC - Trends in Analytical Chemistry*. Elsevier Ltd, 118, pp. 264–276. doi: 10.1016/j.trac.2019.05.031.

Giglio, D. *et al.* (2005) 'Altered muscarinic receptor subtype expression and functional responses in cyclophosphamide induced cystitis in rats', *Autonomic Neuroscience: Basic and Clinical*, 122(1–2), pp. 9–20. doi: 10.1016/j.autneu.2005.07.005.

Giglio, D. *et al.* (2007) 'In vitro characterization of parasympathetic and sympathetic responses in cyclophosphamide-induced cystitis in the rat', *Basic and Clinical Pharmacology and Toxicology*, 100(2), pp. 96–108. doi: 10.1111/j.1742-7843.2007.00014.x.

Gill, A., Zajda, J. and Meyerhoff, M. E. (2019) 'Comparison of electrochemical nitric oxide detection methods with chemiluminescence for measuring nitrite concentration in food samples', *Analytica Chimica Acta*. Elsevier Ltd, 1077, pp. 167–173. doi: 10.1016/j.aca.2019.05.065.

Gill, K. *et al.* (2015) 'Urinary ATP as an indicator of infection and inflammation of the urinary tract in patients with lower urinary tract symptoms', *BMC Urology*, 15(1), pp. 1–9. doi: 10.1186/s12894-015-0001-1.

Gladwin, M. T. *et al.* (2005) 'The Emerging Biology of the Nitrite Anion', *Nature Chemical Biology*, 1(6), pp. 308–314. doi: 10.1038/nchembio1105-308.

Goepel, M. *et al.* (1998) 'Muscarinic receptor subtypes in porcine detrusor: Comparison with humans and regulation by bladder augmentation', *Urological Research*, 26(2), pp. 149–154. doi: 10.1007/s002400050038.

Griess, P. (1879) 'Bemerkungen zu der Abhandlung der HH. Weselsky und Benedikt „Ueber einige Azoverbindungen"', *Berichte der deutschen chemischen Gesellschaft*, 12(1), pp. 426–428. doi: https://doi.org/10.1002/cber.187901201117.

Griffith, D. P., Musher, D. M. and Itin, C. (1976) 'Urease. The primary cause of infection-induced urinary stones', *Investigative urology*, 13(5), p. 346—350. Available at: http://europepmc.org/abstract/MED/815197.

Griffiths, D. J. and Fowler, C. J. (2013) 'The micturition switch and its forebrain influences', *Acta Physiologica*, 207(1), pp. 93–109. doi: 10.1111/apha.12019.

de Groat, W. C., Griffiths, D. and Yoshimura, N. (2015) 'Neural control of the lower urinary tract', *Comprehensive Physiology*, 5(1), pp. 327–396. doi: 10.1002/cphy.c130056.

de Groat, William C. and Yoshimura, N. (2015) 'Anatomy and physiology of the lower urinary tract', in *Progrès en Urologie*. 1st edn. Elsevier B.V., pp. 61–108. doi: 10.1016/B978-0-444-63247-0.00005-5.

de Groat, William C and Yoshimura, N. (2015) 'Chapter 5 - Anatomy and physiology of the lower urinary tract', in Vodušek, D. B. and Boller, F. (eds) *Neurology of Sexual and Bladder Disorders*. Elsevier (Handbook of Clinical Neurology), pp. 61–108. doi: https://doi.org/10.1016/B978-0-444-63247-0.00005-5.

Gu, X. and Wang, X. (2021) 'An overview of recent analysis and detection of acetylcholine', *Analytical Biochemistry*. Elsevier Inc., 632(June), p. 114381. doi:

10.1016/j.ab.2021.114381.

Guinn, E. J. *et al.* (2011) 'Quantifying why urea is a protein denaturant, whereas glycine betaine is a protein stabilizer', *Proceedings of the National Academy of Sciences of the United States of America*, 108(41), pp. 16932–16937. doi: 10.1073/pnas.1109372108.

Gutierrez Cruz, A. *et al.* (2023) 'Urinary ATP Levels Are Controlled by Nucleotidases Released from the Urothelium in a Regulated Manner', *Metabolites*, 13(1). doi: 10.3390/metabo13010030.

Häbler, H. J., Jänig, W. and Koltzenburg, M. (1990) 'Activation of unmyelinated afferent fibres by mechanical stimuli and inflammation of the urinary bladder in the cat.', *The Journal of Physiology*, 425(1), pp. 545–562. doi: https://doi.org/10.1113/jphysiol.1990.sp018117.

Hall, S. B., Khudaish, E. A. and Hart, A. L. (1998) 'Electrochemical oxidation of hydrogen peroxide at platinum electrodes. Part II: effect of potential', *Electrochimica Acta*, 43(14–15), pp. 2015–2024. doi: 10.1016/S0013-4686(97)10116-5.

Hamdi, N., Wang, J. and Monbouquette, H. G. (2005) 'Polymer films as permselective coatings for H2O2-sensing electrodes', *Journal of Electroanalytical Chemistry*, 581(2), pp. 258–264. doi: 10.1016/j.jelechem.2005.04.028.

Hanna-Mitchell, A. T. *et al.* (2007) 'Non-neuronal acetylcholine and urinary bladder urothelium', *Life Sciences*. Elsevier Inc., 80(24–25), pp. 2298–2302. doi: 10.1016/j.lfs.2007.02.010.

Hannestad, Y. S. *et al.* (2000) 'A community-based epidemiological survey of female urinary incontinence':, *Journal of Clinical Epidemiology*, 53(11), pp. 1150–1157. doi: 10.1016/S0895-4356(00)00232-8.

Hanno, P. M. *et al.* (2014) *Penn Clinical Manual of Urology, 2nd Edition*. 2nd edn, *ProtoView*. 2nd edn. Beaverton: Copyright Clearance Center PP - Beaverton. Available at: https://www.proquest.com/other-sources/penn-clinical-manual-urology-2nd-edition-online/docview/1651925384/se-2?accountid=9727.

Hashim, H. and Abrams, P. (2006) 'Is the Bladder a Reliable Witness for Predicting Detrusor Overactivity?', *Journal of Urology*, 175(1), pp. 191–194. doi: 10.1016/S0022-5347(05)00067-4.

Hashitani, H., Bramich, N. J. and Hirst, G. D. S. (2000) 'Mechanisms of excitatory neuromuscular transmission in the guinea-pig urinary bladder', *Journal of Physiology*, 524(2), pp. 565–579. doi: 10.1111/j.1469-7793.2000.t01-2-00565.x.

Hasuzawa, N. *et al.* (2020) 'Physiopathological roles of vesicular nucleotide transporter (VNUT), an essential component for vesicular ATP release', *Biochimica et Biophysica Acta (BBA) - Biomembranes*. Elsevier, 1862(12), p. 183408. doi: 10.1016/j.bbamem.2020.183408.

Haylen, B. T. *et al.* (2010) 'An International Urogynecological Association / International Continence Society Joint Report on the Terminology for Female Pelvic Floor Dysfunction', *Neurourology and urodynamics*, 29, pp. 4–20. doi: 10.1007/s00192-009-0976-9.

Heller, A. and Feldman, B. (2010) 'Electrochemistry in diabetes management', *Accounts of Chemical Research*, 43(7), pp. 963–973. doi: 10.1021/ar9002015.

Hellström, D., Johansson, E. and Grennberg, K. (1999) 'Storage of human urine: Acidification as a method to inhibit decomposition of urea', *Ecological Engineering*, 12(3–4), pp. 253–269. doi: 10.1016/S0925-8574(98)00074-3.

Hicks, R. M. (1975) 'The mammalian urinary bladder: an accommodating organ.', *Biological reviews of the Cambridge Philosophical Society*, 50(2), pp. 215–46. Available at: http://www.ncbi.nlm.nih.gov/pubmed/1100129.

Hu, G. *et al*. (2008) 'Electrocatalytic oxidation and simultaneous determination of uric acid and ascorbic acid on the gold nanopartides-modified glassy carbon electrode', *Electrochimica Acta*, 53(22), pp. 6610–6615. doi: 10.1016/j.electacta.2008.04.054.

Hua, L. *et al*. (2008) 'Urea denaturation by stronger dispersion interactions with proteins than water implies a 2-stage unfolding', *Proceedings of the National Academy of Sciences of the United States of America*, 105(44), pp. 16928–16933. doi: 10.1073/pnas.0808427105.

Huang, I. W. *et al*. (2021) 'Electroenzymatic choline sensing at near the theoretical performance limit', *Analyst*. Royal Society of Chemistry, 146(3), pp. 1040–1047. doi: 10.1039/d0an01939a.

Hussain, K. K. *et al*. (2023) 'Exploring Different Carbon Allotrope Thermoplastic Composites for Electrochemical Sensing', *ACS Applied Polymer Materials*. doi: 10.1021/acsapm.3c00349.

Ikariyama, Y. *et al*. (1989) 'Electrochemical Fabrication of Amperometric Microenzyme Sensor', *Journal of The Electrochemical Society*, 136(3), pp. 702–706. doi: 10.1149/1.2096713.

Ikeda, Y. *et al*. (2012) 'Botulinum neurotoxin serotype a suppresses neurotransmitter release from afferent as well as efferent nerves in the urinary bladder', *European Urology*, 62(6), pp. 1157–1164. doi: 10.1016/j.eururo.2012.03.031.

De Irazu, S. *et al*. (2001) 'Multimembrane carbon fiber microelectrodes for amperometric determination of serotonin in human urine', *Analyst*, 126(4), pp. 495–500. doi: 10.1039/b009703i.

Irwin, D. E. *et al*. (2006) 'Population-Based Survey of Urinary Incontinence, Overactive Bladder, and Other Lower Urinary Tract Symptoms in Five Countries: Results of the EPIC Study', *European Urology*, 50(6), pp. 1306–1315. doi: 10.1016/j.eururo.2006.09.019.

Ishihama, H. *et al*. (2006) 'Activation of α 1D Adrenergic Receptors in the Rat Urothelium Facilitates the Micturition Reflex', *Journal of Urology*, 175(1), pp. 358–364. doi: 10.1016/S0022-5347(05)00016-9.

Iverson, N. M., Hofferber, E. M. and Stapleton, J. A. (2018) 'Nitric oxide sensors for biological applications', *Chemosensors*, 6(1). doi: 10.3390/chemosensors6010008.

Jabs, C. M. *et al*. (1990) 'Adenosine, inosine and hypoxanthine/xanthine measured in tissue and plasma by a luminescence method', *Clinical Chemistry*, 36(1), pp. 81–87. doi:

10.1093/clinchem/36.1.81.

Jänig, W. and Morrison, J. F. B. B. (1986) ‘Chapter 7 Functional properties of spinal visceral afferents supplying abdominal and pelvic organs, with special emphasis on visceral nociception’, in Cervero, F. and Morrison, J. F. B. (eds) *Visceral Sensation*. Elsevier (Progress in Brain Research), pp. 87–114. doi: https://doi.org/10.1016/S0079-6123(08)62758-2.

Janoš, P. (2003) ‘Separation methods in the chemistry of humic substances’, *Journal of Chromatography A*, 983(1–2), pp. 1–18. doi: 10.1016/S0021-9673(02)01687-4.

Jayakumar, K., Bennett, R. and Leech, D. (2021) ‘Electrochemical glucose biosensor based on an osmium redox polymer and glucose oxidase grafted to carbon nanotubes: A design-of-experiments optimisation of current density and stability’, *Electrochimica Acta*. Elsevier Ltd, 371, p. 137845. doi: 10.1016/j.electacta.2021.137845.

Jeon, W. Y. *et al.* (2022) ‘A stable glucose sensor with direct electron transfer, based on glucose dehydrogenase and chitosan hydro bonded multi-walled carbon nanotubes’, *Biochemical Engineering Journal*. Elsevier B.V., 187(August), p. 108589. doi: 10.1016/j.bej.2022.108589.

Jespersen, N. D. (1975) ‘A Thermochemical Study of the Hydrolysis of Urea by Urease’, *Journal of the American Chemical Society*, 97(7), pp. 1662–1667. doi: 10.1021/ja00840a006.

Jin, J. *et al.* (2010) ‘Enzymatic flow injection method for rapid determination of choline in urine with electrochemiluminescence detection’, *Bioelectrochemistry*. Elsevier B.V., 79(1), pp. 147–151. doi: 10.1016/j.bioelechem.2009.12.005.

Jost, S. P., Gosling, J. A. and Dixon, J. S. (1989) ‘The morphology of normal human bladder urothelium’, *Journal of anatomy*, 167(PG-103-15), pp. 103–115. Available at: NS -.

Kalimuthu, P., Leimkühler, S. and Bernhardt, P. V. (2012) ‘Low-potential amperometric enzyme biosensor for xanthine and hypoxanthine’, *Analytical Chemistry*, 84(23), pp. 10359–10365. doi: 10.1021/ac3025027.

Kanai, A. and Andersson, K.-E. (2010) ‘Bladder Afferent Signaling: Recent Findings’, *Journal of Urology*, 183(4), pp. 1288–1295. doi: 10.1016/j.juro.2009.12.060.

Kang, B. C., Park, B. S. and Ha, T. J. (2019) ‘Highly sensitive wearable glucose sensor systems based on functionalized single-wall carbon nanotubes with glucose oxidase-nafion composites’, *Applied Surface Science*. Elsevier, 470(September 2018), pp. 13–18. doi: 10.1016/j.apsusc.2018.11.101.

Kapil, V. *et al.* (2020) ‘The noncanonical pathway for in vivo nitric oxide generation: The nitrate-nitrite-nitric oxide pathway’, *Pharmacological Reviews*, 72(3), pp. 692–766. doi: 10.1124/pr.120.019240.

Karunakaran, C. *et al.* (2020) ‘Electrochemical biosensors for point-of-care applications’, *Defence Science Journal*, 70(5), pp. 549–556. doi: 10.14429/DSJ.70.16359.

Kausaite-Minkstimiene, A. *et al.* (2011) ‘Evaluation of amperometric glucose biosensors

based on glucose oxidase encapsulated within enzymatically synthesized polyaniline and polypyrrole', *Sensors and Actuators, B: Chemical*. Elsevier B.V., 158(1), pp. 278–285. doi: 10.1016/j.snb.2011.06.019.

Kawashima, K. and Fujii, T. (2008) 'Basic and clinical aspects of non-neuronal acetylcholine: Overview of non-neuronal cholinergic systems and their biological significance', *Journal of Pharmacological Sciences*. Elsevier B.V., 106(2), pp. 167–173. doi: 10.1254/jphs.FM0070073.

Khandelwal, P., Abraham, S. N. and Apodaca, G. (2009) 'Cell biology and physiology of the uroepithelium', *American journal of physiology. Renal physiology*, 297(6), pp. F1477-501. doi: 10.1152/ajprenal.00327.2009.

Killoran, S. J. and O'Neill, R. D. (2008) 'Characterization of permselective coatings electrosynthesized on Pt-Ir from the three phenylenediamine isomers for biosensor applications', *Electrochimica Acta*, 53(24), pp. 7303–7312. doi: 10.1016/j.electacta.2008.03.076.

Kim, D. Y. *et al.* (2013) 'Heterogeneous electron-transfer rate constants for ferrocene and ferrocene carboxylic acid at boron-doped diamond electrodes in a room temperature ionic liquid', *Electrochimica Acta*. Elsevier Ltd, 94, pp. 49–56. doi: 10.1016/j.electacta.2013.01.140.

Kirsch, S. H. *et al.* (2010) 'Quantification of acetylcholine, choline, betaine, and dimethylglycine in human plasma and urine using stable-isotope dilution ultra performance liquid chromatography-tandem mass spectrometry', *Journal of Chromatography B: Analytical Technologies in the Biomedical and Life Sciences*. Elsevier B.V., 878(32), pp. 3338–3344. doi: 10.1016/j.jchromb.2010.10.016.

Kissinger, P. T. and Heineman, W. R. (1983) 'Cyclic voltammetry', *Journal of Chemical Education*, 60(9), pp. 702–706. doi: 10.1021/ed060p702.

Klingler, C. H. (2016) 'Glycosaminoglycans: how much do we know about their role in the bladder?', *Urologia*, 83, pp. 11–14. doi: 10.5301/uro.5000184.

Van Der Kloot, W. and Molgó, J. (1994) 'Quantal acetylcholine release at the vertebrate neuromuscular junction', *Physiological Reviews*, 74(4), pp. 899–991. doi: 10.1152/physrev.1994.74.4.899.

Kock, R., Delvoux, B. and Greiling, H. (1993) 'A High-Performance Liquid Chromatographie Method for the Determination of Hypoxanthine, Xanthine, Uric Acid and Allantoin in Serum', *Clinical Chemistry and Laboratory Medicine*, 31(5), pp. 303–310. doi: 10.1515/cclm.1993.31.5.303.

Van Koppen, C. J. and Kaiser, B. (2003) 'Regulation of muscarinic acetylcholine receptor signaling', *Pharmacology and Therapeutics*, 98(2), pp. 197–220. doi: 10.1016/S0163-7258(03)00032-9.

Kozub, B. R., Rees, N. V. and Compton, R. G. (2010) 'Electrochemical determination of nitrite at a bare glassy carbon electrode; why chemically modify electrodes?', *Sensors and Actuators, B: Chemical*, 143(2), pp. 539–546. doi: 10.1016/j.snb.2009.09.065.

Krajewska, B. (2009) 'Ureases I. Functional, catalytic and kinetic properties: A review',

Journal of Molecular Catalysis B: Enzymatic, 59(1–3), pp. 9–21. doi: 10.1016/j.molcatb.2009.01.003.

Kreft, M. E. *et al.* (2010) 'Formation and maintenance of blood-urine barrier in urothelium', *Protoplasma*, 246(1), pp. 3–14. doi: 10.1007/s00709-010-0112-1.

Kullmann, F. A. *et al.* (2008) 'Activation of muscarinic receptors in rat bladder sensory pathways alters reflex bladder activity', *Journal of Neuroscience*, 28(8), pp. 1977–1987. doi: 10.1523/JNEUROSCI.4694-07.2008.

Kulyk, B. *et al.* (2022) 'Laser-induced graphene from paper for non-enzymatic uric acid electrochemical sensing in urine', *Carbon*, 197(June), pp. 253–263. doi: 10.1016/j.carbon.2022.06.013.

Kumar, V. *et al.* (2010) 'In Vitro Release of Adenosine Triphosphate from the Urothelium of Human Bladders with Detrusor Overactivity, Both Neurogenic and Idiopathic', *European Urology*. European Association of Urology, 57(6), pp. 1087–1092. doi: 10.1016/j.eururo.2009.11.042.

Kuo, H. C. (2012) 'Potential Biomarkers Utilized to Define and Manage Overactive Bladder Syndrome', *LUTS: Lower Urinary Tract Symptoms*, 4(SUPPL. 1), pp. 32–41. doi: 10.1111/j.1757-5672.2011.00131.x.

Kurtz, T. W. *et al.* (1986) 'Liquid-chromatographic measurements of inosine, hypoxanthine, and xanthine in studies of fructose-induced degradation of adenine nucleotides in humans and rats.', *Clinical Chemistry*, 32(5), pp. 782–786. doi: 10.1093/clinchem/32.5.782.

Langley, J. N. and Anderson, H. K. (1896) 'The Innervation of the Pelvic and adjoining Viscera: Part VII. Anatomical Observations', *The Journal of Physiology*, 20(4–5), pp. 372–406. doi: 10.1113/jphysiol.1896.sp000629.

Lartigue-Mattei, C. *et al.* (1990) 'Plasma and blood assay of xanthine and hypoxanthine by gas chromatography-mass spectrometry: physiological variations in humans', *Journal of Chromatography B: Biomedical Sciences and Applications*, 529(C), pp. 93–101. doi: 10.1016/S0378-4347(00)83810-4.

Laube, N., Mohr, B. and Hesse, A. (2001) 'Laser-probe-based investigation of the evolution of particle size distributions of calcium oxalate particles formed in artificial urines', *Journal of Crystal Growth*, 233(1–2), pp. 367–374. doi: 10.1016/S0022-0248(01)01547-0.

Lee, I. *et al.* (2019) 'Development of a third-generation glucose sensor based on the open circuit potential for continuous glucose monitoring', *Biosensors and Bioelectronics*. Elsevier B.V., 124–125(September 2018), pp. 216–223. doi: 10.1016/j.bios.2018.09.099.

Lewis, S. A. and Lewis, J. R. (2006) 'Kinetics of urothelial ATP release', *American Journal of Physiology - Renal Physiology*, 291(2), pp. 332–340. doi: 10.1152/ajprenal.00340.2005.

Li, Y. *et al.* (2013) 'Highly Sensitive Platinum-Black Coated Platinum Electrodes for Electrochemical Detection of Hydrogen Peroxide and Nitrite in Microchannel', *Electroanalysis*, 25(4), pp. 895–902. doi: 10.1002/elan.201200456.

Li, Y. *et al.* (2014) 'Electrochemical detection of nitric oxide and peroxynitrite anion in microchannels at highly sensitive platinum-black coated electrodes. application to ROS and RNS mixtures prior to biological investigations', *Electrochimica Acta*. Elsevier Ltd, 144, pp. 111–118. doi: 10.1016/j.electacta.2014.08.046.

Li, Y. and Lin, X. (2006) 'Simultaneous electroanalysis of dopamine, ascorbic acid and uric acid by poly (vinyl alcohol) covalently modified glassy carbon electrode', *Sensors and Actuators, B: Chemical*, 115(1), pp. 134–139. doi: 10.1016/j.snb.2005.08.022.

Lielpetere, A. *et al.* (2023) 'Cross-Linkable Polymer-Based Multi-layers for Protecting Electrochemical Glucose Biosensors against Uric Acid, Ascorbic Acid, and Biofouling Interferences', *ACS Sensors*, 8(4), pp. 1756–1765. doi: 10.1021/acssensors.3c00050.

Lim, S. H. *et al.* (2005) 'A glucose biosensor based on electrodeposition of palladium nanoparticles and glucose oxidase onto Nafion-solubilized carbon nanotube electrode', *Biosensors and Bioelectronics*, 20(11), pp. 2341–2346. doi: 10.1016/j.bios.2004.08.005.

Lincoln, J. and Burnstock, G. (1993) *Autonomic innervation of the urinary bladder and urethra*, *Nervous Control of the Urogenital System*. Harwood Academic Publishers.

Lindström, P. and Wager, O. (1978) 'IgG Autoantibody to Human Serum Albumin Studied by the ELISA-Technique', *Scandinavian Journal of Immunology*. John Wiley & Sons, Ltd, 7(5), pp. 419–425. doi: https://doi.org/10.1111/j.1365-3083.1978.tb00472.x.

Lionetto, L. *et al.* (2008) 'HPLC-mass spectrometry method for quantitative detection of neuroendocrine tumor markers: Vanillylmandelic acid, homovanillic acid and 5-hydroxyindoleacetic acid'. doi: 10.1016/j.cca.2008.08.003.

Lips, K. S. *et al.* (2007) 'Acetylcholine and Molecular Components of its Synthesis and Release Machinery in the Urothelium', *European Urology*, 51(4), pp. 1042–1053. doi: 10.1016/j.eururo.2006.10.028.

Liu, N. *et al.* (2021) 'The role of oxidative stress in hyperuricemia and xanthine oxidoreductase (XOR) inhibitors', *Oxidative Medicine and Cellular Longevity*, 2021. doi: 10.1155/2021/1470380.

Loock, H. P. and Wentzell, P. D. (2012) 'Detection limits of chemical sensors: Applications and misapplications', *Sensors and Actuators, B: Chemical*. Elsevier B.V., 173, pp. 157–163. doi: 10.1016/j.snb.2012.06.071.

Luheshi, G. N. and Zar, M. A. (1990) 'Presence of non-cholinergic motor transmission in human isolated bladder', *Journal of Pharmacy and Pharmacology*, 42(3), pp. 223–224. doi: 10.1111/j.2042-7158.1990.tb05396.x.

Lundberg, J. O., Weitzberg, E. and Gladwin, M. T. (2008) 'The nitrate-nitrite-nitric oxide pathway in physiology and therapeutics', *Nature Reviews Drug Discovery*, 7(2), pp. 156–167. doi: 10.1038/nrd2466.

Luo, A. *et al.* (2015) 'Simultaneous determination of uric acid, xanthine and hypoxanthine based on sulfonic groups functionalized nitrogen-doped graphene', *Journal of Electroanalytical Chemistry*. Elsevier B.V., 756, pp. 22–29. doi: 10.1016/j.jelechem.2015.08.008.

Luong, J. H. T. and Vashist, S. K. (2016) *Point-of-care glucose detection for diabetic monitoring and management*. 1 edition. CRC Press.

Magar, H. S. *et al.* (2017) 'A novel sensitive amperometric choline biosensor based on multiwalled carbon nanotubes and gold nanoparticles', *Talanta*. Elsevier B.V., 167(February), pp. 462–469. doi: 10.1016/j.talanta.2017.02.048.

Maloy, J. T. (1983) 'Factors affecting the shape of current-potential curves', *Journal of Chemical Education*, 60(4), pp. 285–289. doi: https://doi.org/10.1021/ed060p285.

Mansfield, K. J. *et al.* (2005) 'Muscarinic receptor subtypes in human bladder detrusor and mucosa, studied by radioligand binding and quantitative competitive RT-PCR: Changes in ageing', *British Journal of Pharmacology*, 144(8), pp. 1089–1099. doi: 10.1038/sj.bjp.0706147.

Martínez-Saénz, A. *et al.* (2011) 'Mechanisms involved in the nitric oxide independent inhibitory neurotransmission to the pig urinary bladder neck', *Neurourology and Urodynamics*, 30(1), pp. 151–157. doi: 10.1002/nau.20960.

Masuda, H. *et al.* (2007) 'Effects of anaesthesia on the nitrergic pathway during the micturition reflex in rats', *BJU International*, 100(1), pp. 175–180. doi: 10.1111/j.1464-410X.2007.06872.x.

Masuda, H. (2008) 'Significance of nitric oxide and its modulation mechanisms by endogenous nitric oxide synthase inhibitors and arginase in the micturition disorders and erectile dysfunction', *International Journal of Urology*, 15(2), pp. 128–134. doi: 10.1111/j.1442-2042.2007.01973.x.

McCreery, R. L. (2008) 'Advanced carbon electrode materials for molecular electrochemistry', *Chemical Reviews*, 108(7), pp. 2646–2687. doi: 10.1021/cr068076m.

McLatchie, L. *et al.* (2021) 'ATP shows more potential as a urinary biomarker than acetylcholine and PGE2, but its concentration in urine is not a simple function of dilution', *Neurourology and Urodynamics*, 40(January), pp. 1–9. doi: 10.1002/nau.24620.

McMahon, C. P. *et al.* (2007) 'Oxygen tolerance of an implantable polymer/enzyme composite glutamate biosensor displaying polycation-enhanced substrate sensitivity', *Biosensors and Bioelectronics*, 22(7), pp. 1466–1473. doi: 10.1016/j.bios.2006.06.027.

McMurray, G., Casey, J. H. and Naylor, A. M. (2006) 'Animal models in urological disease and sexual dysfunction', *British Journal of Pharmacology*, 147(SUPPL. 2), pp. 62–79. doi: 10.1038/sj.bjp.0706630.

Mentana, A. *et al.* (2020) 'Accurate glutamate monitoring in foodstuffs by a sensitive and interference-free glutamate oxidase based disposable amperometric biosensor', *Analytica Chimica Acta*. Elsevier Ltd, 1115, pp. 16–22. doi: 10.1016/j.aca.2020.04.020.

Michel, M. C. and Vrydag, W. (2006) 'α1-, α2- and β-Adrenoceptors in the Urinary Bladder, Urethra and Prostate', *British Journal of Pharmacology*, 147(SUPPL. 2), pp. 88–119. doi: 10.1038/sj.bjp.0706619.

Miftahof, R. N. and Nam, H. G. (2013) *Biomechanics of the human urinary bladder*, *Biomechanics of the Human Urinary Bladder*. doi: 10.1007/978-3-642-36146-3.

Migneault, I. *et al*. (2004) 'Glutaraldehyde: behavior in aqueous solution, reaction with proteins, and application to enzyme crosslinking', *BioTechniques*, 37(5), pp. 790–802. doi: 10.2144/04375RV01.

Milsom, I. *et al*. (2014) 'Global prevalence and economic burden of urgency urinary incontinence: A systematic review', *European Urology*. European Association of Urology, 65(1), pp. 79–95. doi: 10.1016/j.eururo.2013.08.031.

Monti, P. *et al*. (2017) 'Low electro-synthesis potentials improve permselectivity of polymerized natural phenols in biosensor applications', *Talanta*. Elsevier, 162(October 2016), pp. 151–158. doi: 10.1016/j.talanta.2016.10.019.

Moore, K. H., Ray, F. R. and Barden, J. A. (2001) 'Loss of Purinergic P2X3 and P2X5 Receptor Innervation in Human Detrusor from Adults with Urge Incontinence', *The Journal of Neuroscience*, 21(18), pp. RC166–RC166. doi: 10.1523/JNEUROSCI.21-18-j0002.2001.

Moro, C. and Chess-Williams, R. (2012) 'Non-adrenergic, non-cholinergic, non-purinergic contractions of the urothelium/lamina propria of the pig bladder', *Autonomic and Autacoid Pharmacology*, 32(3 PART 4), pp. 53–59. doi: 10.1111/aap.12000.

Moro, C., Leeds, C. and Chess-Williams, R. (2012) 'Contractile activity of the bladder urothelium/lamina propria and its regulation by nitric oxide', *European Journal of Pharmacology*. Elsevier B.V., 674(2–3), pp. 445–449. doi: 10.1016/j.ejphar.2011.11.020.

Moro, C., Uchiyama, J. and Chess-Williams, R. (2011) 'Urothelial/lamina propria spontaneous activity and the role of M3 muscarinic receptors in mediating rate responses to stretch and carbachol', *Urology*. Elsevier Inc., 78(6), pp. 1442.e9-1442.e15. doi: 10.1016/j.urology.2011.08.039.

Mossa, A. H. *et al*. (2020) 'Imbalance of nerve growth factor metabolism in aging women with overactive bladder syndrome', *World Journal of Urology*. Springer Berlin Heidelberg, 39(6), pp. 2055–2063. doi: 10.1007/s00345-020-03422-6.

Munoz, A. *et al*. (2011) 'Overactive and underactive bladder dysfunction is reflected by alterations in urothelial ATP and NO release', *Neurochemistry International*. Elsevier Ltd, 37(2), p. 288. doi: 10.1016/j.neuint.2010.12.002.

Myszka, D. G. (1999) 'Improving biosensor analysis', *Journal of Molecular Recognition*, 12(5), pp. 279–284. doi: 10.1002/(SICI)1099-1352(199909/10)12:5<279::AID-JMR473>3.0.CO;2-3.

Navera, E. N. *et al*. (1993) 'Nafion-coated carbon fiber for acetylcholine and choline sensors', *Electroanalysis*. John Wiley & Sons, Ltd, 5(1), pp. 17–22. doi: https://doi.org/10.1002/elan.1140050105.

NHS England (2018) *Excellence in continence care: practical guidance for commissioners and leaders in health and social care*. Available at: https://www.england.nhs.uk/wp-content/uploads/2018/07/excellence-in-continence-care.pdf.

NICE guideline (2013) *Falls In Older People : Assessing Risk and Prevention*, *NICE Clinical guideline*. Available at:

https://www.nice.org.uk/guidance/cg161/resources/falls-in-older-people-assessing-risk-and-prevention-35109686728645.

Nicholls, M. (2019) 'Nitric oxide discovery Nobel Prize winners', *European Heart Journal*, 40(22), pp. 1747–1749. doi: 10.1093/eurheartj/ehz361.

Nicholson, R. S. and Shain, I. (1964) 'Theory of Stationary Electrode Polarography: Single Scan and Cyclic Methods Applied to Reversible, Irreversible, and Kinetic Systems', *Analytical Chemistry*, 36(7), p. 1212. doi: 10.1021/ac60213a053.

Nöll, T. and Nöll, G. (2011) 'Strategies for "wiring" redox-active proteins to electrodes and applications in biosensors, biofuel cells, and nanotechnology', *Chemical Society Reviews*, 40(7), pp. 3564–3576. doi: 10.1039/c1cs15030h.

Nomiya, M. and Yamaguchi, O. (2003) 'A Quantitative Analysis of mRNA Expression of α1 and β-adrenoceptor Subtypes and Their Functional Roles in Human Normal and Obstructed Bladders', *Journal of Urology*, 170(2), pp. 649–653. doi: 10.1097/01.ju.0000067621.62736.7c.

Noto, H. *et al.* (1989) 'Excitatory and inhibitory influences on bladder activity elicited by electrical stimulation in the pontine micturition center in the rat', *Brain Research*, 492(1), pp. 99–115. doi: https://doi.org/10.1016/0006-8993(89)90893-7.

O'Brien, K. B. *et al.* (2007) 'Development and characterization in vitro of a catalase-based biosensor for hydrogen peroxide monitoring', *Biosensors and Bioelectronics*, 22(12), pp. 2994–3000. doi: 10.1016/j.bios.2006.12.020.

O'Hare, D., Macpherson, J. V. and Willows, A. (2002) 'On the microelectrode behaviour of graphite-epoxy composite electrodes', *Electrochemistry Communications*, 4(3), pp. 245–250. doi: 10.1016/S1388-2481(02)00265-5.

Ocque, A. J., Stubbs, J. R. and Nolin, T. D. (2015) 'Development and validation of a simple UHPLC-MS/MS method for the simultaneous determination of trimethylamine N-oxide, choline, and betaine in human plasma and urine', *Journal of Pharmaceutical and Biomedical Analysis*. Elsevier B.V., 109, pp. 128–135. doi: 10.1016/j.jpba.2015.02.040.

Okuda, T. *et al.* (2000) 'Identification and characterization of the high-affinity choline transporter', *Nature Neuroscience*, 3(2), pp. 120–125. doi: 10.1038/72059.

de Oliveira, P. R. *et al.* (2021) 'Use of beeswax as an alternative binder in the development of composite electrodes: an approach for determination of hydrogen peroxide in honey samples', *Electrochimica Acta*. Elsevier Ltd, 390, p. 138876. doi: 10.1016/j.electacta.2021.138876.

Osuna, V. *et al.* (2022) 'Progress of Polyaniline Glucose Sensors for Diabetes Mellitus Management Utilizing Enzymatic and Non-Enzymatic Detection', *Biosensors*, 12(3), p. 137. doi: 10.3390/bios12030137.

Özdemir, M. and Arslan, H. (2014) 'Choline-sensing carbon paste electrode containing polyaniline (pani)-silicon dioxide composite-modified choline oxidase', *Artificial Cells, Nanomedicine and Biotechnology*, 42(1), pp. 27–31. doi: 10.3109/21691401.2013.768628.

Pakzad, M. *et al*. (2016) 'Contractile effects and receptor analysis of adenosine-receptors in human detrusor muscle from stable and neuropathic bladders', *Naunyn-Schmiedeberg's Archives of Pharmacology*. Naunyn-Schmiedeberg's Archives of Pharmacology, 389(8), pp. 921–929. doi: 10.1007/s00210-016-1255-1.

Palea, S. *et al*. (1993) 'Evidence for Purinergic Neurotransmission in Human Urinary Bladder Affected by Interstitial Cystitis', *Journal of Urology*. The American Urological Association Education and Research, Inc., 150(6), pp. 2007–2012. doi: 10.1016/S0022-5347(17)35955-4.

Pankratov, Y. *et al*. (2006) 'Vesicular release of ATP at central synapses', *Pflugers Archiv European Journal of Physiology*, 452(5), pp. 589–597. doi: 10.1007/s00424-006-0061-x.

Panyachariwat, N. and Steckel, H. (2014) 'Stability of urea in solution and pharmaceutical preparations', *Journal of cosmetic science*, 65(3), p. 187—195. Available at: http://europepmc.org/abstract/MED/25043489.

Parra, K. N. *et al*. (2016) 'Electrochemical degradation of tetracycline in artificial urine medium', *Journal of Solid State Electrochemistry*, 20(4), pp. 1001–1009. doi: 10.1007/s10008-015-2833-8.

Parsons, B. A. and Drake, M. J. (2011) 'Animal models in overactive bladder research', *Handbook of Experimental Pharmacology*, 202, pp. 15–43. doi: 10.1007/978-3-642-16499-6_2.

Partin, A. W. *et al*. (2020) *Campbell Walsh Wein Urology*. 12th edn. Elsevier.

Patel, B. *et al*. (2020) 'Combination drug therapy against OAB normalizes micturition parameters and increases the release of nitric oxide during chemically induced cystitis', *Pharmacology Research and Perspectives*, 8(1), pp. 1–8. doi: 10.1002/prp2.564.

Patel, B. A. *et al*. (2006) 'Detection of nitric oxide release from single neurons in the pond snail, Lymnaea stagnalis', *Analytical Chemistry*, 78(22), pp. 7643–7648. doi: 10.1021/ac060863w.

Patel, B. A. *et al*. (2011) 'ATP microelectrode biosensor for stable long-term in vitro monitoring from gastrointestinal tissue', *Biosensors and Bioelectronics*, 26(6), pp. 2890–2896. doi: 10.1016/j.bios.2010.11.033.

Patel, B. A. (2021) *Electrochemistry for Bioanalysis*. Elsevier.

Pedley, A. M. and Benkovic, S. J. (2017) 'A New View into the Regulation of Purine Metabolism: The Purinosome', *Trends in Biochemical Sciences*. Elsevier Ltd, 42(2), pp. 141–154. doi: 10.1016/j.tibs.2016.09.009.

Peeker, R. *et al*. (2010) 'A prospective observational study of the effects of treatment with extended-release tolterodine on health-related quality of life of patients suffering overactive bladder syndrome in Sweden', *Scandinavian Journal of Urology and Nephrology*, 44(3), pp. 138–146. doi: 10.3109/00365591003709468.

Peteu, S. F. *et al*. (2021) 'An Electrochemical ATP Biosensor with Enzymes Entrapped within a PEDOT Film', *Electroanalysis*, 33(2), pp. 495–505. doi: 10.1002/elan.202060397.

Peyronnet, B. *et al.* (2018) 'Mirabegron in patients with Parkinson disease and overactive bladder symptoms: A retrospective cohort', *Parkinsonism and Related Disorders*. Elsevier, (April), pp. 0–1. doi: 10.1016/j.parkreldis.2018.07.005.

Peyronnet, B. *et al.* (2019) 'A Comprehensive Review of Overactive Bladder Pathophysiology: On the Way to Tailored Treatment(Figure presented.)', *European Urology*, 75(6), pp. 988–1000. doi: 10.1016/j.eururo.2019.02.038.

Pinyou, P. *et al.* (2022) 'Wiring Xanthine Oxidase Using an Osmium-Complex-Modified Polymer for Application in Biosensing.', *ChemElectroChem*, 9(11). doi: 10.1002/celc.202101597.

Pravda, M. *et al.* (1995) 'Amperometric glucose biosensors based on an Osmium (2+/3+) redox polymer-mediated electron transfer at carbon paste electrodes', *Biosensors*.

Price, G. W. *et al.* (2020) 'Examining Local Cell-to-Cell Signalling in the Kidney Using ATP Biosensing', in, pp. 135–149. doi: 10.1007/7651_2020_297.

Pundir, C. S. and Devi, R. (2014) 'Biosensing methods for xanthine determination: A review', *Enzyme and Microbial Technology*. Elsevier Inc., 57, pp. 55–62. doi: 10.1016/j.enzmictec.2013.12.006.

Qi, Y. T. *et al.* (2022) 'Homeostasis inside Single Activated Phagolysosomes: Quantitative and Selective Measurements of Submillisecond Dynamics of Reactive Oxygen and Nitrogen Species Production with a Nanoelectrochemical Sensor', *Journal of the American Chemical Society*, 144(22), pp. 9723–9733. doi: 10.1021/jacs.2c01857.

Rada, M. P. *et al.* (2020) 'The profile of urinary biomarkers in overactive bladder', *Neurourology and Urodynamics*, 39(8), pp. 2305–2313. doi: 10.1002/nau.24487.

Rahimi, P., Ghourchian, H. and Sajjadi, S. (2012) 'Effect of hydrophilicity of room temperature ionic liquids on the electrochemical and electrocatalytic behaviour of choline oxidase', *Analyst*, 137(2), pp. 471–475. doi: 10.1039/c1an15732a.

Rahimi, P. and Joseph, Y. (2019) 'Enzyme-based biosensors for choline analysis: A review', *TrAC - Trends in Analytical Chemistry*. Elsevier Ltd, 110, pp. 367–374. doi: 10.1016/j.trac.2018.11.035.

Rahman, M. M. *et al.* (2010) 'A comprehensive review of glucose biosensors based on nanostructured metal-oxides', *Sensors*, 10(5), pp. 4855–4886. doi: 10.3390/s100504855.

Ren, W., Luo, H. Q. and Li, N. B. (2006) 'Simultaneous voltammetric measurement of ascorbic acid, epinephrine and uric acid at a glassy carbon electrode modified with caffeic acid', *Biosensors and Bioelectronics*, 21(7), pp. 1086–1092. doi: 10.1016/j.bios.2005.04.002.

Ren, X. *et al.* (2009) 'Using gold nanorods to enhance the current response of a choline biosensor', *Electrochimica Acta*, 54(28), pp. 7248–7253. doi: 10.1016/j.electacta.2009.07.036.

Ricci, F. *et al.* (2002) 'Prussian Blue based screen printed biosensors with improved characteristics of long-term lifetime and pH stability', *Biosensors and Bioelectronics*,

18(2–3), pp. 165–174. doi: 10.1016/S0956-5663(02)00169-0.

El Ridi, R. and Tallima, H. (2017) 'Physiological functions and pathogenic potential of uric acid: A review', *Journal of Advanced Research*. Cairo University, 8(5), pp. 487–493. doi: 10.1016/j.jare.2017.03.003.

Rizzi, G. and Tan, K. R. (2017) 'Dopamine and acetylcholine, a circuit point of view in Parkinson's disease', *Frontiers in Neural Circuits*, 11(December), pp. 1–14. doi: 10.3389/fncir.2017.00110.

Rose, C. *et al.* (2015) 'The Characterization of Feces and Urine: A Review of the Literature to Inform Advanced Treatment Technology', *Critical Reviews in Environmental Science and Technology*, 45(17), pp. 1827–1879. doi: 10.1080/10643389.2014.1000761.

Samanidou, V. F., Metaxa, A. S. and Papadoyannis, I. N. (2002) 'Direct simultaneous determination of uremic toxins: Creatine, creatinine, uric acid, and xanthine in human biofluids by HPLC', *Journal of Liquid Chromatography and Related Technologies*, 25(1), pp. 43–57. doi: 10.1081/JLC-100108538.

Sassolas, A., Blum, L. J. and Leca-Bouvier, B. D. (2012) 'Immobilization strategies to develop enzymatic biosensors', *Biotechnology Advances*. Elsevier Inc., 30(3), pp. 489–511. doi: 10.1016/j.biotechadv.2011.09.003.

Sattarahmady, N., Heli, H. and Vais, R. D. (2013) 'An electrochemical acetylcholine sensor based on lichen-like nickel oxide nanostructure', *Biosensors and Bioelectronics*. Elsevier, 48, pp. 197–202. doi: 10.1016/j.bios.2013.04.001.

Seegmiller, J. E. *et al.* (1961) 'Uric acid production in gout', *Journal of Clinical Investigation*, 40(7), pp. 1304–1314. doi: 10.1172/JCI104360.

Senecal, J. and Vinnerås, B. (2017) 'Urea stabilisation and concentration for urine-diverting dry toilets: Urine dehydration in ash', *Science of the Total Environment*. The Authors, 586, pp. 650–657. doi: 10.1016/j.scitotenv.2017.02.038.

Seth, J. H. *et al.* (2013) 'Nerve growth factor (NGF): A potential urinary biomarker for overactive bladder syndrome (OAB)?', *BJU International*, 111(3), pp. 372–380. doi: 10.1111/j.1464-410X.2012.11672.x.

Sexton, C. C. *et al.* (2011) 'Persistence and adherence in the treatment of overactive bladder syndrome with anticholinergic therapy: A systematic review of the literature', *International Journal of Clinical Practice*, 65(5), pp. 567–585. doi: 10.1111/j.1742-1241.2010.02626.x.

Shabir, S. *et al.* (2013) 'Functional expression of purinergic P2 receptors and transient receptor potential channels by the human urothelium', *American Journal of Physiology - Renal Physiology*, 305(3), pp. 396–406. doi: 10.1152/ajprenal.00127.2013.

Shen, J. *et al.* (2005) 'Involvement of the nitric oxide-cyclic GMP pathway and neuronal nitric oxide synthase in ATP-induced Ca2+ signalling in cochlear inner hair cells', *European Journal of Neuroscience*, 21(11), pp. 2912–2922. doi: 10.1111/j.1460-9568.2005.04135.x.

Shen, J. X. and Yakel, J. L. (2009) 'Nicotinic acetylcholine receptor-mediated calcium

signaling in the nervous system', *Acta Pharmacologica Sinica*, 30(6), pp. 673–680. doi: 10.1038/aps.2009.64.

Shergill, R. S. *et al.* (2022) '3D-printed electrochemical pestle and mortar for identification of falsified pharmaceutical tablets', *Microchimica Acta*. Springer Vienna, 189(3), pp. 0–1. doi: 10.1007/s00604-022-05202-y.

Sheyn, D. *et al.* (2020) 'Evaluation of Urine Choline Levels in Women With and Without Overactive Bladder Syndrome', *Female Pelvic Medicine & Reconstructive Surgery*, 26(10), pp. 644–648. doi: 10.1097/SPV.0000000000000639.

Sheyn, D. *et al.* (2022) 'Evaluation of the relationship of cholinergic metabolites in urine and urgency urinary incontinence', *International Urogynecology Journal*. International Urogynecology Journal, 33(5), pp. 1165–1174. doi: 10.1007/s00192-021-04785-z.

Shi, K. and Shiu, K. K. (2001) 'Determination of uric acid at electrochemically activated glassy carbon electrode', *Electroanalysis*, 13(16), pp. 1319–1325. doi: 10.1002/1521-4109(200111)13:16<1319::AID-ELAN1319>3.0.CO;2-C.

Shibli, S. M. A., Beenakumari, K. S. and Suma, N. D. (2006) 'Nano nickel oxide/nickel incorporated nickel composite coating for sensing and estimation of acetylcholine', *Biosensors and Bioelectronics*, 22(5), pp. 633–638. doi: 10.1016/j.bios.2006.01.020.

Silva-Ramos, M. *et al.* (2013) 'Urinary ATP May Be a Dynamic Biomarker of Detrusor Overactivity in Women with Overactive Bladder Syndrome', *PLoS ONE*, 8(5). doi: 10.1371/journal.pone.0064696.

Simm, A. O. *et al.* (2005) 'Boron-doped diamond microdisc arrays: Electrochemical characterisation and their use as a substrate for the production of microelectrode arrays of diverse metals (Ag, Au, Cu) via electrodeposition', *Analyst*, 130(9), pp. 1303–1311. doi: 10.1039/b506956d.

Singh, H. *et al.* (2015) 'Application of 3D printing technology in increasing the diagnostic performance of enzyme-linked immunosorbent assay (ELISA) for infectious diseases', *Sensors (Switzerland)*, 15(7), pp. 16503–16515. doi: 10.3390/s150716503.

Singh Shergill, R. *et al.* (2022) 'Comparing electrochemical pre-treated 3D printed native and mechanically polished electrode surfaces for analytical sensing', *Journal of Electroanalytical Chemistry*. Elsevier B.V., 905(December 2021), p. 115994. doi: 10.1016/j.jelechem.2021.115994.

Sirén, H. and Karjalainen, U. (1999) 'Study of catecholamines in patient urine samples by capillary electrophoresis', *Journal of Chromatography A*, 853(1–2), pp. 527–533. doi: 10.1016/S0021-9673(99)00679-2.

Sjogren, C. *et al.* (1982) 'Atropine Resistance of Transmurally Stimulated Isolated Human Bladder Muscle', *Journal of Urology*, 128(6), pp. 1368–1371. doi: 10.1016/S0022-5347(17)53509-0.

Soliman, S. A. *et al.* (1986) 'Stability of creatinine, urea and uric acid in urine stored under various conditions', *Clinica Chimica Acta*, 160(3), pp. 319–326. doi: 10.1016/0009-8981(86)90200-7.

Soliman, Y., Meyer, R. and Baum, N. (2016) ‘Prevention and ManageMent Update Falls in the Elderly Secondary to Urinary Symptoms’, *Rev Urol*, 18(1), pp. 28–32. doi: 10.3909/riu0686.

Song, Z. *et al.* (2006) ‘Amperometric aqueous sol-gel biosensor for low-potential stable choline detection at multi-wall carbon nanotube modified platinum electrode’, *Sensors and Actuators, B: Chemical*, 115(2), pp. 626–633. doi: 10.1016/j.snb.2005.10.030.

Souza-Filho, M. V. P. *et al.* (1997) ‘Involvement of nitric oxide in the pathogenesis of cyclophosphamide- induced hemorrhagic cystitis’, *American Journal of Pathology*, 150(1), pp. 247–256.

Stav, K., Dwyer, P. L. and Rosamilia, A. (2009) ‘Women Overestimate Daytime Urinary Frequency: The Importance of the Bladder Diary’, *Journal of Urology*, 181(5), pp. 2176–2180. doi: 10.1016/j.juro.2009.01.042.

Stenqvist, J. *et al.* (2017) ‘Urothelial acetylcholine involvement in ATP-induced contractile responses of the rat urinary bladder’, *European Journal of Pharmacology*. Elsevier B.V., 809(December 2016), pp. 253–260. doi: 10.1016/j.ejphar.2017.05.023.

Stenqvist, J. *et al.* (2018) ‘Effects of caveolae depletion and urothelial denudation on purinergic and cholinergic signaling in healthy and cyclophosphamide-induced cystitis in the rat bladder’, *Autonomic Neuroscience: Basic and Clinical*. Elsevier, 213(March), pp. 60–70. doi: 10.1016/j.autneu.2018.06.001.

Stenqvist, J., Carlsson, T., *et al.* (2020) ‘Functional atropine sensitive purinergic responses in the healthy rat bladder’, *Autonomic Neuroscience*. Elsevier, 227(June), p. 102693. doi: 10.1016/j.autneu.2020.102693.

Stenqvist, J., Aronsson, P., *et al.* (2020) ‘In vivo paracrine effects of ATP-induced urothelial acetylcholine in the rat urinary bladder’, *Autonomic Neuroscience: Basic and Clinical*. Elsevier, 227(March), p. 102689. doi: 10.1016/j.autneu.2020.102689.

Stewart, W. F. *et al.* (2003) ‘Prevalence and burden of overactive bladder in the United States’, *World Journal of Urology*, 20(6), pp. 327–336. doi: 10.1007/s00345-002-0301-4.

Su, C. K. (2021) ‘Review of 3D-Printed functionalized devices for chemical and biochemical analysis’, *Analytica Chimica Acta*. Elsevier Ltd, 1158, p. 338348. doi: 10.1016/j.aca.2021.338348.

Sugaya, K. *et al.* (2009) ‘Relationship between lower urinary tract symptoms and urinary ATP in patients with benign prostatic hyperplasia or overactive bladder’, *Biomedical Research*, 30(5), pp. 287–294. doi: 10.2220/biomedres.30.287.

Sugaya, K. *et al.* (2018) ‘Relationship between Voided Urine Volume and Urinary ATP in Healthy Volunteers’, *Open Journal of Urology*, 08(10), pp. 275–280. doi: 10.4236/oju.2018.810031.

Sui, G. *et al.* (2014) ‘Purinergic and muscarinic modulation of ATP release from the urothelium and its paracrine actions’, *American Journal of Physiology - Renal Physiology*, 306(3), pp. 286–298. doi: 10.1152/ajprenal.00291.2013.

Sun, Q. *et al.* (2022) ‘Acetylcholine deficiency disrupts extratelencephalic projection

neurons in the prefrontal cortex in a mouse model of Alzheimer's disease', *Nature Communications*. Springer US, 13(1). doi: 10.1038/s41467-022-28493-4.

Swennen, E. L. R. *et al.* (2008) 'Time-dependent effects of ATP and its degradation products on inflammatory markers in human blood ex vivo', *Immunobiology*, 213(5), pp. 389–397. doi: 10.1016/j.imbio.2007.10.007.

Szabo, S. M. *et al.* (2018) 'The Association Between Overactive Bladder and Falls and Fractures: A Systematic Review', *Advances in Therapy*. Springer Healthcare, 35(11), pp. 1831–1841. doi: 10.1007/s12325-018-0796-8.

Teles-Grilo Ruivo, L. M. *et al.* (2017) 'Coordinated Acetylcholine Release in Prefrontal Cortex and Hippocampus Is Associated with Arousal and Reward on Distinct Timescales', *Cell Reports*. ElsevierCompany., 18(4), pp. 905–917. doi: 10.1016/j.celrep.2016.12.085.

Thiagarajan, S., Tsai, T. H. and Chen, S. M. (2009) 'Easy modification of glassy carbon electrode for simultaneous determination of ascorbic acid, dopamine and uric acid', *Biosensors and Bioelectronics*, 24(8), pp. 2712–2715. doi: 10.1016/j.bios.2008.12.010.

Thomas, A. *et al.* (2006) 'Quantitative Determination of Adrenaline and Noradrenaline in Urine Using Liquid Chromatography-Tandem Mass Spectrometry', *Chromatographia*, 64(9), pp. 587–591. doi: 10.1365/s10337-006-0067-8.

Timóteo, M. A. *et al.* (2014) 'ATP released via pannexin-1 hemichannels mediates bladder overactivity triggered by urothelial P2Y6 receptors', *Biochemical Pharmacology*, 87(2), pp. 371–379. doi: 10.1016/j.bcp.2013.11.007.

Tobin, G. and Sjögren, C. (1995) 'In vivo and in vitro effects of muscarinic receptor antagonists on contractions and release of [3H]acetylcholine in the rabbit urinary bladder', *European Journal of Pharmacology*, 281(1), pp. 1–8. doi: 10.1016/0014-2999(95)00221-6.

Traiffort, E., O'Regan, S. and Ruat, M. (2013) 'The choline transporter-like family SLC44: Properties and roles in human diseases', *Molecular Aspects of Medicine*, 34(2–3), pp. 646–654. doi: 10.1016/j.mam.2012.10.011.

Tubaro, A. (2004) 'Defining overactive bladder: Epidemiology and burden of disease', *Urology*, 64(6 SUPPL. 1), pp. 2–6. doi: 10.1016/j.urology.2004.10.047.

Turner, D. A. *et al.* (2004) 'The cost of clinically significant urinary storage symptoms for community dwelling adults in the UK', *BJU International*, 93(9), pp. 1246–1252. doi: 10.1111/j.1464-410x.2004.04806.x.

Tyagi, P. *et al.* (2017) 'Past, Present and Future of Chemodenervation with Botulinum Toxin in the Treatment of Overactive Bladder', *The Journal of Urology*, 197(4), pp. 982–990. doi: https://doi.org/10.1016/j.juro.2016.11.092.

Uchil, D. *et al.* (2006) 'Continence pads: Have we got it right?', *International Urogynecology Journal*, 17(3), pp. 234–238. doi: 10.1007/s00192-005-1341-2.

Vadgama, P., Desai, M. and Crump, P. (1991) 'Electrochemical transducers for in vivo monitoring', *Electroanalysis*, 3(7), pp. 597–606. doi: 10.1002/elan.1140030703.

Vashist, S. K. *et al*. (2011) 'Technology behind commercial devices for blood glucose monitoring in diabetes management: A review', *Analytica Chimica Acta*. Elsevier B.V., 703(2), pp. 124–136. doi: 10.1016/j.aca.2011.07.024.

Veselá, R. *et al*. (2012) 'Coupled nitric oxide and autonomic receptor functional responses in the normal and inflamed urinary bladder of the rat', *Physiological Research*, 61(4), pp. 371–380. doi: 10.33549/physiolres.932282.

Vizzard, M. A., Erdman, S. L. and de Groat, W. C. (1996) 'Increased expression of neuronal nitric oxide synthase in bladder afferent pathways following chronic bladder irritation', *The Journal of Comparative Neurology*, 370(2), pp. 191–202. doi: 10.1002/(SICI)1096-9861(19960624)370:2<191::AID-CNE5>3.0.CO;2-Y.

Vlaskovska, M. *et al*. (2001) 'P2X3 knock-out mice reveal a major sensory role for urothelially released ATP', *Journal of Neuroscience*, 21(15), pp. 5670–5677. doi: 10.1523/jneurosci.21-15-05670.2001.

Wahono, N. *et al*. (2012) 'Evaluation of permselective membranes for optimization of intracerebral amperometric glutamate biosensors', *Biosensors and Bioelectronics*. Elsevier B.V., 33(1), pp. 260–266. doi: 10.1016/j.bios.2012.01.019.

wakabayashi, Y. *et al*. (1995) 'Acetylcholinesterase-positive afferent axons in mucosa of urinary bladder of adult cats: retrograde tracing and degeneration studies', *Histology and histopathology*. Available at: http://hdl.handle.net/10201/18764.

Wallner, C. *et al*. (2009) 'The Anatomical Components of Urinary Continence', *European Urology*, 55(4), pp. 932–944. doi: 10.1016/j.eururo.2008.08.032.

Wang, J. (2008) 'Electrochemical glucose biosensors', *Chemical Reviews*, 108(2), pp. 814–825. doi: 10.1021/cr068123a.

Wang, J., Liu, G. and Lin, Y. (2006) 'Amperometric choline biosensor fabricated through electrostatic assembly of bienzyme/polyelectrolyte hybrid layers on carbon nanotubes', *Analyst*, 131(4), pp. 477–483. doi: 10.1039/b516038c.

Wang, J. and Musameh, M. (2005) 'Carbon-nanotubes doped polypyrrole glucose biosensor', *Analytica Chimica Acta*, 539(1–2), pp. 209–213. doi: 10.1016/j.aca.2005.02.059.

Wang, J., Musameh, M. and Lin, Y. (2003) 'Solubilization of Carbon Nanotubes by Nafion toward the Preparation of Amperometric Biosensors', *Journal of the American Chemical Society*, 125(9), pp. 2408–2409. doi: 10.1021/ja028951v.

Wang, L. *et al*. (2014) 'Urinary brain-derived neurotrophic factor: a potential biomarker for objective diagnosis of overactive bladder', *International Urology and Nephrology*, 46(2), pp. 341–347. doi: 10.1007/s11255-013-0540-x.

Wang, P., Luthin, G. R. and Ruggieri, M. R. (1995) 'Muscarinic acetylcholine receptor subtypes mediating urinary bladder contractility and coupling to GTP binding proteins', *Journal of Pharmacology and Experimental Therapeutics*, 273(2), pp. 959–966.

Wang, Y. and Tong, L. L. (2010) 'Electrochemical sensor for simultaneous determination of uric acid, xanthine and hypoxanthine based on poly (bromocresol purple) modified

glassy carbon electrode', *Sensors and Actuators, B: Chemical*. Elsevier B.V., 150(1), pp. 43–49. doi: 10.1016/j.snb.2010.07.044.

Watson, D. G. (2016) *Pharmaceutical Analysis*. Fourth Edi. Elsevier.

Webb, A. *et al.* (2004) 'Reduction of nitrite to nitric oxide during ischemia protects against myocardial ischemia-reperfusion damage', *Proceedings of the National Academy of Sciences of the United States of America*, 101(37), pp. 13683–13688. doi: 10.1073/pnas.0402927101.

Wennberg, A. L. *et al.* (2009) 'A Longitudinal Population-based Survey of Urinary Incontinence, Overactive Bladder, and Other Lower Urinary Tract Symptoms in Women', *European Urology*, 55(4), pp. 783–791. doi: 10.1016/j.eururo.2009.01.007.

White, H. L. and Wu, J. C. (1973) 'Choline and Carnitine Acetyltransferases of Heart', *Biochemistry*, 12(5), pp. 841–846. doi: 10.1021/bi00729a009.

Wild, D. *et al.* (no date) *David Wild Eds. The Immunoassay Handbook. Theory and Applications of Ligand Binding, ELISA and Related Techniques 2013 (3) - Copy*.

Winder, M. *et al.* (2014) 'Signalling molecules in the urothelium', *BioMed Research International*, 2014. doi: 10.1155/2014/297295.

Winder, M. *et al.* (2016) 'Proliferation of the human urothelium is induced by atypical β1-adrenoceptors', *Autonomic and Autacoid Pharmacology*, 35(3), pp. 32–40. doi: 10.1111/aap.12036.

Wu, G. *et al.* (2000) 'Identification of Gβγ Binding Sites in the Third Intracellular Loop of the M3-muscarinic Receptor and Their Role in Receptor Regulation', *Journal of Biological Chemistry*. Â© 2000 ASBMB. Currently published by Elsevier Inc; originally published by American Society for Biochemistry and Molecular Biology., 275(12), pp. 9026–9034. doi: 10.1074/jbc.275.12.9026.

Wu, X. R. *et al.* (2009) 'Uroplakins in urothelial biology, function, and disease', *Kidney International*. Elsevier Masson SAS, 75(11), pp. 1153–1165. doi: 10.1038/ki.2009.73.

Wu, Y. and Li, L. (2016) 'Sample normalization methods in quantitative metabolomics', *Journal of Chromatography A*. Elsevier B.V., 1430, pp. 80–95. doi: 10.1016/j.chroma.2015.12.007.

Xiang, L. *et al.* (2008) 'In situ cationic ring-opening polymerization and quaternization reactions to confine ferricyanide onto carbon nanotubes: A general approach to development of integrative nanostructured electrochemical biosensors', *Analytical Chemistry*, 80(17), pp. 6587–6593. doi: 10.1021/ac800733t.

Xu, Y. and Venton, B. J. (2010) 'Microelectrode sensing of adenosine/adenosine-5'-triphosphate with fast-scan cyclic voltammetry', *Electroanalysis*, 22(11), pp. 1167–1174. doi: 10.1002/elan.200900559.

Yamamoto, T., Moriwaki, Y. and Takahashi, S. (2005) 'Effect of ethanol on metabolism of purine bases (hypoxanthine, xanthine, and uric acid)', *Clinica Chimica Acta*, 356(1–2), pp. 35–57. doi: 10.1016/j.cccn.2005.01.024.

Yang, Q. *et al.* (2018) 'Plasmonic ELISA for Sensitive Detection of Disease Biomarkers with a Smart Phone-Based Reader', *Nanoscale Research Letters*. Nanoscale Research Letters, 13. doi: 10.1186/s11671-018-2806-9.

Yoon, E. J., Choi, Y. and Park, D. (2022) 'Improvement of Cognitive Function in Ovariectomized Rats by Human Neural Stem Cells Overexpressing Choline Acetyltransferase via Secretion of NGF and BDNF', *International Journal of Molecular Sciences*, 23(10). doi: 10.3390/ijms23105560.

Yorde, D. E. *et al.* (1976) 'Competitive enzyme-liked immunoassay with use of soluble enzyme/antibody immune complexes for labeling. I. Measurement of human choriogonadotropin.', *Clinical chemistry*. Oxford University Press, 22(8), pp. 1372–1377.

Yoshida, M. *et al.* (2004) 'Management of detrusor dysfunction in the elderly: Changes in acetylcholine and adenosine triphosphate release during aging', *Urology*, 63(3 SUPPL. 1), pp. 17–23. doi: 10.1016/j.urology.2003.11.003.

Yoshida, M. *et al.* (2006) 'Non-neuronal cholinergic system in human bladder urothelium', *Urology*, 67(2), pp. 425–430. doi: 10.1016/j.urology.2005.08.014.

Yoshida, M. *et al.* (2010) 'The forefront for novel therapeutic agents based on the pathophysiology of lower urinary tract dysfunction: Pathophysiology and pharmacotherapy of overactive bladder', *Journal of Pharmacological Sciences*. Elsevier B.V., 112(2), pp. 128–134. doi: 10.1254/jphs.09R12FM.

Yoshimura, N. (2007) 'Lower urinary tract symptoms (LUTS) and bladder afferent activity', *Neurourology and Urodynamics*, 26(S6), pp. 908–913. doi: 10.1002/nau.20487.

Yoshimura, N. and De Groat, W. C. (1997) 'Neural Control of the Lower Urinary Tract', *International Journal of Urology*, 4(2), pp. 111–125. doi: 10.1111/j.1442-2042.1997.tb00156.x.

Young, J. S. *et al.* (2012) 'Inhibition of stretching-evoked ATP release from bladder mucosa by anticholinergic agents', *BJU International*, 110(8b), pp. E397–E401. doi: 10.1111/j.1464-410x.2012.10966.x.

Yuan, C. J. *et al.* (2005) 'Eliminating the interference of ascorbic acid and uric acid to the amperometric glucose biosensor by cation exchangers membrane and size exclusion membrane', *Electroanalysis*, 17(24), pp. 2239–2245. doi: 10.1002/elan.200503359.

Yuen, J. W. M. and Benzie, I. F. F. (2010) 'Hydrogen peroxide in urine as a potential biomarker of whole body oxidative stress', *https://doi.org/10.1080/10715760310001616032*. Taylor & Francis, 37(11), pp. 1209–1213. doi: 10.1080/10715760310001616032.

Zhang, L. *et al.* (2014) 'Improved enzyme immobilization for enhanced bioelectrocatalyticactivity of choline sensor and acetylcholine sensor', *Sensors and Actuators, B: Chemical*. Elsevier B.V., 193, pp. 904–910. doi: 10.1016/j.snb.2013.11.092.

Zhang, X., Ju, H. and Wang, J. (2008) *Electrochemical Sensors, Biosensors and their Biomedical Applications*. 1st Editio. Academic Press.

Zhang, Y. *et al.* (2007) 'Development and analytical application of an uric acid biosensor

using an uricase-immobilized eggshell membrane', *Biosensors and Bioelectronics*, 22(8), pp. 1791–1797. doi: 10.1016/j.bios.2006.08.038.

Zhu, D. *et al*. (2019) 'Non-enzymatic xanthine sensor of heteropolyacids doped ferrocene and reduced graphene oxide via one-step electrodeposition combined with layer-by-layer self-assembly technology', *Sensors and Actuators, B: Chemical*. Elsevier, 281(November 2018), pp. 893–904. doi: 10.1016/j.snb.2018.10.151.

Zhu, W. *et al*. (2009) 'A new microdialysis-electrochemical device for in vivo simultaneous determination of acetylcholine and choline in rat brain treated with N-methyl-(R)-salsolinol', *Biosensors and Bioelectronics*, 24(12), pp. 3594–3599. doi: 10.1016/j.bios.2009.05.023.